PROFILING THE PROTEIN INTERACTIONS OF THE NOVEL ANTICONVULSANT (*R*)-LACOSAMIDE

Steven Wesley Cotten

A dissertation submitted to the faculty of the University of North Carolina at Chapel Hill in partial fulfillment of the requirements for the degree of Doctor of Philosophy in the Eshelman School of Pharmacy.

Chapel Hill
2010

Approved by:

Professor Rihe Liu

Professor Harold Kohn

Professor Michael B. Jarstfer

Professor Qisheng Zhang

Professor T. Kendall Harden

ABSTRACT

STEVEN WESLEY COTTEN: Profiling the Protein Targets of the Novel Anticonvulsant (*R*)-lacosamide
(Under the direction of Professor Rihe Liu)

The full spectrum of proteins that interact with the anticonvulsant (*R*)-lacosamide remain unknown despite the compound's approval in both Europe and the United States for treatment of partial seizures. This dissertation seeks to identify proteins from the mouse brain proteome that bind to (*R*)-lacosamide by integrating chemical biology approaches coupled with mass spectrometry for drug-target discovery. (*R*)-Lacosamide probes functionalized with reactive units and chemical reporters are used to selectively label, detect, and capture target proteins from complex mixtures of mouse brain lysate. Several proteins identified were further evaluated using recombinant protein technology, and the adduction site of the DPYSL2 protein was identified using mass spectrometry. Computational studies modeled the interaction of (*R*)-lacosamide with the known crystal structure of the DPYSL2 protein. One predicted confirmation is consistent with known structure activity relationships of (*R*)-lacosamide *in vivo*. Data evaluating labeling of an (*R*)-lacosamide derivative with a mutant protein lacking the identified adducted residue are presented.

Acknowledgements

The work presented in this dissertation would have been impossible without outstanding help from numerous faculty members, colleagues, friends, and family. My advisor, Professor Rihe Liu, has given me tremendous support, advice, and encouragement during my graduate career. He graciously provided ample working space in his lab and access to resources in the Eshelman School of Pharmacy, School of Medicine, Lineberger Comprehensive Cancer Center and the Carolina Center for Genome Sciences. He frequently encouraged novel "crazy" ideas, which I was more than willing to provide. He holds all members of his lab to a high standard, and I was no exception. It was evident that dedication and perseverance were necessary to tackle the difficult scientific questions being addressed in his lab. I had an opportunity to contribute to a wide variety of projects and as a result feel well versed in several emerging frontiers of science.

Professor Harold Kohn has played a significant role in shaping my time here at UNC. He generously provided financial support for most of my graduate career, allowing me to work in collaboration with others in his lab navigating the field of chemical biology. The interdisciplinary nature of this research has not only challenged me scientifically, but gave me the opportunity to work closely with a diverse team of scientists building critical collaboration skills that are valuable outside the laboratory. The chance to work intimately on a project with such clinical relevance is rare, and I feel

very fortunate that I was asked to participate. I have no doubt that the invitation to participate in Dr. Kohn's research opened many doors, for which I am very grateful. The funding from the National Institute of Health has made my contributions to this project possible.

Professors T. Kendall Harden, Michael B. Jarstfer, and Qisheng Zhang each had a unique impact on my work. Professor Harden allowed me to rotate in his laboratory my second year in graduate school, providing a temporary home outside of the pharmacy school where I received excellent training in the field of receptor biology and pharmacology. Professor Jarstfer provided an impressive stream of scientific banter on the bus traveling to and from school as well as a listening ear to troubleshoot experimental approaches regarding this research. Professor Zhang provided papers, scientific advice, and access to resources at critical times during my research, which has allowed this work to build momentum.

Throughout my time at UNC I have enjoyed the support of friends and colleagues both within and outside the pharmacy school. For almost five years I have shared my time in the Professor Liu's lab with Dr. Alexander Valencia. His scientific training taught me on a day-to-day basis how valuable mentoring is in a graduate student's career. My success would not have been possible in his absence. In addition to his contributions to my research Dr. Valencia played the role of friend, career advisor, counselor, and occasionally, as comedian.

The data presented here would not have been possible without Dr. Ki Duk Park, Dr. Christophe Salome, Elise Salome, and Pierre Morieux from Dr. Kohn's Laboratory. The synthesis of the compounds by this team of chemists during the project has been

essential to my efforts. Dr. Ki Duk Park was especially generous with his time and reagents to help me throughout the course of the project. Onrapak Reamtong, Drs. Claire Eyers and Simon Gaskell at the University of Manchester also played integral roles in establishing a successful transatlantic scientific collaboration for the project and the data they generated provided an amazing wealth of information for me.

Biao Dong, Dongwook Kim, Jason Kim, Chad Petit, Laura Bonifacio, Joana Soares, Vijay Sekeran, Heather Bethea, Dr. Christine Conwell, and Dr. Moo Cho have all provided indispensible suggestions and reagents over five years.

Pierre Morieux has been a companion and colleague throughout the course of the project and perhaps has the greatest insight into my thoughts as a result of our shared collective experience. He provided motivation and set standards for others on the project and in the program. I wish him wonderful scientific success in the future.

Finally I wish to thank my parents, Alice and Jerry Cotten. Their unending love and support have given me the confidence to complete this journey. I feel extremely fortunate to have such amazing parents.

TABLE OF CONTENTS

Page

LIST OF TABLES

LIST OF FIGURES

LIST OF ABBREVIATIONS

$5HT_3$	5-hydroxytryptamine receptor 3
AB	affinity bait
ADNFLE	autosomal dominant nocturnal frontal lobe epilepsy
AMPA	α-amino-3-hydroxyl-5-methyl-4-isoxazole-propionate
ATP	adenosine triphosphate
ATP1A	Na-/K- transporting ATPase alpha 1
BFNC	benign familial neonatal convulsions
BSA	bovine serum albumin
CAMKII	calmodulin kinase II
CAR2	carbonic anhydrase II
CdK5	cyclin-dependent kinase 5
CNS	central nervous system
CR	chemical reporter
CRMP2	collapsin response mediator protein 2
DMSO	dimethyl sulfoxide
DPYSL2	dihydropyrimidinase like 2
EEG	electroencephalography
ELISA	enzyme linked immunosorbant assay
EMEA	European Medicines Agency
ER	endoplasmic reticulum
ESI	electron spray ionization

FAA	functionalized amino acid
FDA	Food and Drug Administration
FHM2	familial hemiplegic migraine type 2
GABA	gamma-aminobuytric acid
GEFS+	generalized epilepsy with febrile seizures plus
GSK-3β	glycogen synthase kinase 3-beta
HEK	human embryonic kidney
HIV	human immunodeficiency virus
HRP	horseradish peroxidase
ILAE	International League Against Epilepsy
i.p.	intraperitoneal
IS	infantile seizures
KD	ketogentic diet
LC	liquid chromatography
MALDI	matrix-assisted laser desorption ionization
MAP	mitogen activated protein
MES	maximal electroshock seizures
MS	mass spectrometry
NA	nicotinic acid
nACh	nicotinic acetylcholine receptor
NM	nicotinamide
NMDA	N-methyl-D-aspartic acid
NSF	N-ethylmaleimide-sensitive factor

PAL	photoaffinity labeling
p.o.	per oral
RISC	RNA induced silencing complex
RNAi	RNA interference
SAR	structure activity relationship
SDS-PAGE	sodium dodecyl sulfate polyacrylamide gel electrophoresis
SHM	sporadic hemiplegic migraine
siRNA	short interfering RNA
SMEI	severe myoclonic epilepsy of infancy
SNARE	soluble NSF attachment protein receptors
SPR	surface plasmon resonance
STXBP1	syntaxin binding protein 1
SV2A	synaptic vesicle association protein 2A
TAMRA	tetramethylrhodamine
TB	tuberculosis
TBTA	tris[(1-benzyl-1H-1,2,3-triazol-4-yl)methyl] amine
TCEP	tris(2-carboxyethyl)phosphine
UV	ultraviolet
VNS	vagus nerve stimulation

CHAPTER 1

FUNCTIONALIZED AMINO ACIDS, LACOSAMIDE, AND CANDIDATE ANTICONVULSANTS

1.1 Epilepsy and seizure disorders

Epilepsy is one the most common neurological disorder of the brain worldwide. It is estimated that 50 million people are affected, and epilepsy accounts for 1 % of the global burden of disease.[1] In developing countries, 80-90% of those affected receive no treatment at all. Much like a headache, epilepsy is simply a *symptom* of an underlying neurological dysfunction. The relationship between the causative disease and manifested symptoms is often complex and currently not fully understood. This in turn creates challenges for the proper treatment and control of epilepsy due to a myriad of potential causes.

The attempt to classify epileptic syndromes highlights the challenge in categorizing such variable conditions. Efforts in classification have used approaches to segregate epilepsies based on seizure origin, frequency, age, idiopathic versus symptomatic, and genetics. Despite these efforts, any current classification system fails to provide insight into choosing treatment, prognosis, or responsiveness to therapy. The International League Against Epilepsy (ILAE) developed the most commonly used classification system in 1981 based on clinically presented manifestations and electroencephalography (EEG) abnormalities (Table 1.1).[2] According to the ILAE classification system, seizures are divided into 3 main groups, namely, partial, generalized, and unclassifiable.

Partial seizures are defined as arising from a specific loci in the cortex of one hemisphere in the brain. These partial seizures are sub-divided into 3 groups: simple, complex, and secondary generalized. A simple partial seizure is defined as a seizure in which consciousness is not impaired with symptoms typically lasting only a few seconds. Complex partial seizures are associated with altered consciousness in the form of motionlessness or a total loss of consciousness. Secondary generalized seizures are initiated as partial seizures but evolve into one form of generalized seizures.

Generalized seizures are the second type of classification. These seizures are exclusively associated with impaired consciousness from the onset and when present, uncontrollable movement. EEG patterns during generalized seizures show strong synchronous and symmetrical activity over both hemispheres of the brain. Generalized seizures are subdivided into 6 categories: absence, myoclonic, clonic, tonic, tonic-clonic, and atonic. Absence seizures are characterized by of a loss of consciousness followed by cessation of motor activity. Myoclonic seizures are brief muscle contractions varying from a twitch to severe jerking with immediate recovery. Clonic seizures consist of rapid jerking with EEG showing fast activity. In contrast to clonic seizures, tonic episodes consist of sustained muscle contraction of the neck, face, eyes and limbs with EEG showing desynchronized fast activity. Tonic-clonic is the most well known form of epileptic seizure initiated by loss of consciousness followed by a tonic phase of muscle contraction preceding a clonic phase of convulsions. Atonic seizures are characterized by an abrupt loss of posture, resulting in a collapse to the ground accompanied by a short seizure.

Seizure profiles that do not match the typical clinical manifestation or EEG patterns are considered to belong in the unclassifiable category. These epileptic episodes may exhibit partial loss of consciousness, novel EEG patterns or altered tonic, atonic, and clonic phases. Up to one-third of seizures are considered unclassifiable using the 1981 ILAE system, a fact that highlights the need for improvement of seizure stratification through investigation into the underlying neurological dysfunction.

Table 1.1 International League Against Epilepsy Seizure Classification System

1981 International League Against Epilepsy Seizure Classification		
Partial	**Generalized**	**Unclassifiable**
Simple	Absence	
Complex	Myoclonic	
Secondary generalized	Clonic	
	Tonic	
	Tonic-clonic	
	Atonic	

1.1.1 Neurotransmission and epilepsy pathophysiology

The central nervous system (CNS) is comprised of highly specialized neuronal cells that transmit chemical and electrical signals and glial cells that support, protect, and to some extent communicate with neuronal cells.[3] Neurons are highly polarized cells consisting of a single, often branched projection termed axon, that transmits electrical signals in the form of action potentials to other target neurons and numerous projections from the cell body. These projections, termed dendrites, receive signals from adjacent cells and subsequently relay the electrical signal. Conversely, glial cells do not fire action potentials but instead communicate via gap junctions and calcium signaling. Glial cells encase neuronal cells in myelin to speed action potentials and form tripartite synapses with pre-synaptic and post-synaptic neuron terminals.[4]

Rapid communication between neurons is mediated by the release of excitatory amino acids glutamate and aspartate and the inhibitory amino acids γ-aminobutyric acid (GABA) and glycine. Other neurotransmitters such as serotonin, dopamine, norepinephrine, histamine, and acetylcholine, as well as neuropeptides such as oxytocin mediate their effects on longer time scales. The balance between inhibitory and excitatory signals are tightly regulated through numerous proteins that dynamically respond to changes in membrane potential, intracellular and extracellular concentrations of ions such sodium, potassium, and calcium, and the release of neurotransmitters.

Signal propagation between neurons in the brain relies on the depolarization and subsequent repolarization of membrane potential mediated by ion channels in the plasma membrane. Ion channels are classified as ligand-gated or voltage-gated based on what type of stimuli open and close the pore of the channel. Ligand-gated channels respond to the binding of small molecules such as ATP, zinc, and the neurotransmitters serotonin, GABA, and glycine, resulting in a conformational change that leads to channel opening.[5]

This class of receptors is sub-divided into 3 categories based on the channel structure. The Cys-loop receptor superfamily includes nicotinic acetylcholine (nACh), 5-hydroxytryptamine type 3 ($5HT_3$), glycine, γ-aminobutyric acid ($GABA_{A/C}$), and zinc activated receptors which form pentameric channels from assembled subunits at the plasma membrane.[6] The glutamate receptor family forms tetrameric channels and includes the N-methyl-D-aspartic acid (NMDA), α-amino-3-hydroxyl-5-methyl-4-isoxazole-propionate (AMPA), and kainate acid receptors. The final group is the P2X receptors that form trimeric channels. Upon binding to ATP, these channels open and allow Na^+ and Ca^{2+} ions to enter the cell.

Voltage-gated ion channels are the second class of receptors responsible for depolarization of neurons. These include voltage-gated sodium, potassium, and calcium channels. Voltage-gated ion channels sense changes in membrane potential that can occur after stimulation of ligand-gated ion channels resulting in an influx of ions at the post-synaptic terminal. Propagation of the signal occurs when the localized depolarization triggers activation of nearby channels resulting in a new influx of sodium ions followed by rapid inactivation of the channel and repolarization through an expulsion of potassium ions. This series of events generate an action potential that travels down the length of the axon ultimately reaching the presynaptic terminal.

To date, a variety of molecular, genetic, environmental, and developmental factors have been attributed to the development of seizure disorders. In developing countries, endemic diseases such as tuberculosis (TB), cysticerosis, human immunodeficiency virus (HIV), and metabolic conditions related to nutrition are common causes of seizures. In addition to these environmental and developmental factors, several single gene mutations have been described that result in "pure epilepsy," or seizures with unrelated neurological disorders which are thought to account for only 1-2% of all cases of epilepsy.[7]

Mutations have been found in genes encoding ligand and voltage gated channels such as the GABA receptor (*GABAR*), neuronal nicotinic acetylcholine receptor (*CHRN*), voltage-gated potassium channels (*KCNA1, KCNQ2, KCNQ3*), and voltage-gated sodium channels (*SCN1A, SCN1B*). Four mutations in the $GABA_A$ receptor channel have been linked with inherited forms of epilepsy.[8-12] Consequences of the mutations range from

alteration of channel gating, decreased current amplitude, loss of current enhancement by benzodiazepines, and lack of receptor transport to the plasma membrane.

Investigation of the genetics related to autosomal dominant nocturnal frontal lobe epilepsy (ADNFLE) identified at least 11 mutations in the nicotinic acetylcholine receptor.[13-22] Modifications are almost exclusively found in the α3 and β2 subunits that result in a gain of function from increased sensitivity to acetylcholine and increased Ca^{2+} permeability.[23] Benign Familial Neonatal Convulsions (BFNC), another rare form of inherited epilepsy, correlates with mutations in 2 voltage-gated potassium channels.[24] BFNC is characterized by frequent, but brief generalized or multifocal seizures starting the third day after birth and resolving spontaneously after several weeks to a month.

A variety of missense, frameshift, and splice mutations have been identified as giving rise to BFNC.[25-29] These genetic changes reduce current amplitude of the expressed channels affecting proper repolarization of the membrane after stimulation resulting in hyperexcitability.[24,30] The mutations do not affect channel selectivity, gating, or expression of wild-type subunits, suggesting the phenotype arises simply from haploinsufficiency.

The voltage-gate sodium channel type 1 alpha subunit is the most frequent clinically encountered gene mutation associated with epilepsy.[31] One-hundred-forty-two mutations have been characterized that give rise to a variety of seizure disorders including: Generalized Epilepsy with Febrile Seizures Plus (GEFS+), Severe Myoclonic Epilepsy of Infancy (SMEI), Borderline SMEI, and Infantile Spasms (IS). The compendium of mutations includes truncations, missense, mis-splicing, and deletions within the gene affecting a wide range of features including channel gating, proper

folding, expression, ion permeability, and recovery. Despite the large number of identified mutations, the correlation between genotype and phenotype is variable between conditions. *SCN1A* mutations only account for 5-10% of GEFS+ cases while mutations in this gene account for 50% for SMEI. This highlights the concept of a polygenic origin for epilepsy in which multiple alterations at the genetic level contribute to seizure susceptibility.

Cryptogenic epilepsy accounts for up to 40% of cases in which the underlying cause of the syndrome is unknown.[7] This exceeds single gene disorders, trauma, infection, congenital malformations, degenerative disorders, and idiopathic epilepsies that may be related to larger genetic syndromes. In these cases, conditions leading to neuron hyperexcitability may occur from a collection of unknown factors leading to seizure susceptibility that makes targeted treatment difficult.

1.1.2 Disease management

Currently there are four broad approaches to managing seizure disorders. The most common and often first choice for therapy are medications that seek to control seizure frequency and severity. In addition to medications, vagus nerve stimulation (VNS), surgery, and a ketogenic diet are used to control seizures. In VNS therapy, a small electrode is implanted in the neck that directly stimulates the vagus nerve, a major afferent fiber that relays sensory information to the brain. Regular pulses administered by an implanted generator send a 30 Hz signal to the nerve for 30 seconds followed by a 5 minute rest period.[32] A 12 year study of VNS therapy showed a 26% decrease in seizures after 1 year, 30% after 5 years, and 52% after 12 years.[33] The precise

mechanism for seizure reduction may involve increased levels of GABA, increased $GABA_A$ receptor density, or an increase in the release of norepinephrine.[34]

In cases in which seizure genesis is consistently localized at one focal point in the brain, surgery can provide an effective treatment.[35] Cortical resection of a small area of the brain is possible only if the affected area is not critical for speech, movement, memory or eyesight. Additionally, corpus collosotomy (severing the nerve bridge between the hemispheres of the brain) can block the spread of synchronous epileptic waves across lobes.

The third alternative to medication is a ketogenic diet (KD). Elimination of carbohydrates and substitution with fat in the patient's diet changes cellular metabolism from glycolysis to ketosis to generate energy.[36] In addition to the generation of ATP, the metabolism of fatty acids ultimately generates acetone, acetoacetic acid, and β-hydroxybutyric acid termed ketone bodies (Figure 1.1). In patients with pharmacoresistant epilepsy, greater than half show at least a 50% reduction in seizures when they follow a ketogenic diet.[37]

Several hypotheses have been proposed to explain the efficacy of a ketogenic diet in seizure reduction. First, KD has been shown to increase the number of mitochondria in the cell potentially resulting in increased energy available in the brain.[38] Glucose restriction from a KD may also activate ATP-sensitive potassium channels (K_{ATP}) leading to hyperpolarization of neurons as intracellular ATP concentrations fall thereby increasing the threshold for seizure development.[39]

It has been proposed that the change from glycolysis to ketosis may also result in a shift in biochemical pathways affecting amino acid metabolism that favor the

production of GABA. Anticonvulsant activity of the ketone bodies, acetone, acetoacetic acid, and β-hydroxybutyric that accumulate to millimolar concentrations in the blood during a KD, may mediate seizure suppression directly or indirectly. Increased levels of norepinephrine (NE) are also observed during a KD and are correlated with anticonvulsant activity. Norepinephrine agonists generally tend to have anticonvulsant activity and NE reuptake inhibitors decrease seizure susceptibility in epileptic prone rats.[40,41]

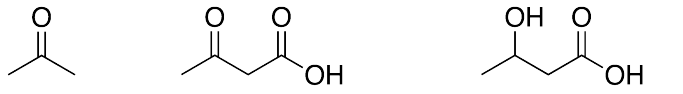

acetone acetocetic acid β-hydroxybutyric acid

Figure 1.1 The three ketone bodies generated during ketosis.

1.1.3 Current drugs and candidates for epilepsy treatment

Currently there are approximately 20 approved medications in the United States for the treatment of epilepsy, of which 15 are distinct chemical entities.[42] Carbamazepine, its 10-keto analog oxcarbazepine, and the prodrug for the active metabolite of oxcarbeazepine, eslicarbazepine acetate, all belong to a class of compounds that bind site II of voltage-gated sodium channels and inhibit their activity (Figure 1.2).[43] While all 3 compounds share a similar mode of action, differences resulting from metabolism result in increasingly superior therapeutic profiles for the second generation (oxcarbazepine) and third generation (eslicarbazepine acetate) agents.

Carbamazepine is metabolized in the liver to carbamazepine-10,11-epoxide which also exerts anticonvulsant activity but is associated with cytochrome P450 induction that results in various side effects and drug interactions. Oxacarbazepine bypasses epoxide

formation to the active metabolite 10,11-dihydro-10-hydroxycarbamazepine and shows decreased induction of cytochrome P450 enzymes.[44] Eslicarbazepine acetate, currently approved only in Europe, is a prodrug of (*S*)-licarbazepine, also know as 10,11-dihydro-10-dihydroxycarbamazepine, the major metabolite of oxacarbazepine. Metabolism of eslicarbazepine acetate generates a 95:5 *R* to *S* ratio *in vivo* that results in a 16% greater bioavailability compared to an equivalent dose of oxacarbazepine.[45]

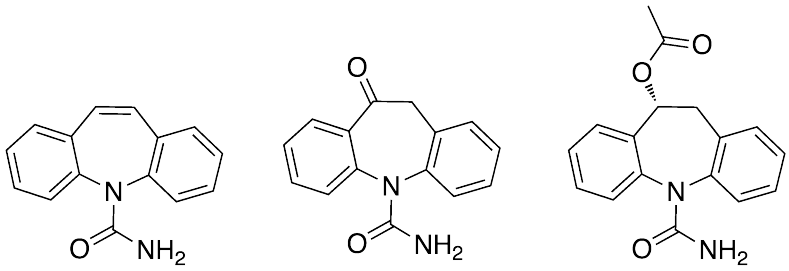

Figure 1.2 Structures of carbamazepine, oxcarbazepine and eslicarbazepine

Phenytoin inhibits activity of voltage-gated sodium channels through binding to the fast-inactivation state following depolarization.[46] The clinical use of phenytoin is complicated by a variety of drug interactions and wide variability rates of metabolism *in vivo*.[47] Despite these consequences, it is predicted that phenytoin is the most commonly prescribed anticonvulsant in the U.S.[48]

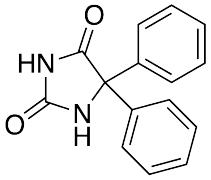
Phenytoin

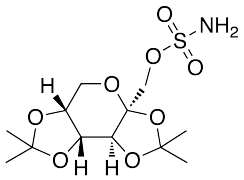
Topiramate

Topiramate is a sulfated fructose-derived monosaccharide originally developed as an antidiabetic drug. Multiple cellular activities are thought to be responsible for its anticonvulsant activity. In addition to inhibiting sodium currents through an interaction with

voltage-gated sodium channels, topiramate is a selective inhibitor for activity of the GluR5 kainate receptor, promotes GABA release, and enhances GABA induced Cl^- influx.[49-53] Topiramate likely acts indirectly on presyntapic GluR5 kainate receptors, evident through its slow-inactivation of the receptor. It is postulated that the drug binds the receptor in the unphosphorylated state acting as a negative allosteric regulator.[54]

Phenobarbital and the prodrug primidone have been used clinically for the treatment of epilepsy since 1912 and 1950, respectively.[55] Primidone is metabolized to phenobarbital and phenylethylmalonamide *in vivo*, but it remains unclear whether phenylethylmalonamide exerts activity independent of the major metabolite phenobarbital (Figure 1.3). The anticonvulsant property of phenobarbital is attributed to extending the duration of $GABA_A$ channel opening without affecting firing frequency.[56-58] This results in enhanced activation of $GABA_A$ receptors by suppressing epileptic transmissions and hyperpolarizing neurons.

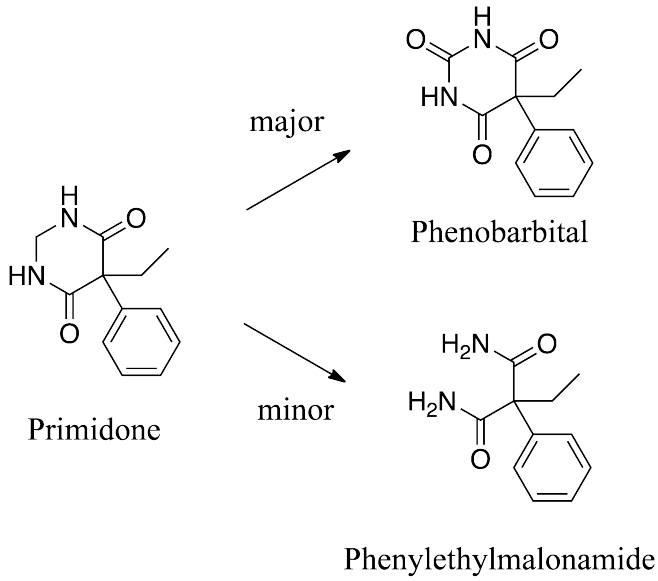

Figure 1.3 Routes of metabolism for primidone. The major route is metabolism to phenobarbital that exerts anticonvulsant action by affecting $GABA_A$ channel opening. It is unclear whether the minor metabolite phenylethylmalonamide has activity independent of phenobarbital.

Valproic acid was originally synthesized as an organic solvent in 1882 and was serendipitously discovered as an effective anticonvulsant while being used as a solvent for drug screening in the 1960s.[7] The simple branched chain fatty acid structure has been shown to possess numerous biological activities that contribute to its efficacy. Valproic acid has been shown to increase GABA concentrations in the brain via inhibition of succinic semialdehyde dehydrogenase that results in accumulation of succinic semialdehyde, an inhibitor of GABA transaminase.[59]

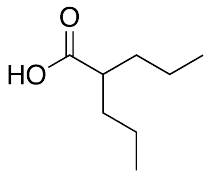

Valproic acid

Modulation of voltage-gated sodium channels by valproic acid resulting in inhibition of repetitive high frequency firing in neurons has also been observed.[60] Recent reports also show valproic acid is an inhibitor of protein kinase C epsilon (PKC-ε), brain microsomal long-chain fatty acyl-CoA synthetase, and histone deacetylase (HDAC).[61-63] Inhibition of

these enzymes has ramifications in cellular signaling related to neurite outgrowth, arachidonic acid metabolism, and modulation of gene expression at the genomic level.

Currently there are three approved therapies that are derivatives of the neurotransmitter GABA. Although gabapentin, pregabalin, and vigabatrin were all rationally designed to act as GABA analogs, none of them show activity as agonists at the GABA receptor (Figure 1.4). Gabapentin and pregabalin both bind the α2δ subunit of L-type Ca^{2+} channels preventing proper trafficking to the plasma membrane resulting in decrease functional receptors at the synpase.[64] Vigabatrin greatly elevates levels of GABA in the brain through inhibition of GABA transaminase, a GABA metabolizing enzyme present intracellularly in neurons and glial.[65] Administration of vigabatrin (50 mg/kg) results in elevated levels of GABA (> 1.8 mmol/kg) and a 50% decrease in seizure frequency.[66]

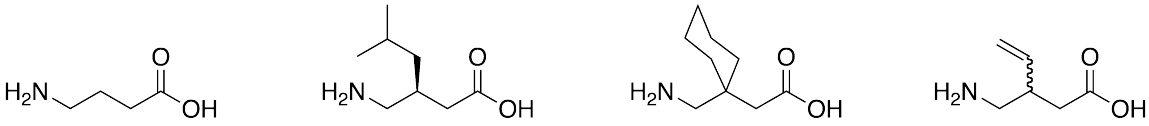

GABA Pregabalin Gabapentin Vigabatrin

Figure 1.4 GABA and anticonvulsant derivatives of GABA.

Clobazam and clonazepam belong to the family of benzodiazapine drugs that are commonly used for treatment of epilepsy and anxiety disorders. Both compounds are $GABA_A$ receptor agonists that bind similarly as other benzodiazepines (Figure 1.5). This results in enhanced chloride conductance of the channel by increasing the channel opening frequency thus hyperpolarizing the neuronal cells.[67]

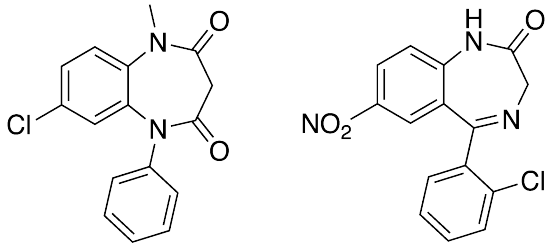

Clobazam Clonazepam

Figure 1.5 The benzodiazepine derivatives clobazam and clonazepam.

Ethosuximide is a succinimide drug specifically approved for the treatment of absence seizures. The compound selectively blocks voltage-gated T-type calcium channels in the thalamus, preventing bursts of absence seizure activity.[68] Originally developed in the 1950s as a member of a family of anticonvulsant compounds, ethosuximide is the only remaining succinimide drug still used for the treatment of epilepsy and is considered the first-line therapy for absence seizures.

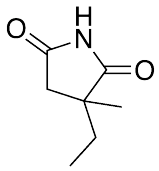

Ethosuximide

Approved in 2003, the sulphonamide derivative zonisamide inhibits T-type calcium channels, voltage-gated sodium channels, and binds to the benzodiazepine site on $GABA_A$ receptors. Clinically relevant concentrations of zonisamide have been shown to prevent Ca^{2+}-dependent low-threshold spikes from calcium channels as well as stabilize the fast-inactivated state of voltage-gated sodium channels.[69-71] Furthermore, zonisamide has been shown to block muscimol binding to the $GABA_A$ receptor and modulate its function similar to benzodiazepines.[72]

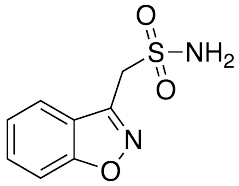

Zonisamide

Lamotrigine was first developed in the 1960s as an antifolate agent to mimic the properties of phenytoin and phenobarbital.[73] Despite these intentions, the compound

showed little activity with regard to folate biosynthesis but remarkable anticonvulsant activity.[74] Research showed that lamotrigine, similar to phenytoin, blocks sustained repetitive firing of voltage-gated sodium channels by stabilizing the fast-inactivated state.[75] Subsequent work has demonstrated a conserved motif responsible for binding to voltage-gated sodium channels and identified conserved interacting residues among lamotrigine, phenytoin, and carbamazepine.[46]

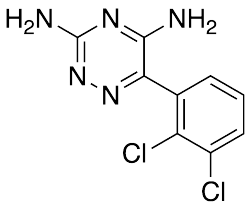

Lamotrigine

Tiagabine is a derivatized version of the GABA uptake inhibitor nipecotic acid (Figure 1.6). Attachment of the lipophilic side chain allows for permeability across the blood brain barrier not afforded by the parent compound.[76] As predicted, tiagabine elevates GABA levels through inhibition of GABA reuptake in the synaptic cleft by GABA transporters present on both neuronal and glial cells.[77] The results of lingering GABA retained in the synaptic cleft allows for sustained inhibitory signaling on the postsynaptic cell.

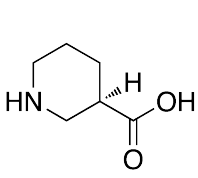

Nipecotic acid

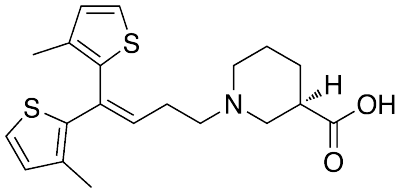

Tiagabine

Figure 1.6 The structures of nipecotic acid and tiagabine.

Felbamate was approved in 1993 in the United States for the treatment of partial seizures and Lennox-Gastuat Syndrome, a difficult form of childhood epilepsy appearing between the ages of 2 and 6. A year after approval, concerns over severe hepatic toxicity and the development of aplastic anemia greatly limited widespread adoption of

felbamate.[78] The drug inhibits voltage-gated sodium channels *in vitro*, specifically binds and blocks NR2B containing NMDA receptor complexes, and intracellularly mediates $GABA_A$ receptor activity.[79-83] Felbamate is unique in that it directly modulates both glutametergic and GABA signaling through two distinct mechanisms.

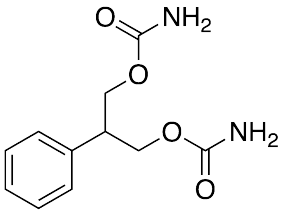

Felbamate

Levetiracetam and the current drug candidate brivaracetam belong to a family of chemically distinct pyrrolidine compounds that show anticonvulsant activity (Figure 1.7). Using photoaffinity labeling of crude synaptosomes, the synaptic vesicle protein SV2A was identified as the target for levetiracetam.[84] This glycoprotein found on the membranes of synaptic vesicles is implicated in the coordination of vesicle exocytosis and presynaptic neurotransmitter release. SV2A knockout mice develop severe seizures and die postnatally, and cultured cells lacking SV2 proteins accumulate extracellular calcium causing abnormal increases in neurotransmitter release.[85] Screening for SV2A ligands identified brivaracetam, a propyl derivative of levetiracetam, that shows a 10-fold higher affinity to SV2A than levetiracetam.[86] In mouse models for epilepsy brivaracetam is 6-12 times more potent than levetiracetam suggesting that binding to SV2A is correlated with anticonvulsant activity. Unlike levetiracetam, brivaracetam also inhibits sodium currents in cultured neurons.[87]

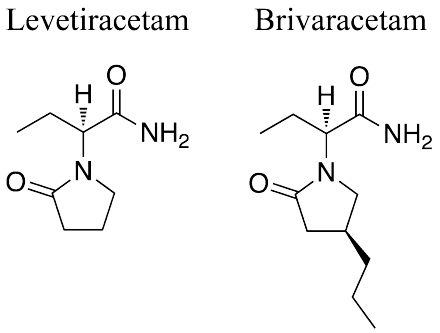

Figure 1.7 SV2A binding anticonvulsants levetiracetam and brivaracetam

Rufinamide is a recently approved anticonvulsant showing broad efficacy in a variety of epilepsy models.[88] Tentative evidence has been presented suggesting that rufinamide reduces sodium currents and limits repetitive firing of sodium channels *in vitro*.[89] It is currently approved as an adjunct therapy for seizures associated with Lennox-Gastaut syndrome.

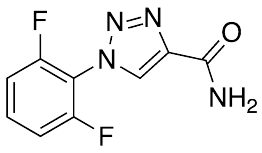

Rufinamide

Collectively, the anticonvulsants currently available for the treatment of epilepsy have varied modes of action. Traditional therapies target suppression of glutametergic signaling or enhance GABA signaling via modulation of ion channels. Emerging drugs have revealed new targets such as SV2A that could provide new approaches to seizure management. New activities are also being discovered for old therapies such as the histone deacetylase inhibitor activity of valproic acid that may provide new avenues to explore novel mechanisms of actions for older drugs.

1.2 Functionalized amino acids and (*R*)-lacosamide

(*R*)-Lacosamide, commercially marketed as Vimpat® by UCB group, was approved by the Food and Drug Administration in 2008 as an adjunctive therapy for the treatment

of partial-onset seizures in adults.[90] The development of (*R*)-lacosamide represents a collaboration among academia, government, and multiple pharmaceutical companies in both the United States and Europe. In addition to possessing anticonvulsant activity, the drug's effectiveness in models of neuropathic pain is also being evaluated.[91] Despite receiving market approval in both the U.S. and Europe, its mechanism of action remains unclear.

1.2.1 Rationale for the series

(*R*)-Lacosamide, (*R*)-N-benzyl-2-acetamido-3-methoxypropionamide, is a member of a class of compounds showing anticonvulsant activity called functionalized amino acids (FAAs). Structural requirements for the library of compounds were designed after careful observation of common motifs found in neurologically active agents such as hydantoins, piperazines, and benzodiazepines. It was recognized that drugs such as phenytoin and diazepam contain 3 basic units: (1) two nitrogen atoms separated by two carbons, (2) an oxygen atom off the ethylene bridge between the two nitrogens, and (3) an aromatic ring one carbon removed from one of the nitrogens.[92] The resulting criteria generate 3 amino acid-like scaffolds to derivatize (Figure 1.8).

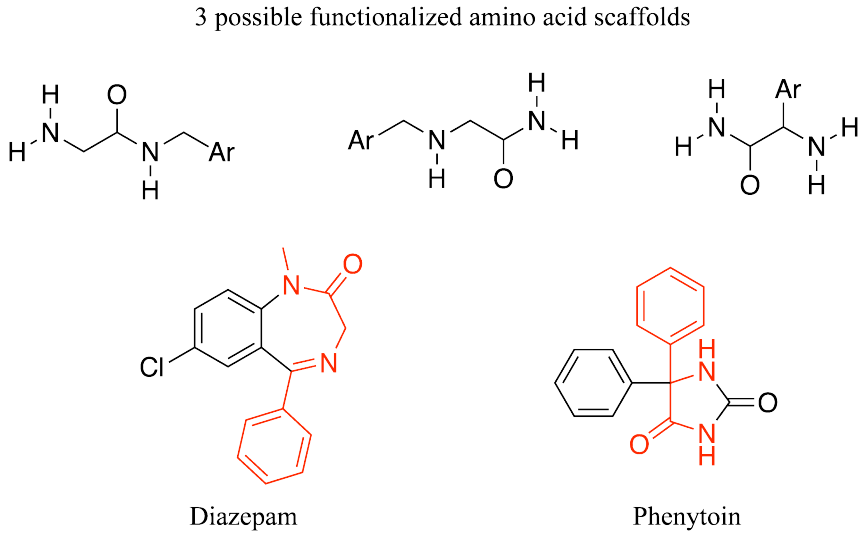

Figure 1.8 Functionalized amino acid scaffolds and neurologic agents. Three possible scaffolds can be generated with the criteria set forth for functionalized amino acids. Both diazepam and pheyntoin contain the basic units of FAAs (outlined in red).

Approximately 300 FAAs have been synthesized and evaluated in the Anticonvulsant Screening Program by Eli Lily and the National Institute for Neurological Disorders and Stroke over 25 years. Two acute seizure models have been used, the first being a maximal electroshock seizure (MES) model and the second a subcutaneous pentylenetetrazol seizure threshold (scMet) model. In the MES test, corneal electrodes are used to administer high frequency electrical stimulation inducing characteristic tonic hind limb extension that is thought to provide a good model for primary and secondary generalized tonic-clonic seizures.[93] The majority of the approved drugs for epilepsy show good protection in this model except for ethosuximide, tiagabaine, vigabatrin, and levetiracetam.

The generation of functionalized amino acids based on the first scaffold in Figure 1.8 structural requirements for anticonvulsant activity were interrogated by using a variety of substitutions on the acyl, central amino acid, and terminal amine units.

Extension of the acyl unit and either extension or contraction of the *N*-benzyl group leads to a sharp drop in anticonvulsant activity.[94] Substitutions on the central amino acid illustrated that the presence of a heteroatom one carbon away from the central backbone greatly enhances activity.[92,95-98] There was no trend observed in potency whether the substitution was electron rich or deficient.

The FAAs show an interesting trend when enantiomericly pure compounds are prepared containing substitutions off the central amino acid. Greater potency is consistently observed in the amino acid derivatives possessing the D-configuration (corresponding to the (*R*)-stereoisomer) than those with the L-configuration (corresponding to the (*S*)-stereoisomer), with at least a 10-fold loss of activity when the chiral center is inverted.[94] Small substitutions at the *para* and *meta* positions off the *N*-benyzl ring can be tolerated such as electron withdrawing groups like fluorine as well as an isothiocyanate group.[96,99]

1.2.2 (*R*)-Lacosamide

The realization that substitution of heteroatoms one atom away from the C(2) position enhanced anticonvulsant activity led to the synthesis of 12 derivatives of *N*-benzyl-2-acetamidopropionamide with 6 different heteroaromatic substitutients.[98] One compound, (*N*-benzyl-2-acetamido-3-methoxypropionamide), showed remarkable activity in mice i.p. and rat p.o. MES models with ED_{50}s of 4.5 mg/kg and 3.9 mg/kg, respectively (Figure 1.9). Consistent with other FAAs, the corresponding (*S*) enantiomer was substantially less active with ED_{50} 100-300 mg/kg and >30 mg/kg. These activities

were superior to phenytoin (mice i.p. ED_{50} ~6.5 mg/kg) and the eudismic ratio between *R* and *S* was greater than 22-fold.

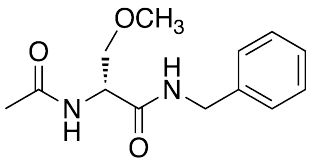

Mice i.p. ED_{50} = 4.8 mg/kg

Rat p.o. ED_{50} = 3.9 mg/kg

Figure 1.9 Structure and antiseizure activity of (*R*)-lacosamide

(*R*)-Lacosamide has been extensively evaluated in a variety of rodent models for epilepsy.[100] Initial screening in the MES test showed lacosamide effectively prevented seizures with ED_{50}s of 4.5 mg/kg and 3.9 mg/kg for mice i.p. and rat p.o. respectively. It was shown to be ineffective in protecting against seizures induced by the GABA antagonists pentylenetetrazol, bicuculline, and picrotoxin. In the 6 Hz psychomotor seizure test, (*R*)-lacosamide showed good activity with an ED_{50} of 10 mg/kg, exceeding the potency of new antiepileptic drugs such as levetiracetam. Activity in 6 Hz psychomotor seizure tests is often correlated with effectiveness in treating pharmacoresistant epilepsy.

Evaluation of (*R*)-lacosamide in the rat kindling model for complex partial seizures demonstrated excellent protection (ED_{50} 13.5 mg/kg). Cobalt induced status epilepticus showed that lacosamide exhibited moderate protection of seizure induction (ED_{50} 45.5 mg/kg) but activity was greatly potentiated by the addition of 0.75 mg/kg diazepam which lowers lacosamide's ED_{50} by 90% to 3.85 mg/kg.

Collectively, the results of the animal models illustrate that (*R*)-lacosamide has broad-spectrum anticonvulsant action that is markedly different from current therapies. Lacosamide's excellent activity both in the MES and 6 Hz seizure models is unqiue compared to most traditional anticonvulsants, and the potent synergy between lacosamide and diazepam in the cobalt induced status epilepticus model warrants further investigation.

1.2.3 Clinical progression and market approval

Phase I clinical trials of (*R*)-lacosamide were carried out by Harris FRC and subsequently picked up for phase II by Schwarz Pharma.[101] A total of 7 clinical trials were carried out by Schwarz Pharma and UCB group, evaluating (*R*)-lacosamide as an adjunct therapy for the treatment of partial-onset seizures.[102] Quantities of 200, 400, 600 mg per day were initially evaluated, but doses above 400 mg/day were discontinued due to slight risk of fainting.

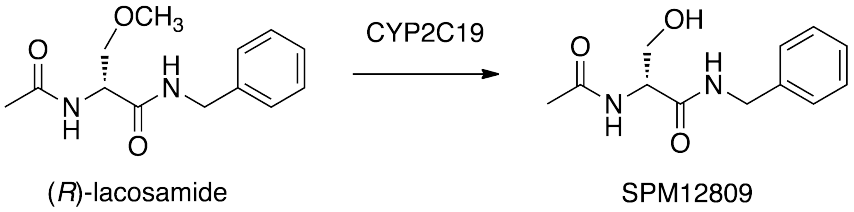

Figure 1.10 Major metabolism of (*R*)-lacosamide in humans.

The drug's half-life in humans is estimated at 11-16 hours. The major metabolite (SPM12809) observed *in vivo* results from the conversion of the methoxy group to a hydroxyl group that is excreted in the urine (Figure 1.10).[102] No significant conversion

between *R* or *S* is observed *in vivo*. The median reduction in seizure frequency relative from lacosamide was between 23-35% for 200 mg/day, 35-40% for 400 mg/day, and 35-40% for 600 mg/day with placebo groups between 8-20%. Patients enrolled were previously uncontrolled on 1-3 concomitant anticonvulsants and almost half had tried 7 or more currently marketed drugs.

The most common side effects of (*R*)-lacosamide include dizziness, headache, and nausea. There is an association with increased cardiac risk potentially associated with a prolonged PR interval (the time corresponding to the onset of atrial depolarization but preceding ventricular depolarization) and chest pain with several patient populations although no predicting factors such as age, race, or gender could be identified. As a result, the 600 mg/day dose was withdrawn from the new drug application. Lacosamide was approved in 2008 by the EMEA and FDA as an adjunct therapy for the treatment of partial-onset seizures in patients over 17. The drug is marketed as Vimpat® in both the United States and Europe. Currently there are several clinical trials completed that evaluated lacosamide as a treatment for fibromyalgia and diabetic neuropathy showing mixed results.

1.2.4 Potential mechanism of action

Despite gaining approval in both the U.S. and Europe for partial-onset seizures, a clear understanding of the mechanism of action responsible for (*R*)-lacosamide's efficacy has not been developed. To date, lacosamide has been implicated to interact with slow-inactivated voltage-gated sodium channels, dihydropyrimidinase-like protein 2 (DPYSL2) (also known as CRMP-2), and various isoforms of human carbonic

anhydrase.[103-106] Errington and coworkers initially showed (*R*)-lacosamide enhanced entry of sodium channels into the slow-inactivated state after sustained depolarization (10 or 30 s) in N1E-115 neuroblastoma cells.[105] Additionally, (*R*)-lacosamide induced hyperpolarization of slow-inactivation voltage curves but did not affect recovery of sodium channels out of the inactive state. No effect was seen when the (*S*)-enantiomer was used.

Sheets and coworkers used HEK293 cells expressing individual sodium channels or cultured dorsal root ganglion cells (DRGs) from adult male Sprague-Dawley rats to investigate the effect of (*R*)-lacosamide on the slow inactivation of individual receptor populations.[104] The effects of (*R*)-lacosamide, lidocaine, and carbamazepine on slow-inactivated sodium channels was investigated for $Na_v1.3$-, $Na_v1.7$-, and $Na_v1.8$-type channels. IC_{50} values for inhibition of slow-inactivated $Na_v1.3$-type channels for (*R*)-lacosamide, lidocaine, and carbamazepine were 415 μM, 284 μM, and 900 μM, respectively. Inhibition of slow-inactivated $Na_v1.7$ currents was calculated to be 182 μM, 44 μM, and 406 μM for (*R*)-lacosamide, lidocaine, and carbamazepine. (*R*)-Lacosamide also exhibited a similar ability to inhibit inactivated $Na_v1.8$ type channels in DRG cells. The inhibition values of (*R*)-lacosamide for the resting state of the sodium channels were 100-257 larger compared to the inactivated channel state.

The results show that (*R*)-lacosamide can selectively discriminate between slow-inactivated versus fast-inactivated sodium channels to a greater extent than lidocaine and carbamazepine. This finding has implications in selectively blocking neurons that are chronically depolarized in neurological disorders such as epilepsy and neuropathic pain.

Recently a systematic screening of newer anticonvulsants against inhibition of carbonic anhydrase *in vitro* revealed (*R*)-lacosamide shows potent to moderate activity against a variety of human isoforms.[106] Inhibition constants ranged from 331 nM (CAII) to 4.56 μM (CAXII). X-ray crystallography identified that (*R*)-lacosamide binds to the coumarin binding region on the CAII enzyme, a region distal to the site occupied by traditional anticonvulsants such as sulfonamides and sulfamates.

It has also been implicated that (*R*)-lacosamide interacts with DPYSL2, a protein involved in growth cone guidance and neuronal outgrowth.[103] No evidence for direct binding has been reported, but recently we reported that endogenous and recombinant DPYSL2 can be labeled *in vitro* by affinity bait containing derivatives of (*R*)-lacosamide.[107] DPYSL2 and its potential role in epilepsy and the interaction with (*R*)-lacosamide are discussed in detail in chapter 4.

1.3 Concluding remarks

The discovery, development, and approval of (*R*)-lacosamide are the result of collaboration among academia, government, and industry. The anticonvulsant profile of (*R*)-lacosamide shows the compound has broad-spectrum anticonvulsant activity with a potentially complex network of interactions that contribute to its efficacy. Investigating the full spectrum of proteins that interact with (*R*)-lacosamide is crucial to understand how its effects are exerted in models for both epilepsy and potentially neuropathic pain, as well as the development of the next generation anticonvulsant derivatives.

CHAPTER 2

PROFILING SMALL MOLECULE PROTEIN INTERACTIONS AND DRUG TARGET DISCOVERY: CONVENTIONAL AND EMERGING STRATEGIES

2.1 Introduction

Chapter 1 discussed the pharmacological complexity of currently approved anticonvulsants in the context of their numerous interacting proteins and subsequent effects on the central nervous system. New applications for simple molecules such as valproic acid that have been approved for decades continue to emerge in the literature.[63] Such diverse pharmacology highlights the challenges of elucidating a clear mode of action when target proteins are unknown.

In the case of (*R*)-lacosamide, discovery in an animal model circumvented insight into molecular actions with specific proteins in the brain. This lack of drug-target information can be common in pharmaceutical development, especially with neurological agents. Because many neurological disorders are multifactorial, the benchmark for efficacy is often beneficial outcomes, rather than targeted protein interactions. A variety of approaches have been developed that seek to identify proteins that interact with small molecules in a meaningful way and contribute to their efficacy.

2.2 Direct identification

The most commonly used approach in small molecule-target identification involves biochemical purification of interacting proteins from complex cell lysates or tissues coupled with some form of mass spectrometry. Efficient capture usually requires structural modification of the target compound for immobilization on a solid surface or enhancement of binding affinity through the introduction of reactive groups. Both approaches have been used as a means to identify drug targets.

2.2.1 Immobilized affinity chromatography

Isolation and enrichment of target proteins using immobilized ligands dominate efforts in drug-target identification. Using this approach, drug derivatives are synthesized to introduce linkers at a site that allows for chemical modification without disrupting biological activity. Such linkers can facilitate the coupling of the drug derivatives via assorted chemistry to various types of resins. Conjugation of the drug linker to the resin allows for display of the ligand on the solid surface that can then bind to target proteins within complex protein mixtures. Numerous examples illustrate the utility of this approach.

Using this methodology, target proteins for the diarylquinoline R207910 (TMC207), a candidate for the treatment of tuberculosis, were recently identified.[108] Immobilization of an amine functionalized R207910 analog on sepharose resin captured the α and β subunits of ATP synthase from *M. smegmatis* membrane lysate. Interestingly, analysis of binding using BIAcore of the recombinant α and β subunits to immobilized R207910 showed no direct interaction. Only subunit γ showed binding to

the diarylquinoline with K_d value of 500 nM. The authors suggest that the hydrophobic nature of the γ subunit prevented 2D electrophoresis prior to mass spectrometry, thereby inhibiting peptide identification.

The EGFR tyrosine kinase inhibitor gefitinib (Iressa) is approved for the treatment of non-small cell lung cancer and as a third line chemotherapuetic. Originally developed specifically to target EGFR tyrosine kinase, affinity chromatography of sepharose-conjugated gefitinib identified 25 additional kinases with low micro to nanomolar IC_{50} values for the compound.[109] The proteomic screen did not identify related receptor tyrosine kinases, which is consistent with the *in vitro* selectivity of gefitinib.

Numerous other protein targets have been identified for small molecules and drug candidates using affinity chromatography. Schreiber and coworkers identified the protein target of the macrolide immunosuppressant FK506 (Tacrolimus) as cis-trans peptidyl-proplyl isomerase and the antiproliferative cyclotetrapeptide trapoxin as histone deactylase 1 (HDAC-1) using a similar approach.[110,111]

2.2.2 Photocrosslinking

A second method for direct identification of protein targets uses photoreactive groups that upon light activation form covalent adducts with adjacent residues on the target proteins. A variety of photoreactive groups can be incorporated in the biologically active compound. Aryl azides, benzophenones, and diazirines are frequently used as photoaffinity probes for crosslinking small molecules and proteins (Figure 2.1).[112] Aryl azides can be activated under mild conditions (>300 nm) but maximum absorption is

characterized at 280 nm, which is generally considered undesirable due to protein degradation.

The major route after excitation results in ring expansion, then subsequent attack by a local nucleophile.[113] Benzophenones are activated at ~350 nm generating a reactive diradical which can form C-C bonds with unreactive C-H bonds on target proteins. Diazirines, specifically 3-(trifluoromethyl)diazirines, have been adopted as useful photoaffinity reagents for the selective labeling of proteins.[114] Activation at 360 nm results in the formation of highly reactive but short-lived carbenes that form covalent adducts with adjacent residues.

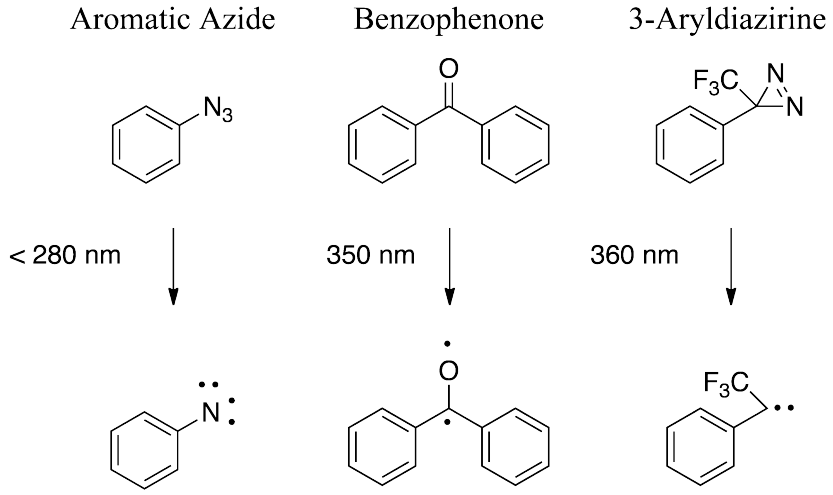

Figure 2.1 Common photoaffinity probes for drug-protein labeling (adapted from ref. [113])

Photoaffinity labeling (PAL) with various probes has been used extensively to identify target proteins, discover binding sites, and understand binding kinetics for drug-receptor complexes.[115] Fuks and coworkers identified the synaptic vesicle protein 2 (SV2A) as the binding site for the levetiracetam in rat brain membranes using a radiolabeled analog containing an aromatic azide.[116,117] Validation showed levetiracetam

and the photoaffinity probe exclusively bound to SV2A with no appreciable binding to SV2B or SV2C. All other anticonvulsants tested showed no binding to SV2A.

Similarly, using a leucine analog containing a diazirine moiety incorporated into the antifungal cyclodespeptide HUN-7293, the integral ER membrane protein Sec61α was identified as a potential target.[118] The Sec61 complex is a transmembrane channel responsible for regulating the translocation of newly synthesized proteins into the ER membrane. HUN-7293 was previously reported to block translocation of vascular cell adhesion molecule (VCAM) expression and the identification of Sec61α provided a clear mechanism for its cellular activity. The utility and specificity achievable with photoaffinity probes provide an alternative to direct affinity chromatography where binding may be conditional or weak.

2.2.3 Electrophillic labeling

In addition to light-activated probes as affinity labeling of target proteins, electrophilic probes targeting nucleophiles have been adopted for labeling strategies. This approach has traditionally been applied in two ways. The first major application seeks to identify specific amino acid residues involved in binding between small molecules and target proteins. The second application of electrophilic probes screens the proteome for small-molecule protein interactions based on selectivity toward various catalytically reactive nucleophiles.

Traditionally, derivitized ligands for G-protein coupled receptors and ion channels have incorporated electrophilic moieties such as isothiocyanates and aldehydes to increase binding affinity. Ligands for the opioid (μ, δ, and κ), NMDA, $GABA_A$,

cannabinoid, α-adrenergic, dopamine receptors and GABA chloride channels have been proven to be effective in forming covalent modifications with target proteins in the brain fractions *in vitro* and *in vivo*.[119-129] For adduction to occur between the protein and chemical probe, an adjacent nucleophile such as lysine or cysteine must be present in order to form the covalent interaction. The extent of labeling can be titrated by various controllable factors such as pH, temperature, and reaction time that control both reactivity and selectivity.

The second application of electrophilic probes profiles protein reactivity. This approach, often termed activity-based proteomics, targets specific enzyme super families sharing catalytic activity using various structural scaffolds paired with nucleophilic reactive units.[130] Chemical probes targeting serine proteases, serine hydrolases, cysteine proteases, phosphatases, carbon electrophiles, and kinases have been used to identify numerous proteins via mass spectrometry.[131-135]

The results provide insight into metabolic activation of proteins previously not known to be involved in disease states such as cancer. Probing using a sulfonate ester library identified γ–glutathione-S-transferase to be highly activated in breast cancer cells.[136] Activity profiling for inhibitors of cysteine proteases in *Plasmodium falciparum* identified a specific inhibitor falcipain-1, a protease active during the invasive stage of the malaria-causing parasite.[137] The functional profiling against protease activity coupled with the chemical screen provided a new drug target for the treatment of malaria and a lead structure for the design of new therapeutics.

2.2.4 Limitations of affinity chromatography and affinity labeling

Despite their effectiveness in identifying targets for approved drugs and drug-candidates there are several drawbacks to direct identification with affinity chromatography and photoaffinity labeling. The introduction of bulky tags required for immobilization may diminish or abolish drug binding to its cognate proteins. The use of a biologically inactive compound may therefore prohibit the proper identification of target proteins. Additionally, the drug scaffold may not be amenable to easy introduction of linkers regions for immobilization. Lack of SAR information regarding critical regions on the chemical structure necessary for biological activity further complicates the process. The successful creation of an immobilized small molecule requires both the availability of a synthetic route and the retention of biological activity (binding) despite structural modification.

Another drawback to affinity chromatography is the potential for proteins to interact non-specifically with the solid surface used to display the small molecule. This can greatly decrease the chance of proper identification if the target protein is in low abundance. Non-specifically bound proteins on the resin often overwhelm mass spectrometry signals thereby masking rare peptide sequences. Using ampicillin as a model system for affinity chromatography, Rechenberg and coworkers evaluated the ability of various resins to capture ampicillin-binding proteins from *E. coli*.[138] Agarose, acrylamide, and magnetic beads were amine coupled with ampicillin followed by incubation with *E. coli* lysate. After extensive washing, enriched proteins were identified with mass spectrometry via on bead digestion followed by LC-MS/MS. Although all resins correctly identified a variety β-lactamase isoforms, their relative ratios between

resins were not equal. The acrylamide resin showed very high enrichment of non-specifically bound ribosomal proteins that were much lower in the magnetic and agarose bead samples. This study highlights the potential for biased identification of proteins based on the type of solid surface used for immobilization.

Photoaffinity labeling for protein target identification possesses similar limitations. Incorporation of the photolabile moiety may decrease affinity between the small molecule and protein target(s). If an aromatic group is present on the small molecule then it may be possible to introduce an azide of diazirine without substantial loss of binding. If no aromatic ring is present, however, incorporation of the large benzophenone, aromatic azide, or aromatic diazirine units into the scaffold could significantly alter the activity. Efficient labeling of target proteins versus non-specific proteins must be carefully titrated based on intensity of the light used for activation, reaction time and temperature, and the amount of target protein present. Finally, the presence of appropriate nucleophiles inside the binding pocket of the target protein may be required with some photo probes for successful adduction.

2.3 Indirect identification

The second strategy for drug-target identification uses indirect methods to deconvolute biochemical pathways altered by drug treatment. Changes at the RNA, protein, and metabolite level can be monitored in the presence or absence of drugs to identify specific pathways or genes that respond to drug treatment. More recently, phenotypic assays using model organisms has allowed for rapid screening of the responsiveness of known genotypic knockouts following drug treatment. All methods

generate large volumes of data making analysis labor-intensive, yet can provide meaningful insight into a drug's mode of action.

2.3.1 Gene expression profiling

One frequent approach to validate drug targets is to monitor changes in gene expression profiles using microarray analysis. Whole genome chips for both human and yeast provide a means to observe global changes in gene expression as a result of drug treatment. Comparison with untreated samples can reveal which signaling pathways the target compound alters. This approach was used to discriminate between the modes of action of the immunosuppressant drugs cyclosporin and FK506.[139] RNA from wild-type yeast strains treated with FK506 and cyclosporin exhibited a specific gene expression profile relative to untreated samples. It was found that thirty-six genes changed expression at least 2 fold upon drug treatment.

Both compounds have been shown to inhibit the calcineurin-signaling pathway, and mutant analysis of a calcineurin deletion strain showed strong correlation with the genotypic profiles of FK506 and cyclosporin. Because pharmacological inhibition of the calcineurin signaling might occur at multiple steps, individual protein targets in the pathway were analyzed in the presence or absence of compounds. Deletion stains of the most abundant immunophilins in yeast (*CPH1* and *FPR1*) upstream of calcineurin were profiled to discriminate individual target proteins. In the FPR1 deletion mutant, FK506 was not able to generate a gene expression profile similar to that in the wild type or the calcineurin deletion, suggesting that *FPR1* is the target for FK506. Conversely, when the

CPH1 deletion mutant was used, cyclosporin did not produce the signature expression profile.

Taken together, this illustrates that FK506 targets FPR1, while cyclosporin targets CPH1. In addition to identifying the proteins responsible for calcineurin inhibition, several other genes showed induction by treatment with FK506. These proteins, implicated in drug-resistance, illustrate that gene expression profiling for drug-target discovery can provide insight into both primary and off-target effects.

Gene expression profiling has also been used for generating models to predict drug action. Gunther and coworkers generated microarray profiles from primary human neuronal precursor cells treated with 36 neurological agents including antidepressants, antipsychotics, and opiates.[119] Using the compendium of drug-efficacy profiles, computational models were built with the objective of predicting the class of drug (antidepressant, antipsychotics, or opiate) to which an "unknown" drug may belong. Each class of drug contained chemically and functionally diverse compounds. The models were able to assign the correct drug class with more than 80% accuracy based upon the expression profile of unknown samples. Even though the biochemical class could be determined, specific proteins could not be definitively assigned. Comparisons with subclasses of chemically or mechanistically similar compounds could further detail the mechanism of action.

2.3.2 RNAi

RNA interference (RNAi) has been adopted as another powerful tool in drug discovery that allows for silencing gene expression of specific genes and observation of

knock-down phenotypes at both the cellular and organism levels.[140] This phenomenon involves the delivery of 21-23 long double stranded RNA sequences to cells that are complementary to target messenger RNA. Degradation of the mRNA is induced by activation of the RNA induced silencing complex (RISC) whose endonuclease activity cleaves the target mRNA strand, ideally resulting in a decrease of protein expression. This method has been used generally to validate known drug targets by evaluating the drug efficacy in the knock-down phenotype. Recent efforts have attempted to couple RNAi platforms with chemical screens to identify new drug targets. This approach does not provide a means, however, to deorphanize drugs with unknown binding partners.

2.3.3 Metabolomics

Recently, advances in mass spectrometry have enabled the development of platforms that simultaneously detect and quantify hundreds of metabolites as a means to understand changes in cellular biochemistry. This technology has been applied to drug-target discovery and is proving to be a useful new tool in drug development. Using this approach, Watson and coworkers identified the protein target of the GMX1777, a prodrug in Phase I clinical trials for the treatment of cancer.[141] A total of 88 metabolites were measured in IM-9 cells after 6 h treatment with 30 nM GMX1777. Comparative biochemical profiles between treated and untreated cells revealed that NAD levels dropped 1.5 fold after drug treatment. To understand which branch of the NAD biosynthetic pathway was specifically targeted, [^{14}C] labeled substrates of nicotinamide (NM) and nicotinic acid (NA), enzymes feeding into NAD biosynthesis, were used to measure the generation of [^{14}C]NAD. Analysis revealed that phosphoribosyltransferase

(NAMPT), the enzyme upstream of the NM branch of the NAD pathway, is specifically targeted by the drug.

2.4 Limitations of indirect target identification approaches

Despite success using indirect methods for drug target identification, these approaches have several drawbacks. First, most indirect methods generate large amounts of data that require extensive analysis. Gene expression profiling and metabolomics can be computationally intensive, and identification of candidate targets requires careful experimental design with proper controls. Phenotypic based methods such as RNAi generally are not amenable to drug target identification unless comprehensive screening with a large pool of potential targets is performed. For all approaches, the results need to be validated using a more direct method to confirm relevance of the putative target(s).

2.5 Concluding remarks

Several methods have been described for identifying unknown drug targets. Direct methods aim at physically enriching relevant proteins from complex mixtures through the use of reactive groups and immobilized ligands. Indirect methods look for changes in biochemistry measured by gene expression profiling, cellular metabolites, or phenotypic screens to identity signaling pathways affected by the drug. These approaches have a variety of drawbacks and biases, including non-specific interactions with solid surfaces, proper display of immobilized ligands, and intensive data analysis. Novel methods are therefore needed that minimize these drawbacks while utilizing their advantages.

CHAPTER 3

CHEMICAL BIOLOGY APPROACHES FOR (*R*)-LACOSAMIDE DRUG TARGET DISCOVERY

3.1 Introduction

Sixty percent of the currently marketed anticonvulsants have a complex or unclear mechanism of action. This fact highlights the need for new approaches in drug target discovery, particularly for neurological agents. Conventional technologies for direct identification of protein targets can be biased for stable or abundant proteins and do not account for protein complexes present *in vivo*. Indirect methods such as microarray analysis tend to generate more questions regarding modes of action from the sheer volume of data generated rather than providing biochemical insight. Therefore, improvement in approaches for drug target discovery are needed that allow for selective and specific investigation of protein-drug interactions.

Immobilization of small molecules on a solid surface for affinity purification of targets can potentially limit the ability of target proteins to correctly recognize the small molecule as well as introduce surfaces for non-specific interactions. Liberation of the molecule from the solid surface allows greater conformational flexibility for both the small molecule and protein that can greatly enhance the affinity between the two interacting partners. The ligand also potentially has access to binding pockets in intact protein complexes that may not be accessible when immobilized on a solid surface. Recent advances in chemical biology have permitted the capture and detection of protein-

ligand complexes using the Cu(I)-catalyzed Huisgen 1,3 cycloaddition between an azide and alkyne to form a triazole as a tool for drug discovery (Figure 3.1).[142,143] This reaction, also known as "click chemistry," is a superior tool for drug-target discovery because of the chemoselectivity between the azide and alkyne, mild reaction conditions in water and ambient temperature, and the small functional groups involved.[144] The azide and alkyne functional units have been installed on intracellular constituents such as proteins, lipids, and glycans for *in vivo* capture and detection of a variety of biomolecules.[145-148] These bioorthogonal ligations have also been exploited to target and detect various protein classes in a proteome. Alkynes have been incorporated into chemical probes for histone deaceytlases, serine hydrolases, and other proteases to map enzyme activity based on their substrate specificity.[131-133] In addition to this activity-based proteomics, affinity-based proteomics seeks to profile binding partners for small molecules in complex protein mixtures. Probes for the cancer biomarker galectin-3 and an irreversible inhibitor of RSK1/RSK2 have been evaluated using this chemoselective ligation method.[146,149]

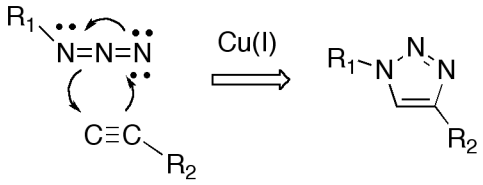

Figure 3.1 The click chemistry reaction. Cu(I) promotes the formation of a triazole ring under mild aqueous conditions.

The mutually exclusive reactivity between the azide and alkyne circumvents the need to immobilize the small molecule drug/candidate, thereby allowing specific capture of the drug-protein complex after binding has occurred unhindered in solution. Using

this approach we applied the click chemistry reaction to identify potential protein targets of (*R*)-lacosamide.

3.2 Results and Discussion

3.2.1 Rationale and design strategy

Like other anticonvulsants, (*R*)-lacosamide's efficacy may result from multiple specific protein interactions that affect multiple pathways involved in epilepsy and neuropathic pain. Previous efforts failed to observe any appreciable binding after screening a variety of cloned receptors, suggesting that (*R*)-lacosamide may exhibit weak or modest binding to its endogenous protein target(s).[150] Based on the simple structure of (*R*)-lacosamide, we suspect that the potential for identifying strong affinity interactions may be low. Therefore a method to stabilize the interaction between (*R)*-lacosamide and its protein targets is needed to enhance the chance of target identification.

To address this need, we designed a series of drug analogs that allow for a two-step process of labeling and capture of (*R*)-lacosamide binding proteins (Figure 3.2). Labeling of proteins is enhanced by the addition of a moderately reactive group, termed affinity bait (AB), allowing for the formation of irreversible covalent drug-protein adducts under selective controllable conditions. This affinity bait assists in labeling under conditions where binding is modest or protein abundance is low. Post-labeling, the drug-protein adducts are detected by utilizing the paired azide and alkyne functional units, termed chemical reporters (CR), installed on the drug analogs and probes used for detection or purification.

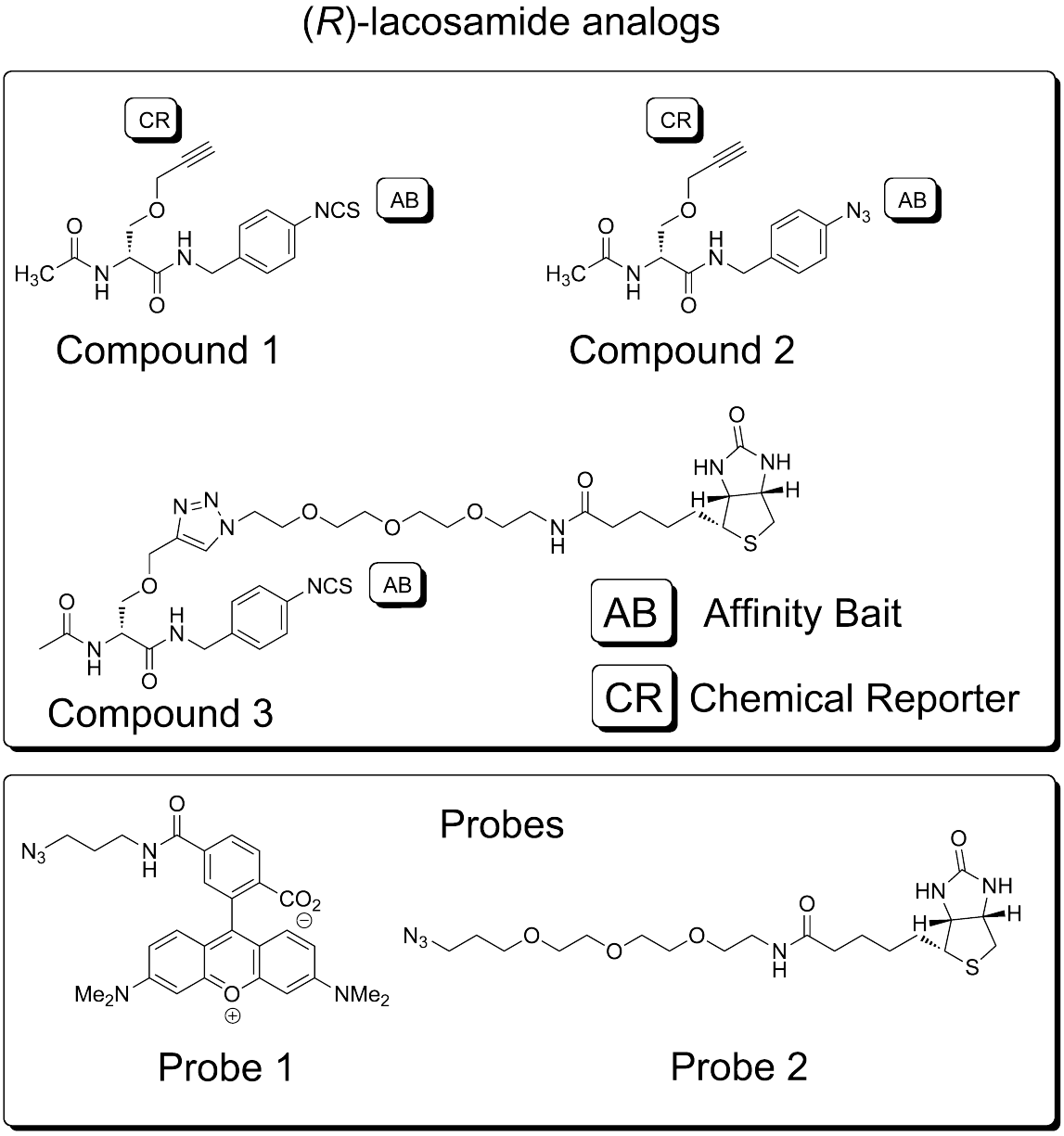

Figure 3.2 Chemical structures of (*R*)-lacosamide analogs and probes for detection and purification of target proteins. Two derivatives of lacosamide were synthesized containing reactive affinity bait groups to form covalent adducts with target proteins and chemical reporter groups to detect and purify the drug-protein adducts using click chemistry. Compound 3 contains a reactive isothiocyanate and a biotin group that can be used directly to label and purify proteins from mouse brain lysate. Two probes were synthesized, one containing a fluorescent TAMRA group and the other a biotin group, to detect and purify the labeled proteins.

Compound 1 contains an isothiocyanate at the 4'-benzylamide that is expected to react with lysines or cysteines to form thioureas and dithiocarbamates, respectively. Compound 2 contains an aromatic azide at the 4'-benzylamide that upon exposure to UV light (312 nm) undergoes either ring expansion followed by nucleophilic attack or C-H insertion with target proteins. Placement of the AB and CR groups within the lacosamide scaffold was selected based on previous pharmacologic data for other lacosamide derivatives that had been extensively examined in the Kohn laboratory.[151-154] Perturbation of the (*R*)-lacosamide scaffold at the meta-position for the *N*-benzyl amide and the *N*-acetamido group results in modest loss of pharmacological activity.[153] To minimize loss of activity from addition of the chemical moieties, the AB group was installed at the para position of the *N*-benzyl amide ring and the CR group at the (C)2 side chain, both of which can tolerate modification while retaining modest activity *in vivo* as shown previously.

3.2.2 Affinity bait (AB) reactivity

The electrophilic isothiocyanate affinity bait in compound 1 provides a pH- and temperature-dependent probe for potential nucleophiles present inside the protein binding pocket (Figure 3.3). Presumably the moderately basic ε-amine present on lysine residues is protonated at a neutral pH making it partially reactive towards electrophilic adduction. At pH 8.0 and above, the deprotonation of the terminal ammonium group greatly increases reactivity leading to increased adduction. Raising the pH or temperature and increasing the labeling time allows for control over the extent of modification. Lowering the pH below 8.0 results in protonation of the terminal amines present on lysines,

reducing their reactivity toward the isothiocyanate affinity bait. Improving reactivity by raising the pH, however, does make the affinity bait more susceptible to inactivation through hydolysis in the presence of water.

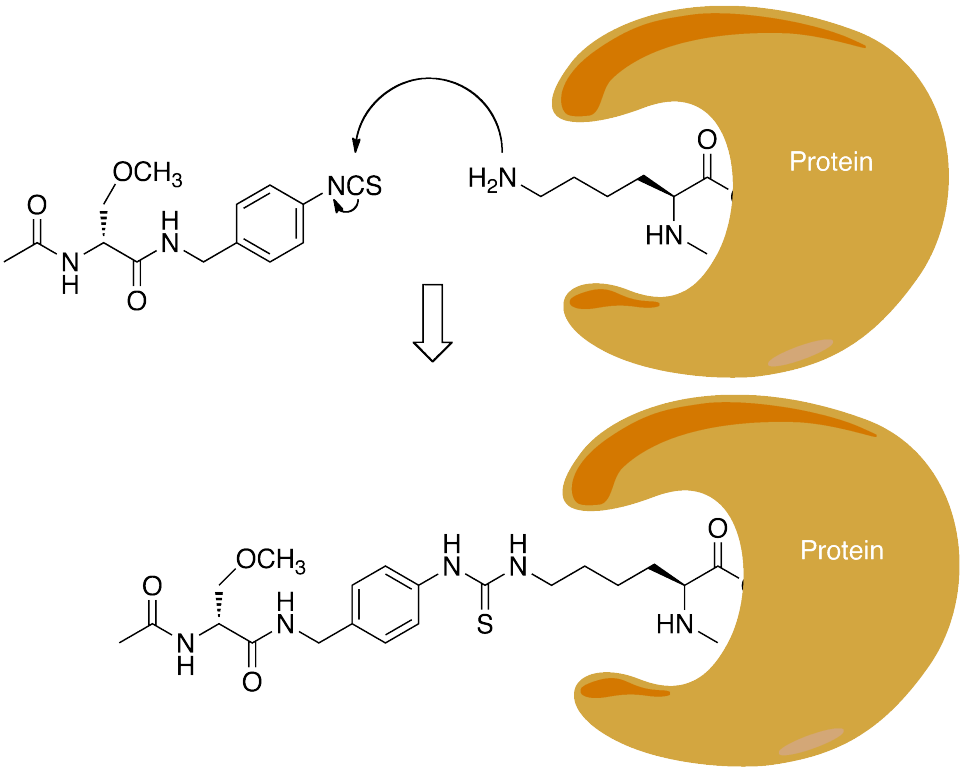

Figure 3.3 Reactivity of an (*R*)-lacosamide analog containing an AB (isothiocyanate) group with lysine residues in the drug-binding pocket on target proteins. Incubation of the affinity bait containing drug analog is expected to react with nucleophilic lysine residues to form a stable thiourea creating the drug-protein adduct.

To capture those protein targets lacking nucleophiles in the binding pocket, we designed an aromatic azide photoaffinity bait (compound 2). Activation of the affinity bait by excitation with UV light (312 nm) can generate adducts through three mechanisms (Figure 3.4).

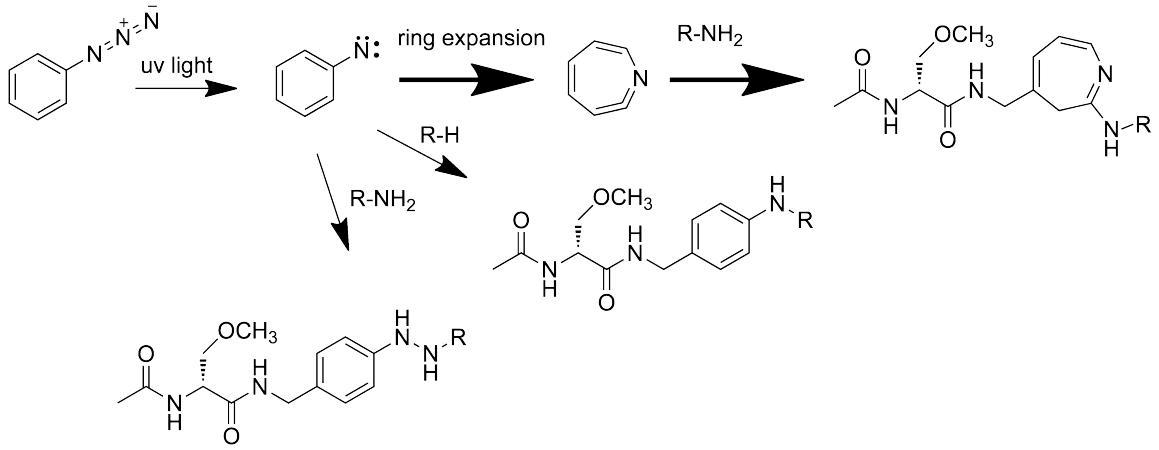

Figure 3.4 The three routes of adduction by activation of compound 2 with UV light. Activation by UV light generates a reactive nitrene that favorably undergoes ring expansion followed by nuceophilic attack from adjacent residues.

Activation of the aromatic azide can occur under relatively mild conditions (> 300 nm) but absorption is characterized by λ_{max} < 280 nm. Upon exposure to UV light, formation of the reactive nitrene can undergo insertion into C-H or N-H bonds. The most favored pathway, however, is considered ring expansion followed by rapid reaction with adjacent nucleophiles on binding proteins. The half-life for the nitrene intermediate is estimated between 0.1-5 msec during which the intermediate can undergo ring expansion or react with O_2 forming less reactive species. The reaction time can be adjusted according to the extent of labeling desired, however, protein degradation may result from long crosslinking times and an increase in temperature.

3.2.3 Chemical reporter (CR) reactivity

Selective capture of the drug-protein adducts utilizes installation of cognate partners for the click chemistry reaction on the drug analogs and chemical probes. Non-specific side reactions resulting in background labeling of proteins occur in association

with both the alkyne and azide functional units when added to lysate mixtures. Nevertheless, slightly lower background has been reported for the azide unit when it is installed on the chemical probe.[155] The alkyne functional unit was incorporated, therefore, in the lacosamide scaffold and the azide into the chemical probes (probes 1 and 2) to reduce non-specific labeling of proteins by the probe during the click chemistry reaction.

The cycloaddition reaction between the alkyne containing lacosamide analog and azide containing reporter probes is greatly accelerated by the presence of Cu(I) in aqueous solution.[156,157] Generation of Cu(I) under aqueous conditions requires copper sulfate ($CuSO_4$), a reducing agent tris (2-carboxyethyl) phosphine (TCEP) and the Cu(I) stabilizing ligand tris [(1-benzyl-1H-1,2,3-triazol-4-yl)methyl] amine (TBTA). Generation of the triazole product begins by the association of two Cu(I) atoms forming a copper acetylide species from Cu(I) and activated azide. Simultaneous complexation of the intermediates with the stabilizing TBTA ligand brings the acetylide and activated azide together allowing for cyclization to form the triazole product (Figure 3.5).[158]

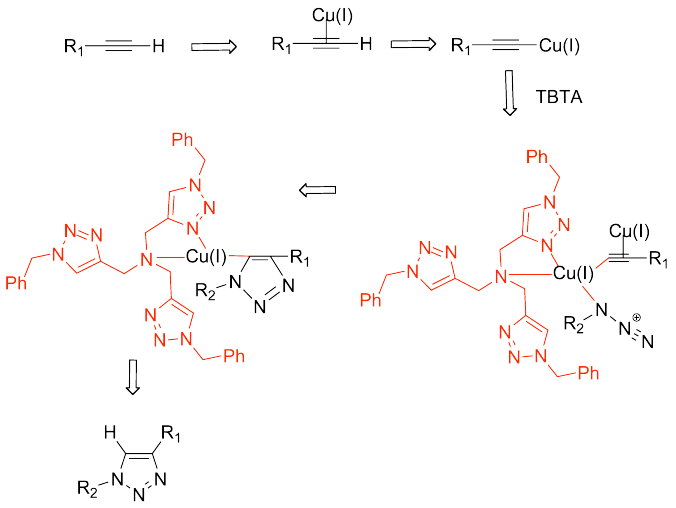

Figure 3.5 The mechanism of the click chemistry reaction. Formation of the copper acetylide species allows for complexation with the stabilizing TBTA ligand (red). This brings the alkyne and azide in close proximity, promoting cyclization.

Two reporter probes were synthesized in the Kohn laboratory to fluorescently detect (probe 1) or purify (probe 2) affinity-labeled drug-protein adducts using click chemistry. Probe 1 contains a tetramethylrhodamine (TAMRA) fluorophore with a C3 azide. Drug-protein adducts reacted with probe 1 can be detected by excitation with UV light at 532 nm and absorption at 580 nm. Probe 2 contains a biotin group, which after reacting with drug-protein adducts, allows for enrichment and purification of labeled proteins using immobilized streptavidin.

3.2.4 Validation of the AB & CR strategy

Prior to investigation of the lacosamide analogs containing AB and CR units in mouse brain lysate, suitability of the compounds to undergo click chemistry was evaluated using an enzyme linked immunosorbent assay (ELISA). The affinity bait in compound 1 is designed to react with lysine residues on target proteins; therefore, a

polylysine plate was used as a solid surface to immobilize the drug. Specifically, compound 1 was incubated overnight at 4 °C in the poly-lysine coated 96-well plate to immobilize the lacosamide AB and CR through reaction with its affinity bait. Click chemistry was performed with the biotin containing probe (probe 2) for 4 h. The plate was washed extensively and streptavidin-HRP conjugate was incubated to detect the presence of biotin. After removing unbound streptavidin-HRP, HRP substrate was added and color intensity measured (Figure 3.6). The right column shows wells where DMSO was substituted for compound 1 as a negative control. The reactions were performed in triplicate. Probe 2 was omitted in row four to illustrate the background signal of the streptavidin-HRP conjugate. The results show that the signal is dependent on the presence of the alkyne and that it appears the drug scaffold does not hinder the cycloaddition.

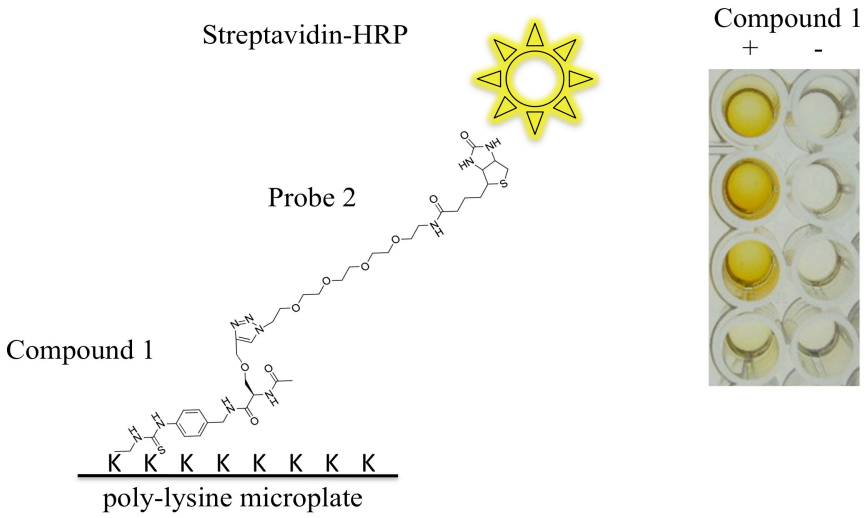

Figure 3.6 Evaluation of click chemistry using an ELISA assay. Compound 1 (1 mM) was immobilized in lane 1 on a poly-lysine plate through its affinity bait by incubation overnight at 4 °C. Click chemistry was performed for 1 hour at room temperature by the addition of Probe 2 (40 μM), TCEP (500 μM), TBTA (250 μM), and $CuSO_4$ (1 mM) to introduce a biotin group. Probe 2 was omitted from the click chemistry step for samples in the bottom row. Streptavidin-HRP was added to detect the presence of biotin. The reactions were performed in triplicate.

Assessment of the pharmacological activity of compounds 1 and 2 is critical to ensure that their usage for the labeling and identification of candidate proteins can provide meaningful results. Modified compounds such as compounds 1 and 2 with poor activity may be indicative of abolishment of binding to endogenous protein receptors and are perhaps unsuitable for target identification. Drug analogs containing single AB or CR units as well as the fully functionalized (AB and CR) compounds 1 and 2 were evaluated for anticonvulsant activity in the maximal electroshock seizure (MES) mouse model through a collaboration with the National Institute for Neurological Disorder and Stroke's Anticonvulsant Screening Program. This test is an acute electroshock seizure models that provide mechanistic independent insight for protection against tonic-clonic (MES).

Results of the pharmacological evaluation are summarized in Table 3.1. Introduction of a single AB or CR unit resulted in a modest loss of activity compared to (*R*)-lacosamide. Subsequent evaluation of bi-functionalized compounds 1 and 2 in a mouse (i.p.) MES test for electroconvulsant seizures showed good activity (ED_{50} = 45 mg/kg, 20 mg/kg respectively).[107] Consistent with lacosamide derivatives, diminished activity is observed with the *S* enantiomer (L-configuration). Collectively, the results indicate that compound 1 and 2 remain biologically active *in vivo* in a manner consistent with (*R*)-lacosamide. Activity is not abolished by installation of the AB and CR units that are designed for labeling and capture of (*R*)-lacosamide binding proteins during screening.

Table 3.1 Pharmacological evaluation of AB and CR lacosamide derivatives

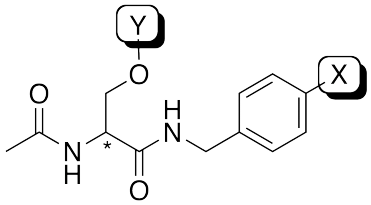

Compound				Mice (ip), (mg/kg)		
Compd	Stereo	X	Y	MES, ED_{50}	Tox, TD_{50}	6 Hz, ED_{50}
1	*R*	NCS	$CH_2C{\equiv}CH$	45	110	53
	S	NCS	$CH_2C{\equiv}CH$	> 300	> 300	ND
(AB)	*R*	NCS	CH_3	24	47	ND
(AB)	*S*	NCS	CH_3	> 100, < 300	> 30, < 100	ND
(CR)	*R*	H	$CH_2C{\equiv}CH$	16	59	29
(CR)	*S*	H	$CH_2C{\equiv}CH$	> 300	> 300	> 100
2	*R*	$CH_2C{\equiv}CH$	N_3	20	82	< 10
	S	$CH_2C{\equiv}CH$	N_3	160	>300	ND
(AB)	*R*	CH_3	N_3	8.4	46	ND
(AB)	*S*	CH_3	N_3	> 100, < 300	> 300	~ 100
(CR)	*R*	$CH_2C{\equiv}CH$	H	16	59	< 30
(CR)	*S*	$CH_2C{\equiv}CH$	H	> 300	> 300	> 100

ND: not determined adapted from Ref [107]

3.2.5 TAMRA-based probe for in-gel fluorescence

After confirmation of biological activity *in vivo* and aptness to undergo click chemistry via an ELISA assay, compounds 1 and 2 were evaluated in mouse brain lysate. The tetramethylrhodamine (TAMRA) containing probe (probe 1) was used to label adducted proteins in crude homogenates of mouse brain lysate. The soluble fraction from

the crude homogenate of mouse brain lysate was used for initial in-gel fluorescence studies. Mouse brains were homogenized to a final protein concentration of 4 mg/ml in 50 mM HEPES pH 7.4 and 150 mM NaCl followed by centrifugation at 14,000 rpm for 30 minutes. The supernatant (soluble fraction) was removed and used for labeling experiments. Small aliquots (50 μl) were labeled with compound 1 or 2 for a defined period of time, followed by addition of probe 1, TCEP, TBTA, and $CuSO_4$ for click chemistry. The reaction was allowed to proceed for 1 h followed by addition of SDS-PAGE loading buffer to terminate the reaction. Samples were resolved on a 10% SDS-PAGE gel and scanned for fluorescence (excitation 532 nm and emission 580 nm).

Labeling of soluble mouse brain lysate for 1 hour at room temperature with compound 1 showed dose dependent adduct formation that could be detected with probe 1 (Figure 3.7). Discrete TAMRA labeled protein bands were observed in proteins with a wide range of sizes (<25 and >175 kDa). Nine major bands showed intense labeling compared to other protein bands within the gel. In the absence of compound 1 or the chemical reporter unit (AB-*R*-LCM), minimal background fluorescence appeared to be generated by the TAMRA chemical reporter probe. A small amount of background fluorescence is observed in the control lanes potentially corresponding to highly abundant proteins such as actin and tubulin.

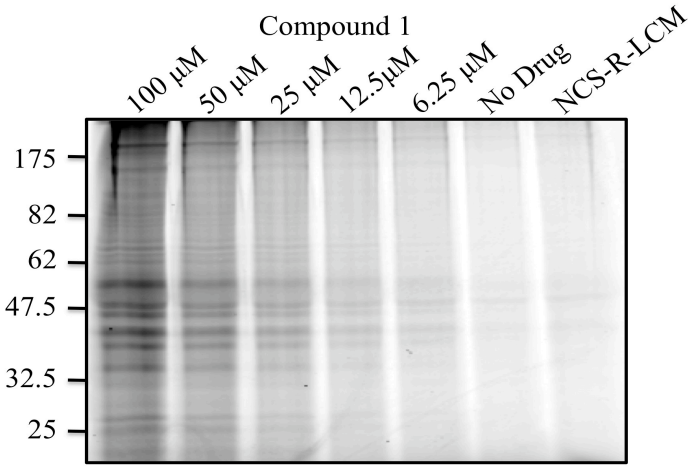

Figure 3.7 Dose dependent labeling of soluble mouse brain lysate with compound 1. After labeling the lysate with compound 1, adducted proteins were detected using click chemistry with the TAMRA chemical probe. Proteins were resolved on a 10% SDS-PAGE gel and detected using in-gel fluorescence (excitation 532 nm / emission 580 nm). Compound 1 shows dose dependent labeling across the concentrations studied and very little background labeling is observed when the chemical reporter is absent from drug analog.

Compound 2 was designed to react with proteins lacking a nucleophile in the binding pocket. Therefore, the reactivity of the photoaffinity bait was separately evaluated in soluble mouse brain lysate. Controlling the extent of labeling by varying labeling time was first investigated with compound 2. Activation of the aromatic azide by UV light allows for temporal control of the adduct formation. Incubation of soluble mouse brain lysate with compound 2 (50 μM) for 30 minutes followed by activation of the aromatic azide by using UV at 312 nm for various times showed a positive correlation between activation time and the extent of labeling as detected by the TAMRA probe (probe 1). Maximal labeling at 50 μM for compound 2 was achieved between 5 and 10 minutes (Figure 3.8). Banding patterns generated with compound 1 and compound 2, although similar, were not identical, indicating each affinity bait labeled distinct proteins. These differences illustrate that compounds 1 and 2 provide a more comprehensive

coverage of potential (*R*)-lacosamide targets by reacting with both nucleophillic and electrophillic residues present on potential (*R*)-lacosamide binding proteins in the mouse brain proteome.

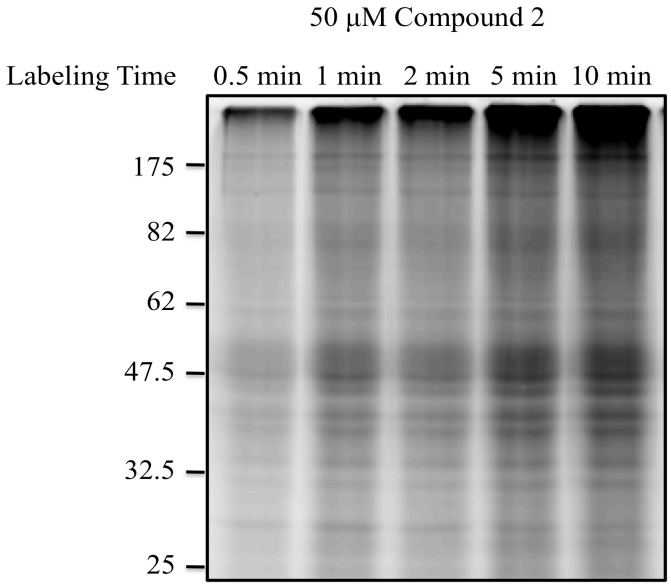

Figure 3.8 Time dependent labeling of mouse brain lysate with compound 2. After activation of compound 2 (50 μM) at 312 nm for various times, adducted proteins were detected using click chemistry with the TAMRA chemical probe (probe 1). Proteins were resolved on a 10% SDS-PAGE gel and detected using in-gel fluorescence (excitation 532 nm / emission 580 nm).

The specificity of compound 1 and sensitivity of the TAMRA probe (probe 1) were evaluated using mouse brain lysate spiked with bovine serum albumin (BSA) functionalized to contain an alkyne chemical reporter unit (BSA-alkyne). Labeling of compound 1 in mouse brain lysate was compared with samples containing 1 μg BSA-alkyne or 3 μg enolase protein. After click chemistry, TAMRA labeled proteins were resolved on an SDS-PAGE gel and individual band intensities were quantified. Protein samples containing the BSA-alkyne showed very strong detection with the TAMRA probe (probe 1) (Figure 3.9). If we assume the click reaction was 100% efficient, the

band represents 28.9 ng of BSA protein, which is equivalent to approximately 17% of the total 1 μg input.

Integration of pixel intensity for the BSA band and band 1 was 4404 and 291 respectively. Using the integrations to compare relative protein amounts, quantification of the protein amount for band 1 was estimated to be 2 nanograms. Therefore, most of the bands may represent picogram amounts of individual proteins in the lysate labeled by compound 1. No reactivity was seen toward enolase (lane 2) despite the fact that it was the most abundant protein in the lysate mixture. This suggests that the isothiocyanate group shows minimal non-specific reactivity toward abundant proteins under the conditions used and labeling most likely occurs through a specific interaction with a nucleophillic lysine or cysteine side chain present inside a pocket within the interacting protein. The detection limit of probe 1 to discriminate individually labeled proteins was estimated to be in the sub-nanogram range.

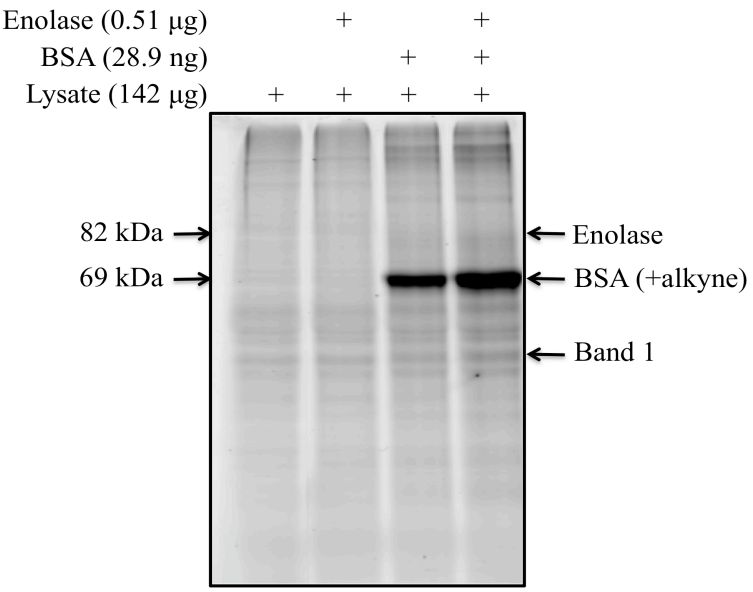

Figure 3.9 The selectivity of compound 1 and sensitivity of probe 1 in mouse brain lysate assayed through in-gel fluorescence. Soluble mouse brain lysate samples (142 μg) spiked with enolase protein (0.51 μg) and/or alkyne functionalized BSA protein (28.9 ng) or lysate alone were reacted with compound 1 for 1 hour at room temperature followed by click chemistry with probe 1 for 1 hour. Samples were resolved on a 10% SDS-PAGE gel and scanned for fluorescence (ex.: 532 nm, em.: 580 nm). Molecular weight makers are shown for BSA (69 kDa) and enolase (82 kDa).

Collectively, the in-gel fluorescence results demonstrate that the pharmacologically active compounds 1 and 2 can label potential target proteins present in the soluble fraction of the mouse brain proteome. Both affinity baits show dose and time dependent labeling which can be controlled through drug concentration or labeling reaction time.

3.2.6 Enrichment of target proteins with the biotin probe

Previous efforts using probe 1 to detect proteins adducted with compound 1 or 2 demonstrated that sub-nanogram quantities of adducted proteins in mouse brain lysate were detected via in-gel fluorescence after labeling. The adducted proteins remained in

the complex mixture of mouse brain lysate and were therefore unsuitable for mass spectrometry. Absolute identification of protein targets is not possible without purification and enrichment of adducts prior to mass spectrometry analysis. Detection limits for mass spectrometry vary by application and analysis conditions but picomolar or potentially low femtomolar quantities are sufficient for protein identification through MALDI and ESI, respectively.[159] Despite these sensitivities, enrichment is paramount for detection of (*R*)-lacosamide labeled proteins that may be present in low abundance in the mouse brain.

The preparation of the mouse brain lysate should include as many proteins as possible to increase the likelihood of finding the putative targets. Exclusion of membrane or nuclear fractions will reduce the complexity of the lysate mixture, potentially eliminating many protein targets relevant to epilepsy. Fractionation may also disrupt native protein complexes present *in vivo*. For instance, omission of proteins in the membrane fraction would eliminate targets such as GABA receptors, sodium channels, AMPA receptors, and calcium channels; all of which are known targets for anticonvulsants. Subsequently, omission of the soluble fraction would remove targets such as carbonic anhydrase and GABA transaminase; also targets for the treatment of seizure disorder.

Simultaneous screening of isolated protein fractions is labor intensive and likely disrupts protein complexes present *in vivo*. A rapid, facile method that incorporates both membrane and soluble proteins without denaturation is ideal for our proteomic search. The water-soluble ionic detergent deoxycholate is often used to solubilize components of cellular membranes. Deoxycholate has been used to solubilize and purify native NMDA

receptor complexes from brain tissue, illustrating its suitability to retain native protein conformations.[160] Unlike Triton X-100 or octylglucoside, the presence of deoxycholate does not inhibit tubulin polymerization *in vitro* indicating it is a mild non-denaturing detergent.[161] Because the NMDA receptor and related synaptic protein complexes represent classes of proteins that are validated drug targets, 1% deoxycholate was used to partially solubilize intact membrane complexes in the preparation of mouse brain lysate. For the NMDA receptor, it is estimated that 35% of the total receptor complexes present in lysate can be solubilized using 1% deoxycholate.[160]

Our initial studies evaluated the ability to enrich with the biotin probe proteins that were labeled with compounds 1, 2 and 3. Lysate labeled with compounds 1 and 2 (40 μM) were reacted with the biotin probe (probe 2), after which biotin labeled adducts were captured with beads coated with streptavidin or mutein streptavidin, a streptavidin mutant with a lower affinity for biotin. After extensive washing, captured proteins were eluted with SDS-PAGE loading buffer (for streptavidin bead samples) or buffer supplemented with 1 mM biotin (for mutein streptavidin bead samples). Proteins were resolved via SDS-PAGE, followed by transferring to a nitrocellulose membrane and detected with a streptavidin Alexa Fluor® 488 conjugate (Figure 3.10).

The results in lane 6 indicate the presence of two endogenously biotinylated proteins above 52 kDa present in the mouse brain lysate that require removal before labeling experiments are performed. Comparison of the capture and elution efficiency between the streptavidin and mutein streptavidin beads revealed much lower enrichment with the mutein beads. Despite the theoretical advantage for milder elution conditions

with the mutein beads resulting from a lower K_d with biotin (1.3×10^{-7} versus 4×10^{-14}), a lower recovery was observed compared to streptavidin beads.

Contrasting lanes 2 and 5 revealed that the efficiency of the click chemistry step to introduce biotin residue (lane 2) substantially lowered the yield compared to compound 3. The two-step labeling and capture afforded by compounds 1 and 2 should, however, provide sufficient material for mass spectrometry identification. Banding patterns between the two samples appeared identical, but overall yield was higher in lane 5 when the click chemistry step was circumvented.

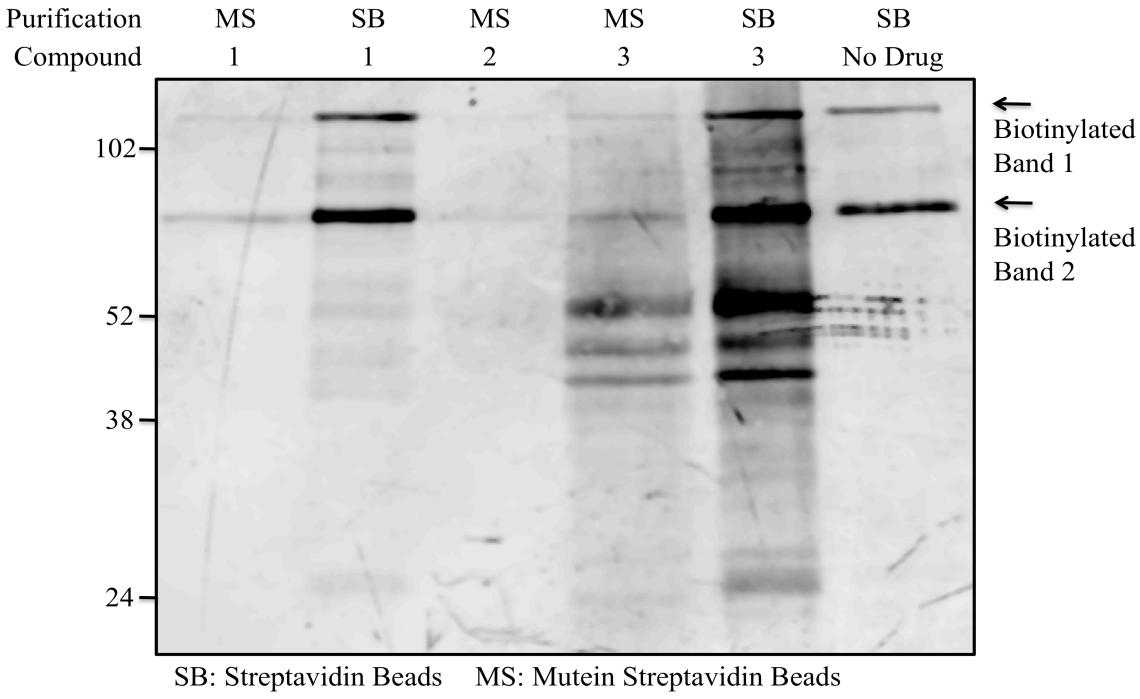

Figure 3.10 The enrichment of biotinylated proteins using probe 2. Lysate incubated with compound 1 or compound 3 for 1 hour at room temperature were clicked with probe 2 followed by capture with streptavidin beads. Purified proteins were resolved on a 10% gel then transferred to a nitrocellulose membrane followed by detection of biotinylated proteins using streptavidin Alexa Fluor® 488. Two endogenously biotinylated bands were strongly enriched using both mutein and streptavidin beads. Compounds 1 and 2 showed a lower number of proteins captured compared to compound 3 where click chemistry is not necessary for enrichment.

Based on these findings, the protocol was modified so the lysate was precleared by incubating with streptavidin beads to remove any endogenously biotinylated proteins. Additionally, washing steps utilized regular streptavidin beads coupled with stringent washing (2X with 50 mM HEPES + 150 mM NaCl + 0.2 % SDS, 2X 6 M urea, 2X 50 mM HEPES + 150 mM NaCl) to strip the non-specifically bound proteins from the matrix. Activation of the affinity bait by UV light at 312 nm for compound 2 was extended to 20 minutes to ensure maximal labeling. Application of such conditions for purification resulted in the enrichment of more bands compared to previous experiments (Figure 3.11). Distinct differences in enriched proteins were observed between lysate labeled with 40 μM of compounds 1 and 2. Furthermore, the two endogenous biotinylated proteins were effectively eliminated. (*S*)-Lacosamide (2 mM) was added to the lysate as a way to reduce the labeling and capture of non-specific proteins. It is assumed that the presence of the inactive stereoisomer of the drug will saturate off-target proteins that may have non-specific interactions with the lacosamide scaffold. Surprisingly, no differences were observed when a competing excess of (*S*)-lacosamide was added to the labeling reaction.

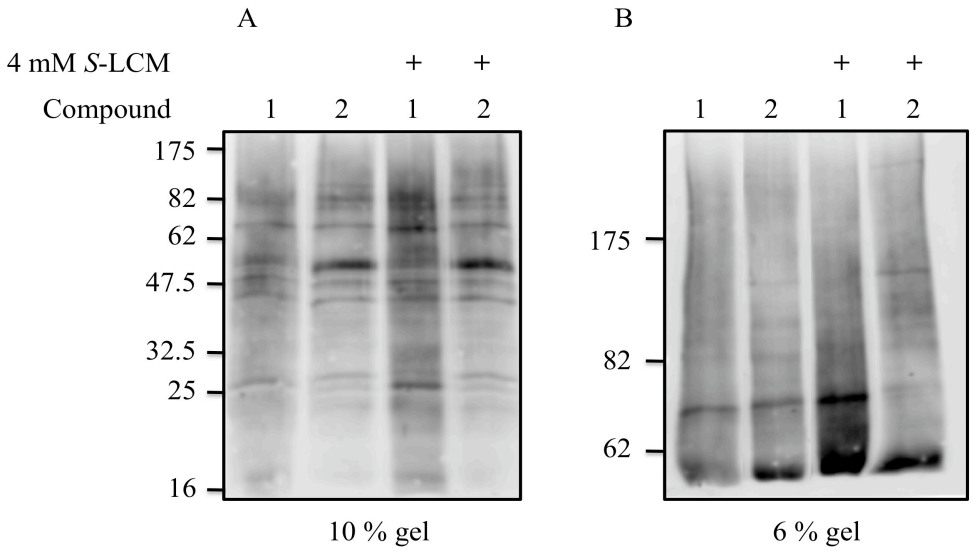

Figure 3.11 Proteins purified from mouse brain lysate using the optimized enrichment conditions with compounds 1 and 2. Mouse brain lysate was incubated with 40 μM of compound 1 or 2 followed by click chemistry with probe 2. *S*-Lacosamide (1 mM) was added to investigate the non-specific labeling by the isothiocyanate affinity bait. Proteins adducted with the biotin probe were captured using streptavidin beads followed by washing 2X (1 ml) with 50 mM HEPES + 150 mM NaCl + 0.2 % SDS, 2X (1 ml) 6 M urea, and 2X (1 ml) 50 mM HEPES + 150 mM NaCl. The beads were boiled for 5 minutes in 40 μl of SDS-PAGE loading buffer. Samples were resolved on SDS-PAGE gels then transferred to a nitrocellulose membrane followed by detection of biotin using streptavidin Alexa Fluor 488®.

The successful development of a protocol that achieves enrichment of discrete bands from mouse brain lysate containing both soluble and membrane solubilized proteins allowed for the preparation of high quality samples for mass spectrometry.

3.2.7 Mass spectrometry identification of enriched proteins

The sensitivity of mass spectrometry to identify proteins using nanogram to femtogram quantities provides an excellent tool for identification of protein-drug targets. Despite this sensitivity, challenges remain for purification of individual proteins using a multistep process of labeling, tagging, purifying, and eluting proteins from complex

mixtures. Regulatory proteins are often rare or in low abundance compared to the total protein content of the cell. These classes of proteins embody attractive drug targets due to their ability to amplify signal transduction cascades.

Identification of regulatory proteins poses challenges because their expression remains tightly controlled and they tend to have rapid turnover in the cell. Degradation and stability may hinder enrichment of sufficient quantities needed for mass spectrometry. Once removed from an environment with a high protein concentration, target proteins may precipitate in the absence of chaperones, binding partners, or co-factors. One of the major challenges in preparing samples for mass spectrometry is elution off the matrix used for enrichment. The strong affinity between biotin and streptavidin creates an almost covalent interaction between the matrix and target proteins. Even with harsh solvents and high temperatures it is estimated that only 10-20% of the bound material is released; therefore, we developed two approaches for preparation of samples for identification by mass spectrometry (Figure 3.12).[162]

In method 1, SDS-PAGE loading buffer supplemented with 1 mM biotin was added to the beads followed by boiling at 95ºC for 5 minutes. Supernatant containing the eluted proteins was loaded to an SDS-PAGE gel and proteins were detected via silver stain. Visualized bands were cut and submitted for in-gel trypsinization.

In method 2, the beads were washed once with water after purification from the lysate and the proteins were directly trypsinized off the streptavidin bead matrix. Method 1 could potentially provide information regarding the site of adduction on the protein because the intact protein would be released, allowing for identification of signature lacosamide ions associated with adduction; the efficiency of release is expected to be

low, however. Method 2 does not allow for identification of the modification site because the adducted portion of the protein will remain immobilized on the matrix. Rare or non-abundant proteins that are captured, however, have a better chance of being identified from the release of trypsinized peptides. Both methods were used to interrogate the proteins that interact with compounds 1 and 2.

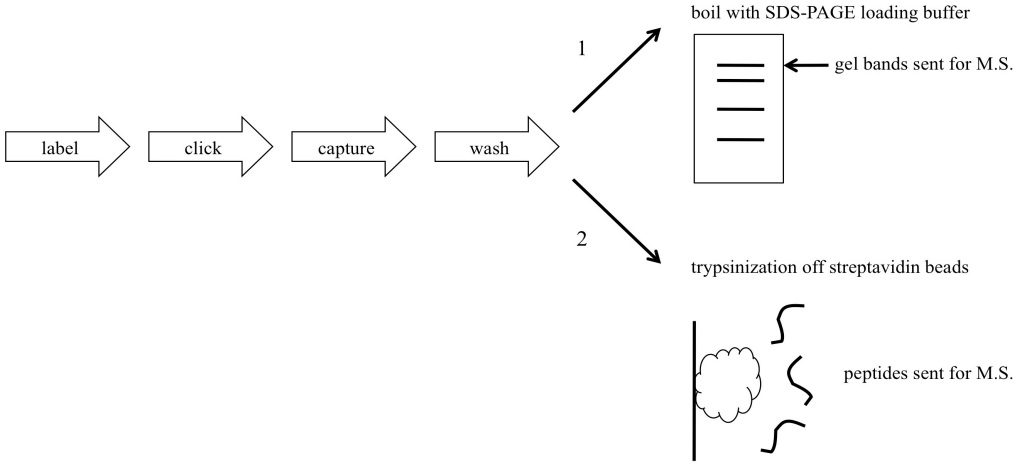

Figure 3.12 Strategies for processing enriched samples for protein identification with mass spectrometry. Method 1 relies on separation of enriched proteins on SDS-PAGE gels followed by excision of silver stained gel bands. Method 2 uses trypsinization of captured proteins directly off streptavidin beads.

Mouse brain lysate was labeled with compounds 1 and 2 or their inverse entantiomers ((*S*)-configuration) followed by reaction with the biotin containing probe (probe 2) and enriched with streptavidin beads. Purified drug-protein adducts were either submitted directly for trypsinization off the streptavidin beads or boiled with loading buffer and resolved on an SDS-PAGE gel. Silver stained gel bands were cut and submitted to the Michael Barber Centre for Mass Spectrometry at the University of Manchester. Results of the mass spectrometry analysis identified approximately 73 unique proteins from methods 1 and 2. These are listed in Table 3.2.

Table 3.2 Complete list of proteins identified during the proteomic screen

Ref Seq ID	Protein Description	MW (kDa)
NP_034053	2',3'-cyclic-nucleotide 3'-phosphodiesterase	46.992
NP_061223	3-monooxygenase/tryptophan 5-monooxygenase activation protein beta/alpha	27.955
NP_033562	3-monooxygenase/tryptophan 5-monooxygenase activation protein epsilon	29.058
NP_035868	3-monooxygenase/tryptophan 5-monooxygenase activation protein eta	28.081
NP_061359	3-monooxygenase/tryptophan 5-monooxygenase activation protein gamma	28.172
NP_061224	3-monooxygenase/tryptophan 5-monooxygenase activation protein sigma	27.575
NP_035869	3-monooxygenase/tryptophan 5-monooxygenase activation protein theta	27.647
NP_035870	3-monooxygenase/tryptophan 5-monooxygenase activation protein zeta/delta	27.64
NP_766549	4-aminobutyrate aminotransferase, mitochondrial precursor	56.321
NP_071864	Abhydrolase domain-containing protein 8	48.158
NP_031419	Actin, cytoplasmic 1	41.606
NP_031476	ADP/ATP translocase 1	32.773
NP_031477	ADP/ATP translocase 2	32.8
NP_848473	ADP/ATP translocase 4	35.157
NP_075608	Alpha enolase	47.01
NP_033809	AP-2 complex subunit mu-1	49.524
NP_034454	Aspartate aminotransferase, cytoplasmic	46.117
NP_031531	ATP synthase subunit alpha, mitochondrial precursor	59.622
NP_058054	ATP synthase subunit beta	56.17
NP_081671	Brain acid soluble protein 1	21.955
NP_001074767	Calcium-independent alpha-latrotoxin receptor	166.504
NP_033931	Carbonic anhydrase 2	28.901
NP_080720	Citrate synthase	51.606
NP_001003908	Clathrin heavy chain	191.426
NP_083146	Clathrin light chain B	23.043
NP_031713	Cofilin 1	18.428
NP_067248	Creatine kinase B type	42.582
NP_034027	Creatine kinase, ubiquitous mitochondrial precursor	46.873
NP_031791	Dihydropyrimidinase related protein 1	62.037
NP_034085	Dihydropyrimidinase related protein 2	62.147
NP_034195	Dynamin 1	97.154
NP_034236	Elongation factor 1-alpha 1	49.983
NP_001070982	Excitatory amino acid transporter 2	61.899
NP_031464	Fructose-bisphosphate aldolase A	39.225
NP_033787	Fructose-bisphosphate aldolase C	39.264
Q8R050	G1 to S phase transition protein 1 homolog	68.396
NP_038537	Gamma enolase	47.166
NP_032159	Glutamate dehydrogenase 1, mitochondrial precursor	61.206
NP_032110	Glyceraldehyde-3-phosphate dehydrogenase	35.679
NP_032110	Glyceraldehyde-3-phosphate dehydrogenase	35.679
NP_001106855	Guanine nucleotide-binding protein G(o) subunit alpha 1	39.905
NP_034609	Heat shock 70 kDa protein	69.948
NP_112442	Heat shock cognate 71 kDa protein	70.74

NP_080784	Heat shock protein 75 kDa	80.078
NP_034610	Heat shock protein HSP 90-alpha	84.657
NP_032328	Heat shock protein HSP 90-beta	83.15
NP_032246	Hemoglobin subunit beta-1	15.617
NP_835582	Histone H4 (MW 11360)	11.236
NP_032644	Malate dehydrogenase, cytoplasmic	36.337
NP_035253	Myelin proteolipid protein	29.946
NP_032933	Peptidyl-prolyl cis-trans isomerase A	17.84
NP_598429	Phosphate carrier protein, mitochondrial precursor	39.501
NP_032854	Phosphoglycerate kinase1	44.42
NP_112467	Phosphoglycerate kinase2	44.752
NP_033853	Plasma membrane calcium-transporting ATPase 2	132.457
NP_035229	Pyruvate kinase isozymes M1/M2	57.714
NP_083770	Ras related protein Rab-30	22.927
NP_033027	Ras related protein Rab-3A	24.839
NP_035377	Retinoblastoma-binding protein 6	199.457
NP_035627	Serine/threonine-protein kinase 6	47.042
NP_033784	Serum albumin precursor	68.562
NP_659149	Sodium/potassium-transporting ATPase subunit alpha	112.852
NP_848492	Sodium/potassium-transporting ATPase subunit alpha-2	112.087
NP_659170	Sodium/potassium-transporting ATPase subunit alpha-3	115.838
NP_033851	Sodium/potassium-transporting ATPase subunit beta-1	35.064
NP_849245	Spermatogenesis-associated protein 7 homolog	65.524
NP_084477	Stress-70 protein, mitochondrial precursor	51.578
NP_062684	Structural maintenance of chromosomes protein 1A	143.085
NP_075770	Succinate dehydrogenase [ubiquinone] flavoprotein subunit	72.455
NP_080881	Symplekin	142.49
NP_077725	Syntaxin-1B	33.114
NP_001107041	Syntaxin binding protein1	68.605
NP_033441	Triosephosphate isomerase	26.582
NP_035783	Tubulin alpha-1A chain	50.005
NP_033476	Tubulin beta-2A chain	49.776
NP_075768	Tubulin beta-3 chain	50.288
NP_080175	Ubiquinol-cytochrome-c reductase complex core protein 2	48.104
NP_277044	Vang like protein 2	59.64
NP_032766	N-ethylmaleimide sensitive fusion protein	82.483

The number of proteins identified from method 1 was significantly less than from method 2. Only 3 proteins were identified exclusively through method 1 and all were from samples labeled with compound 2 or its enantiomer (Table 3.3). Conversely, 32 proteins were found exclusively from method 2, including 7 different protein isoforms from 3 protein families previously identified by method 1 (Table 3.4).

Table 3.3 Proteins identified exclusively from method 1

Ref Seq ID	Protein Description	MW (kDa)	Compound
NP_033931	Carbonic anhydrase 2	28.901	2 (*S*)
NP_080175	Ubiquinol-cytochrome-c reductase complex core protein 2	48.104	2 (*S*)
NP_032766	N-ethylmaleimide sensitive fusion protein	82.483	2 (*R*)

Table 3.4 Proteins identified exclusively from method 2

Ref Seq ID	Description	MW (kDa)
NP_035086	2-oxoglutarate dehydrogenase E1 component, mitochondrial precursor	112.53
NP_033562	3-monooxygenase/tryptophan 5-monooxygenase activation protein epsilon	29.058
NP_061359	3-monooxygenase/tryptophan 5-monooxygenase activation protein gamma	28.172
NP_061224	3-monooxygenase/tryptophan 5-monooxygenase activation protein sigma	27.575
NP_766549	4-aminobutyrate aminotransferase, mitochondrial precursor	56.321
NP_071864	Abhydrolase domain-containing protein 8	48.158
NP_058054	ATP synthase subunit beta	56.17
NP_001003908	Clathrin heavy chain	191.426
NP_031713	Cofilin 1	18.428
NP_067248	Creatine kinase B-type	42.582
NP_034195	Dynamin 1	97.154
NP_001070982	Excitatory amino acid transporter 2	61.899
Q8R050	G1 to S phase transition protein 1 homolog	68.396
NP_080784	Heat shock protein 75 kDa, mitochondrial precursor	80.078
NP_034610	Heat shock protein HSP 90-alpha	84.657
NP_032328	Heat shock protein HSP 90-beta	83.15
NP_032246	Hemoglobin subunit beta 1	15.617
NP_835582	Histone H4	11.236
NP_032933	Peptidyl-prolyl cis-trans isomerase A	17.84
NP_033853	Plasma membrane calcium-transporting ATPase 2	132.457
NP_035229	Pyruvate kinase isozymes M1/M2	57.714
NP_083770	Ras related protein Rab-30	22.927
NP_033027	Ras related protein Rab-3A	24.839
NP_035377	Retinoblastoma-binding protein 6	199.457
NP_035627	Serine/threonine-protein kinase 6	47.042
NP_659149	Sodium/potassium-transporting ATPase subunit alpha	112.852
NP_848492	Sodium/potassium-transporting ATPase subunit alpha-2 precursor	112.087
NP_033851	Sodium/potassium-transporting ATPase subunit beta-1	35.064
NP_062684	Structural maintenance of chromosomes protein 1A	143.085
NP_075770	Succinate dehydrogenase [ubiquinone] flavoprotein subunit	72.455
NP_080881	Symplekin	142.49
NP_277044	Vang like protein 2	59.64

The results of screening the deoxycholate solublized mouse brain lysate with compounds 1 and 2 identified various nuclear, cytoplasmic, and membrane associated proteins. Several proteins were identified as mitochondrial precursor isoforms suggesting that the deoxycholate detergent preparation was able to solubilize not only plasma membrane associated proteins, but proteins found in organelles such as the mitochondria and endoplasmic reticulum. The number of unique proteins identified was surprising due to the stringent washing conditions applied to the streptavidin beads during purification. The strong denaturing property of 6 M urea is expected to eliminate most non-specific interactions between proteins and the streptavidin matrix. Therefore, most proteins identified by mass spectrometry should have been retained on the matrix through their biotin-streptavidin interaction.

3.2.8 Selectivity of enantiomers and affinity baits

Comparison of the enantioselectivity of compounds 1 and 2 to capture individual proteins could potentially provide insight into which targets are most likely responsible for (*R*)-lacosamide's efficacy. Pharmacological data for (*R*)-lacosamide and other functionalized amino acids clearly show biological activity is enantioselective for the (*R*) stereoisomer (D-configuration). This trend of enantioselective biological activity could be extended to correlate with the binding affinity of (*R*)-lacosamide to its cognate protein targets. We could expect the (*R*) stereoisomers for compounds 1 and 2 to preferentially interact and label the correct protein targets better than the (*S*) stereoisomers. For this hypothesis to be true, increased biological activity resulting from differences in pharmacokinetics, metabolism, transport, or efflux must be considered negligible.

Currently no studies exist evaluating any of these factors for individual enantiomers. The number of peptide fragments identified for each protein from individual entantiomers with compound 1 is listed in Table 3.5.

Table 3.5 The number of peptides identified with *R* versus *S* for compound 1.

	Protein Description	**(*R*)**	**(*S*)**
	2',3'-cyclic-nucleotide 3'-phosphodiesterase	5	6
	3-monooxygenase/tryptophan 5-monooxygenase activation protein epsilon		7
	3-monooxygenase/tryptophan 5-monooxygenase activation protein gamma		4
	3-monooxygenase/tryptophan 5-monooxygenase activation protein theta		3
	3-monooxygenase/tryptophan 5-monooxygenase activation protein zeta/delta	5	8
	4-aminobutyrate aminotransferase, mitochondrial precursor		1
	Actin, cytoplasmic 1	15	17
	ADP/ATP translocase 1	7	5
*	ADP/ATP translocase 2	2	
*	ADP/ATP translocase 4	5	3
	ATP synthase subunit alpha, mitochondrial precursor	4	4
	ATP synthase subunit beta	9	4
	Clathrin heavy chain	3	9
	Cofilin 1	1	
	Creatine kinase B-type	2	5
*	Dihydropyrimidinase related protein 2	8	5
	Dynamin 1		2
*	Elongation factor 1-alpha 1	1	
	Excitatory amino acid transporter 2		2
*	Fructose-bisphosphate aldolase A	6	
*	Gamma enolase	2	
	Glyceraldehyde-3-phosphate dehydrogenase	2	6
	Guanine nucleotide-binding protein G(o) subunit alpha 1	3	3
	Heat shock 70 kDa protein (can not identify isoform)		2
	Heat shock cognate 71 kDa protein	2	6
	Heat shock protein HSP 90-alpha	2	2
	Hemoglobin subunit beta-1	3	3
	Histone (can not identify isoform)	1	2
	Malate dehydrogenase, mitochondrial precursor		4
	Myelin proteolipid protein	3	3
*	Peptidyl prolyl cis trans isomerase A	3	
*	Plasma membrane calcium-transporting ATPase 2	1	
	Potassium transporting ATPase alpha chain 1	2	3
	Pyruvate kinase isozymes M1/M2	2	2

	Ras related protein (can not identify isoform)		1
*	Ras related protein Rab-30	2	
*	Ras related protein Rab-3A	2	
	Serine/threonine-protein kinase 6		1
*	Sodium/potassium-transporting ATPase subunit alpha-1 precursor	17	6
*	Sodium/potassium-transporting ATPase subunit alpha-2 precursor	21	9
*	Sodium/potassium-transporting ATPase subunit alpha-3	25	22
	Sodium/potassium-transporting ATPase subunit beta-1	2	1
	Succinate dehydrogenase [ubiquinone] flavoprotein subunit, mitochondrial precursor		2
	Syntaxin binding protein 1	2	3
	Triosephosphate isomerase	3	4

* indicates proteins where more peptides were identified with the *R* than the *S*

For several proteins, more peptides were identified with the *R* enantiomer versus the *S* enantiomer. Although the mass spectrometry approaches used in methods 1 and 2 are not quantitative, identification of more peptides with one enantiomer versus another may represent a trend in the preference of one configuration to label certain proteins in the lysate. The proteins with the largest enrichment (i.e. number of peptides) for the *R* enantiomer using compound 1 were the sodium/potassium-transporting ATPase subunit alpha 1, sodium/potassium-transporting ATPase subunit alpha 2, fructose bisphosphate aldolase A, ATP synthase subunit beta, and dihydropyrimidinase related protein 2.

Compound 2 labeled and captured a distinct set of proteins compared to compound 1 (Table 3.6). The enantiomeric preference for the sodium/potassium-transporting ATPase subunits, fructose bisphosphate aldolase A, and ATP synthase subunit beta was not observed with compound 2. The *R* versus *S* preference for dihydropyrimidinase related protein 2 was the only protein that showed a common stereo-specificity between compound 1 and 2. Additionally, triosephosphate isomerase, syntaxin binding protein 1 (also known as MUNC18-1), N-ethylmaleimide sensitive

fusion protein, and pyruvate kinase isozymes M1/M2 showed a preference of (*R*) versus (*S*) when compound 2 was used.

Table 3.6 The number of peptides identified with *R* versus *S* using compound 2

	Protein Description	**(*R*)**	**(*S*)**
	2 oxoglutarate dehydrogenase E1 component, mitochondrial precursor		2
	2',3' cyclic nucleotide 3' phosphodiesterase		4
	3-monooxygenase/tryptophan 5-monooxygenase activation protein gamma	3	3
	3-monooxygenase/tryptophan 5-monooxygenase activation protein sigma	2	2
	3-monooxygenase/tryptophan 5-monooxygenase activation protein zeta/delta	3	
	3-monooxygenase/tryptophan 5-monooxygenase activation protein zeta/delta		6
	Actin, cytoplasmic 1	23	21
	ADP/ATP translocase 1		8
	ADP/ATP translocase 2		5
	Alpha-enolase		2
	ATP synthase subunit alpha, mitochondrial precursor		9
	ATP synthase subunit beta		3
	Carbonic anhydrase 2		3
	Clathrin heavy chain		4
	Creatine kinase B-type		1
*	Dihydropyrimidinase related protein 2	6	
	Elongation factor 1-alpha 1		3
	Fructose-bisphosphate aldolase A		2
	G1 to S phase transition protein 1 homolog		1
	Gamma enolase	2	3
	Glyceraldehyde-3-phosphate dehydrogenase	1	6
	Guanine nucleotide-binding protein G(o) subunit alpha 1		2
	Heat shock cognate 71 kDa protein	4	3
	Heat shock protein 75 kDa, mitochondrial precursor		1
	Heat shock protein HSP 90-alpha		2
	Heat shock protein HSP 90-beta		2
	Hemoglobin subunit beta 1		1
	Histone (can not identify isoform)		2
	Malate dehydrogenase, cytoplasmic		1
	Malate dehydrogenase, mitochondrial precursor		3
	Myelin proteolipid protein	3	5
*	Pyruvate kinase isozymes M1/M2	3	
	Retinoblastoma-binding protein 6	1	
	Sodium/potassium-transporting ATPase subunit alpha 1 precursor		5
	Sodium/potassium-transporting ATPase subunit alpha 2 precursor	7	6
	Sodium/potassium-transporting ATPase subunit alpha 3	9	13

	Sodium/potassium-transporting ATPase subunit beta 1		1
	Structural maintenance of chromosomes protein 1A		1
*	Symplekin	2	
*	Syntaxin binding protein 1	3	
*	Triosephosphate isomerase	4	
	Ubiquinol cytochrome-c reductase complex core protein 2,		3
	Vang like protein 2	1	
*	N-ethylmaleimide sensitive fusion protein	3	

* Indicates proteins where more peptides were identified with the *R* versus the *S*

3.2.9 Prioritization of candidate target proteins

The proteomic search using mass spectrometry methods 1 and 2 identified numerous proteins that were labeled and enriched by compound 1 and 2 from mouse brain lysate. Each affinity bait identified a set of unique proteins, some of which showed apparent enrichment when the *R* enantiomer was used for labeling. Because it is impossible to study all these proteins simultaneously, the identified proteins were prioritized to choose the best potential drug target candidates for further examination. For every identified protein, a precedent for role in epilepsy or neurotransmission, pattern of expression in the brain, and involvement in signaling pathways were investigated further. The identified proteins were classified into five major groups based on their role in the cell: pre-synaptic vesicle regulation, actin/cytoskeleton dynamics, signaling proteins, cellular energetics, and housekeeping proteins (Figure 3.13).

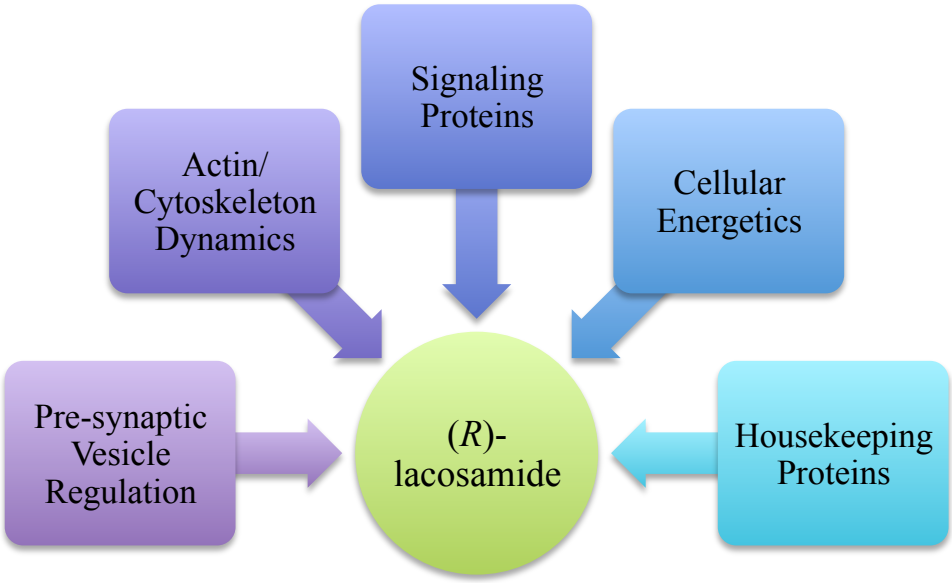

Figure 3.13 Classes of (*R*)-lacosamide interacting proteins identified from the proteome search. Proteins identified via mass spectrometry were grouped based on their cellular functions.

Eight proteins are involved in pre-synaptic regulation of neurotransmitter loaded vesicles and receptor mediated endocytosis: clathrin heavy chain (CLTC), clathrin light chain B (CLTB), ras related protein Rab 3A (RAB3A), ras related protein Rab 3D (RAB3D), syntaxin binding protein 1 (STXBP1), N-ethylmaleimide sensitive fusion protein (NSF), dynamin 1 (DNM1), and syntaxin 1B (STX1B). Of these 8 proteins, RAB3A, RAB3D, STXBP1, NSF, and STX1B are all intimately involved in the coordination of vesicle exocytosis via the soluble NSF attachment protein receptor (SNARE) complex.[163] RAB3A and RAB3D are small GTPases found on the outer membrane of synaptic vesicles that contribute to maintaining the pool of filled vesicles for release at the plasma membrane.[164] STXBP1 regulates SNARE complex formation and maturation while NSF dissembles the SNARE complex after exocytosis.[165,166] The identification of a number of synaptic proteins suggests that (*R*)-lacosamide may

modulate the rate of synaptic vesicle maturation and release, providing a novel intracellular mechanism for control of neurotransmission.

Eight proteins involved in cytoskeleton dynamics within the cell were identified: actin (ACTB), tubulin alpha 1A (TUBA1A), tubulin beta 2A (TUBB2A), tubulin beta 3 (TUBB3), cofilin 1 (CFL1), vang like protein 2 (VANGL2), dihydropyrimidinase related protein 2 (DPYSL2), and dihydropyrimidinase related protein 1 (DPYSL1). Actin and tubulin are ubiquitously expressed proteins that make up the cytoskeleton of all cells. In the brain, these proteins undergo constant remodeling at synapse terminals in response to stimuli and provide the scaffold for branching and connectivity during neurite outgrowth. CFL1 disassembles actin filaments in neurons and its inactivation through phosphorylation by LIM kinase 1 results in increased neurite outgrowth.[167]

VANGL2 mediates planar cell polarity as it relates to neural tube formation during development.[168] Microarray data has recently suggested a role for VANGL2 in nociception and may represent a novel drug target for pain management.[169] DPYSL1 and DPYSL2 are members of a protein family that are highly expressed during development and contribute to axon guidance.[170] Phosphorylation of DPYSL2 by glycogen synthase kinase-3β (GSK-3β) inactivates DPYSL2 and results in decreased axon outgrowth.[171] The identification of a group of proteins involved in remodeling of the cytoskeleton and their potential role in synaptic plasticity highlights the possibility that (*R*)-lacosamide may affect a neuron's response to repeated stimuli through alteration of cellular architecture.

A variety of other signaling proteins were also identified during the proteomic search including 2-monoxygenase/tryptophan 5-monooxygenase activation protein

(YWHA), calcium-independent alpha-latrotoxin receptor (LPHN2), guanine nucleotide-binding protein G_o subunit alpha 1 (GNAO1), and brain abundant membrane attached signal protein (BASP1). Several isoforms of YWHA, also known as 14-3-3, were captured with compounds 1 and 2. These proteins form dimers that bind phosphoserine or phosphothreonine residues in conserved motifs of target proteins. Recently, isoforms of YWHA have been shown to reduce inactivation of voltage dependent 2.2 calcium channels ($Ca_v2.2$).[172] Calcium-independent alpha-latrotoxin receptor (LPHN2) is a member of the latrophilin subfamily of G-protein coupled receptors. The endogenous ligand remains unknown, but the family of receptors has been shown to bind the latrotoxin, a black widow spider venom peptide, triggering vesicle exocytosis of GABA, glutamate or acetylcholine in a calcium independent fashion.[173]

Guanine nucleotide-binding protein G_o subunit alpha 1 (GNAO1) belongs to a class of signal transduction proteins coupled to transmembrane receptors that upon agonist activation switch from the inactivated GDP bound form to the activate GTP bound state and modulate downstream effector proteins.[174] $G_{\alpha o}$ and $G_{\alpha i}$ can comprise almost 1% of the total membrane protein in the brain. The major downstream effector of $G_{\alpha o}$ is adenylyl cyclase that upon binding, blocks the generation of the secondary messenger cyclic adenosine monophosphate (cAMP).[175]

Brain abundant membrane attached signal protein (BASP1) plays a role in neurite outgrowth through organization of lipid rafts at the plasma membrane.[176] Recruitment of BASP1 to the membrane via myristoylation results in reorganization of secondary messengers such at PIP_2 affecting the dynamics of the actin cytoskeleton. Collectively,

the identified signaling proteins provide numerous possible avenues for regulation of a variety of signaling pathways by (*R*)-lacosamide.

In the class of identified candidates involved in cellular energetics, 3 proteins stand out as interesting targets. Creatine kinase B (CKB) is a cytoplasmic enzyme responsible for generating energy reservoirs of rapidly accessible ATP through the synthesis of phosphocreatine.[177] Energy homeostasis has been shown to be important for proper neuron function and knockdown of creatine kinase in mice results in a decrease in seizures. It is hypothesized that the lack of available ATP required for energy intensive periods during seizure development and spread could play a role in the knockdown phenotype.[178]

Carbonic anhydrase 2 (CAR2), a validated target for other anticonvulsants such as topiramate and zonisamide, was also identified from the screen. In the cell, CAR2 and other carbonic anhydrase isoforms control pH and CO_2 homeostasis affecting biosynthetic pathways such as gluconeogenesis, lipogenesis, and ureagenesis. (*R*)-Lacosamide was shown recently to be a potent inhibitor (331 nM) of human CAR2, by interacting with the coumarin binding site on the protein.[179] This result suggests that CAR2 can interact with a structurally diverse set of ligands with various affinities.

In addition to CAR2, the alpha and beta subunits of the sodium/potassium-transporting ATPase (ATP1A, ATP1B) were identified. These proteins are involved in maintenance of electrochemical gradients in the cell by transporting monovalent cations across the plasma membrane. Mutations in ATP1A3 have been linked to a hyperexcitability phenotype in neurons of mice.[180] Clinically observed mutations in

ATP1A3 have also been attributed to a variety of neurological disorders, including rapid-onset dystonia, bipolar disorder, and Parkinsonism.[181]

Of the proteins discussed, DPYSL2, STXBP1, NSF, and ATP1A were chosen for further study because of their implications in epilepsy pathogenesis based on current literature. DPYSL2 was selected for additional study because an interaction with (*R*)-lacosamide has been suggested previously.[103] Its role in axonal guidance and neuronal sprouting also provides an interesting and novel mechanism for seizure control. STXBP1 and NSF were elected for further study because regulation of the SNARE complex could affect seizure development or pathways involved in neuropathic pain. Recent genetic analysis demonstrated that heterozygous missense mutations in the *stxbp1* gene could be associated with early infantile epileptic encephalopathy (EIEE).[182] STXPB1 and NSF were exclusively identified with the *R* enantiomer when compound 2 was used, a phenomenon that is consistent with the pharmacological data related to (*R*)-lacosamide and other functionalized amino acids. Finally, ATP1A was chosen because of the extensive clinical data associated with mutations in the protein resulting in neurological disorders as well as the availability of an enzymatic screen to assay protein function. The validation and characterization of these proteins with (*R*)-lacosamide are discussed in the following chapter.

3.3 Alternative approach to target discovery

The results of the proteomic screen identified numerous potential protein targets through affinity bait labeling and enrichment followed by mass spectrometry. The possibility of missing the endogenous target does remain, however. Biases from lysate

preparation, age of the animal tissue used, or instability of proteins may not provide comprehensive coverage of rare or non-abundant proteins. An alternative strategy was designed, therefore, to provide a means for candidate protein identification that allows for iterative enrichment of interacting proteins.

3.3.1 mRNA-display technology

mRNA-display is a protein selection technology that uses a protein-mRNA fusion molecule as the unit for *in vitro* selection. Creation of the mRNA-protein fusion is accomplished by synthesis of an mRNA template attached to a short DNA adapter molecule containing a 3′ puromycin, an antibiotic that mimics the 3′ end of aminoacyl tRNA. During *in vitro* translation, when the ribosome reaches the DNA linker, translation pauses and the puromycin enters the ribosomal "A" site and reacts with the C-terminus of the growing peptide. Incorporation of puromycin as the last amino acid in the nascent peptide results in the mRNA-protein fusion.

This fusion molecule is then purified from the ribosome complex and used for selection. Because the genotype and phenotype are covalently linked in a single molecule, target proteins isolated can be amplified and enriched through the mRNA portion of the molecule after each round of selection. Furthermore, because the mRNA-protein complex is created entirely *in vitro*, it circumvents the need for bacterial transformation allowing for rapid generation of large comprehensive libraries.

There are several advantages to using mRNA-display to identify drug-protein targets. The covalent linkage of the genotype to the phenotype allows for rapid identification of isolated proteins and enrichment of proteins that bind specifically to the

target of interest. No bacterial transformation is needed; large libraries can thus be generated easily from different experimental conditions. The diversity of each library may easily reach 10^{13} displayed proteins reflecting the diversity of all of the proteins and their domains in the proteome. Each gene will be represented multiple times in the library, allowing for a greater likelihood of retaining rare genes during selection. mRNA-display also allows for greater flexibility in selection conditions. *In vitro* selection permits for adjustments in cofactors, temperature, metal ions, chelating agents, pH, detergents, and ionic concentrations. Furthermore, *in vitro* protein expression also minimizes biases from mis-folding, post translation modification, or transport *in vivo*.

It is possible that some of the targets of (*R*)-lacosamide could be membrane bound receptors. Previous selections using mRNA-display for both human and C. *elegans* proteome libraries indicate that membrane bound proteins could be well displayed.[183,184] Selection of binding to calmodulin (CaM) identified many membrane bound proteins, including plasma membrane Ca^{2+}-ATPase, mitochondrial H^+ transporting ATP synthase, voltage gated sodium channel, receptor 5-hydroxytryptamine 2C, neurotransmitter-gated ion-channel subunit, and a receptor from the nicotinic family. Of these isolated membrane bound proteins, only the intracellular domains were identified during selection, presumably because calmodulin is a cytosolic intracellular protein. Moreover, proper folding of membrane bound proteins could be encouraged during *in vitro* translation in the presence of microsomal membrane, a technique that is widely used for *in vitro* expression of proteins whose function may rely on membrane insertion.

3.3.2 Library construction

Four mRNA-displayed mouse brain proteome libraries were created from four experimental conditions: normal (sham stimulated), (*R*)-lacosamide treated (20 mg/kg), 6 Hz stimulated (32 mA 3 sec), and 6 Hz stimulated (*R*)-lacosamide treated. Psychomotor seizure was induced in 3 to 5-month-old mice through corneal electrodes. After stimulation, the mice were sacrificed and brain tissue prepared according to established procedures. Total RNA was isolated from brains of mice treated with each experimental condition using Trizol RNA isolation followed by purification of mRNA with oligo d(T) cellulose from Ambion. Novagen's Orient Express cDNA synthesis kit was used for creation of cDNA.

Mouse brain mRNA (0.5 μg) was reversed transcribed by MMLV reverse transcriptase with 0.125 μg of a random hexamer oligo T primer (T_2N_6) at 37 °C for 1 hour, followed by second strand synthesis and digestion of RNA at 15 °C for 90 minutes with DNA polymerase I and RNase H respectively. Methylated dNTPs were used for first and second strand synthesis. DNA ends were flushed with T4 DNA polymerase in the presence of unmethylated dNTPs for 20 minutes at 11 °C. Flushed cDNA was ligated with directional linkers containing a 5' EcoR I and partial 3' Hind III site. Upon ligation, ends were digested with EcoR I and Hind III for 1 hour. Digested ends were ligated to the upstream (containing a T7 promoter, E Tag, and PKA recognition site) and the downstream anchor sequences (containing a His Tag, and Flag Tag, respectively). The resulting ligation products were size fractionated using SizeSep400 Spun Columns (GE Healthcare) pre-equilibrated with ligation buffer. The library was then amplified with Roche Expand Long Template PCR kit. Figure 3.14 shows total RNA, mRNA and the

cDNA libraries created for selection. The size distribution for each library ranges from transcripts below 500 bp to approximately 3 kb, suggesting each library contains complete coverage of all potential proteins in the mouse proteome.

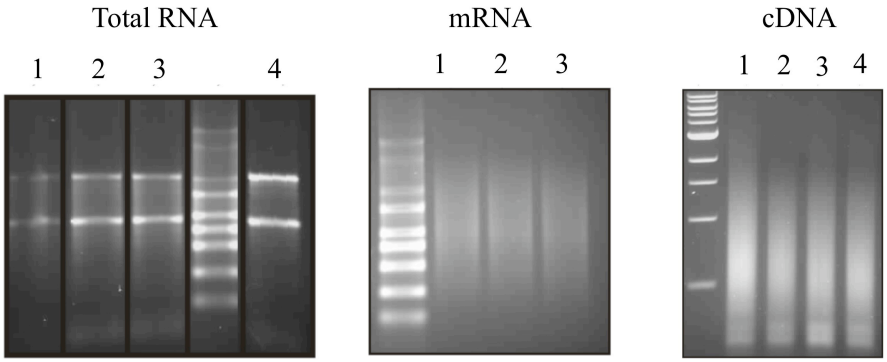

Figure 3.14 Total RNA, mRNA and cDNA libraries generated from individual tissue treatments. RNA was extracted from four experimental tissue treatments followed by generation of cDNA libaries using Orient Express cDNA synthesis kit (Novagen).

Each tissue treatment received a unique nucleotide tag incorporated into the downstream consensus region during PCR amplification of the ligated libraries (Figure 3.15). After incorporation of the tissue specific tag, the libraries were pooled. Following a potential selection the nucleic acid tag could be used to identify the library of origin for genes isolated.

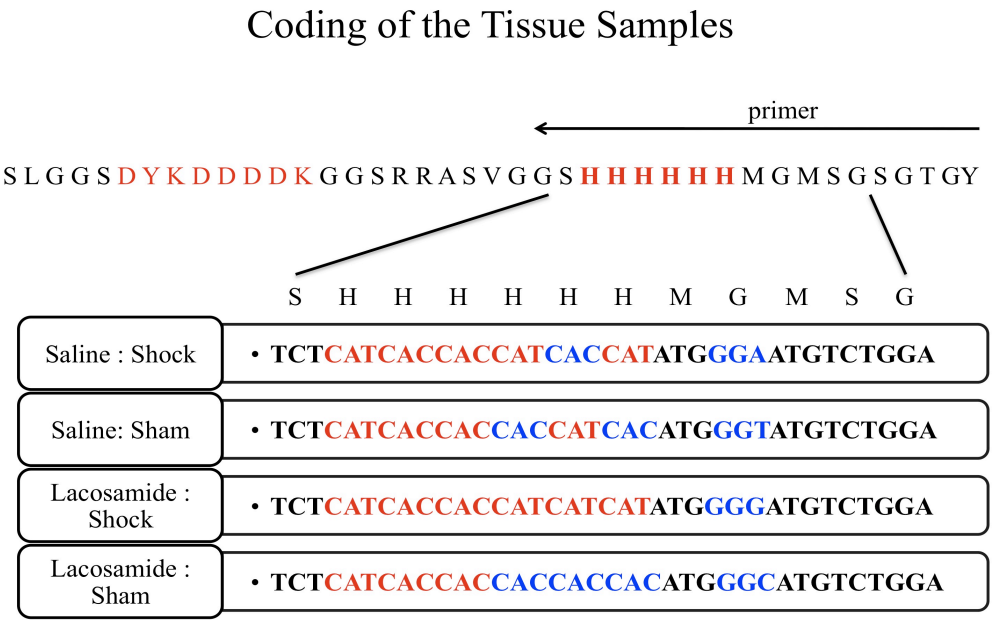

Figure 3.15 Strategy for encoding proteins displayed from individual libraries. cDNA from each tissue treatment was amplified with a primer containing a unique sequence in the region near the HIS tag.

3.3.3 Preparation of the libraries for *in vitro* selection

An mRNA-displayed library was generated using mRNA from four experimental treatments. One round of selection consists of seven major steps: transcription, 3' conjugation of a DNA-puromycin linker [psoralen-$(ATAGCCGGTG)_{2'\text{-Ome}}$-$dA_{15}$-CC-puromycin], *in vitro* translation and fusion, purification of fusion molecules based on FLAG tag, binding to target, capture of bound molecules, and PCR amplification of eluted molecules (Figure 3.16).

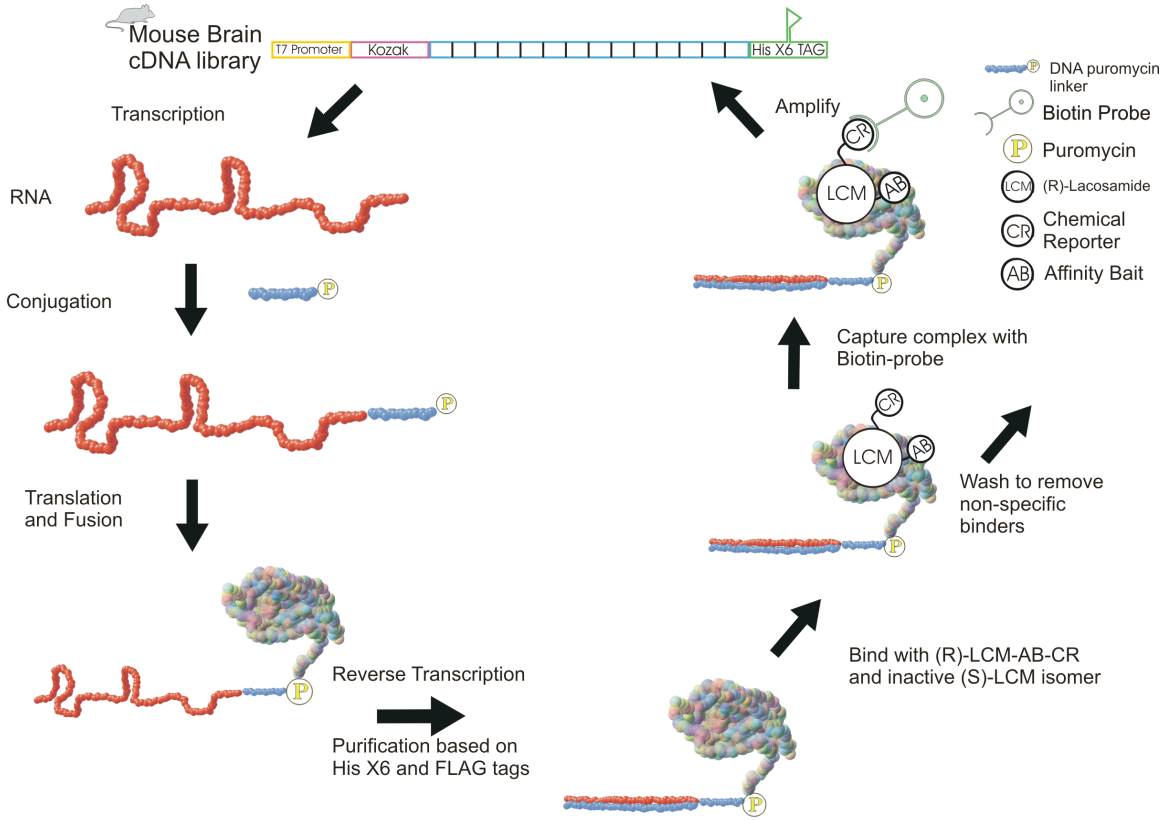

Figure 3.16 Selection scheme for identification of (*R*)-lacosamide-binding targets using mRNA-display. RNA is transcribed *in vitro* from the mouse brain cDNA library followed by conjugation with a puromycin containing DNA linker. The linked RNA is used for *in vitro* translation in rabbit reticulocyte lysate and purified using oligo d(T) and FLAG affinity tags. The purified fusion molecules are incubated with a lacosamide analog and captured using biotin streptavidin chemistry. The selected cDNA library is regenerated using the nucleic acid portion of the enriched molecules.

Prior to initiation of selection, out of frame transcripts were removed through generation and purification of the individual mRNA-displayed libraries, followed by regeneration of the new cDNA library. Each library was individually transcribed, fused, and translated, followed by purification using oligo d(T) and FLAG affinity tags. Efficiency of the purification steps was monitored by measurement of the radiolabeled fusion molecules. Elution profiles of the oligo d(T) and FLAG purification are shown in Figure 3.17. For the oligo d(T) purification, the percentage of counts was 4 times greater

for the library generated from the (*R*)-lacosamide/sham tissue treatment. Upon FLAG purification the percent recovery of eluted molecules from all libraries were equal at approximately 10%. Immediately following FLAG purification, the eluted cDNA libraries were regenerated and pooled together at equal molar concentrations.

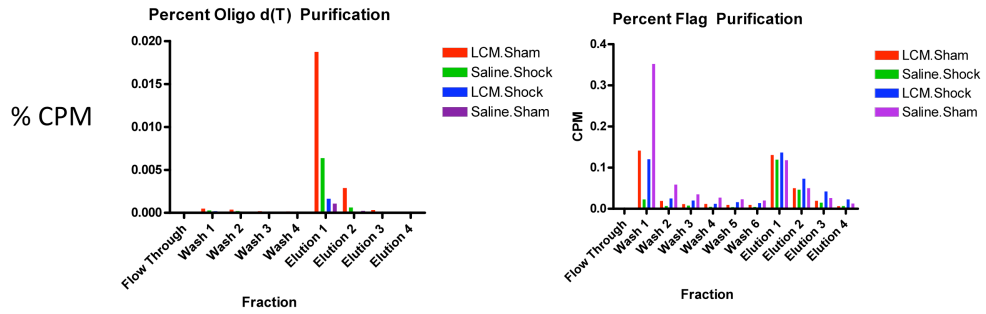

Figure 3.17 Elution profiles of individual cDNA libraries. Fusion molecules generated during the *in vitro* translation reaction are purified using 1 mg of oligo d(T) beads. The beads are washed four times with TBST buffer followed by elution of the captured molecules using distilled water. One percent of each fraction is counted for radioactivity to monitor the purification efficiency (left panel). Fusion molecules present in elution 1 for each library were further purified using anti-flag (M2) resin. After washing the resin six times with TBST, the bound molecules were eluted with TBST plus FLAG peptide (1 mg/ml). One percent of each fraction is counted for radioactivity to monitor the purification efficiency (right panel). The flowthrough fractions are omitted from the graph for clarity.

The results indicate successful creation of four libraries, each originating from separate experimental treatments that are suitable for an mRNA-display selection to identify (*R*)-lacosamide binding proteins. The pooled libraries contain total coverage of mRNAs expressed in mouse brain tissue with sizes ranging from less than 500 bp to greater than 3 kb. Utilization of the generated libraries for mRNA-displayed selection could be used to complement the mass spectrometry methods described here by identifying specific binding regions within individual proteins or by identifying rare proteins not found during the proteomic search.

3.4 Concluding remarks

Chemical biology approaches were applied to drug target discovery for the approved anticonvulsant (*R*)-lacosamide. Labeling techniques were developed for (*R*)-lacosamide derived probes, allowing for discrimination of sub-nanogram quantities of individual proteins with a TAMRA fluorescent probe within a complex mixture of mouse brain lysate. Using a preparation of mouse brain lysate containing both soluble and membrane bound proteins, proteins interacting with the lacosamide derived probes were specifically purified and enriched utilizing click chemistry with a biotin containing probe.

The enrichment of proteins was paired with two approaches for protein identification with mass spectrometry. Trypsinization of purified proteins captured on the beads provided the greatest diversity of identified proteins. The proteomic screening with biologically active lacosamide related probes identified approximately 73 unique proteins via mass spectrometry. The identified proteins included G-protein coupled receptors (GPCR), ion and small molecule transporters, cytosolic, and nuclear proteins.

The identified proteins could be segregated into 5 classes of proteins involved in synaptic vesicle regulation, cytoskeletal dynamics, cellular energetics, and housekeeping functions. Included in this list were two proteins that have already been validated or suggested to be (*R*)-lacosamide targets, CAR2 and DPYSL2 respectively.[103,179] The implications of this finding suggest that the methods developed can provide insight into the physiologically relevant network of (*R*)-lacosamide interacting proteins.

3.5 Materials and Methods

3.5.1 Synthesis of compounds and pharmacology

Compounds 1, 3, 4, 5 were synthesized as previously described.[107] Biological activity for compound 1 and 2 were evaluated by the National Institute of Health's Anticonvulsant Screening Program. Experiments were performed in male rodents (albino Carworth Farms no. 1 mice intraperitoneal route ip). Housing and care were in accordance with recommendations from the "Guide for the Care and Use of Laboratory Animals". Anticonvulsant activity was evaluated using the MES test and scMET test using previously reported methods.[153]

3.5.2 ELISA assay

Compound 1 (20 mM) in DMSO was immobilized in the wells of poly-lysine plates (Corning 3665) overnight at 4 ºC. The solution was removed and wells washed extensively with TBST (50 mM Tris pH 7.4, 150 mM NaCl, 0.1% Tween-20). Non-specific sites were blocked with 5% bovine serum album (Pierce) in TBST for 1 h at 4 ºC. After extensive washing with TBST, the cycloaddition reaction was initiated by sequential addition of probe 2 (20 mM) in DMSO, 500 μM TCEP (Pierce 20490) in water, 250 μM TBTA (Sigma-Aldrich 678937) in DMSO, and 1 mM $CuSO_4$ (Sigma-Aldrich 209201) in water. The reaction was allowed to proceed for 4 h at room temperature. After washing extensively (200 μl, 4 times) with TBST, streptavidin-HRP (Pierce N100) in TBST plus 5% BSA was added to each well. After incubation for 1 h at room temperature, the wells were washed extensively (200 μl, 4 times) with TBST followed by addition of o-phenylenediamine (OPD) substrate, 1 mg/ml (Pierce #34005)

dissolved in stable substrate buffer (Pierce #34062). The reaction was allowed to proceed for several minutes followed by addition of 10% H_2SO_4. Color absorbance (440 nm) was quantified with a Nanodrop 2000 (Thermo Scientific).

3.5.3 Preparation of mouse brain lysate

Mouse brains (male, 2 month, ICR, euthanized by CO_2, stripped of meninges (Rockland Immunochemicals)) were homogenized in 50 mM HEPES pH 7.4 followed by addition of 1% deoxycholate (Pierce 89904). The slurry was rotated at 37 ºC for 1 h followed by centrifugation at 100,000g. After centrifugation, 0.1% Triton X-100 was added to the supernatant and dialyzed overnight at 4 ºC against 3 L of 50 mM HEPES pH 7.4, 150 mM NaCl and 0.1% Triton X-100. The resulting liquid was centrifuged at 100,000g for 1 hour. The supernatant was collected and stored at -80 ºC until use.

3.5.4 In-gel fluorescence with compounds 1 and 2

For each reaction, 30 μl of mouse brain lysate was aliquoted into PCR strip tubes (VWR# 53509-304) followed by the addition of an appropriate amount of compound 1 or 2 (in DMSO). The reaction volume was brought up to 50 μl with distilled water. The reaction for compound 1 was allowed to proceed for the designated time at room temperature. For compound 2, the reaction was equilibrated in the dark at 4ºC followed by activation of the photoaffinity probe by exposure to UV light (312 nm Spectroline EB-280C, 115V, 60 Hz, 0.4 Amps) at distance of 2 millimeters for 10 minutes. The labeling reaction for compound 1 was terminated by addition of 4 mM methylhydrazine for 30 minutes. After labeling, cycloaddition reaction was initiated by 50 μM probe 1 (1 μl of 7

mM stock in DMSO), 500 μM TCEP (5 μl of 7 mM in water), 250 μM TBTA (0.87 μl of 20 mM stock in DMSO), and 1 mM $CuSO_4$ (5 μl of 14 mM stock in water). Samples were wrapped in foil and rotated at room temperature for 1 h followed by addition of 20 μl of 4X SDS-PAGE loading buffer. The samples were boiled at 95 ºC for 5 minutes followed by loading 10 μl to a 10% SDS-PAGE gel. Proteins were resolved at 180 volts for 50 minutes followed by washing the gel twice in distilled water for 5 minutes. The gel was scanned using a Typhoon Scanner (GE Healthcare) (excitation 532 nm / emission 580 nm).

3.5.5 Enrichment of labeled proteins with probe 2

Mouse brain lysate (500 μl per reaction) was pre-cleared of endogenously biotinylated proteins by the addition of 25 μl of high capacity streptavidin beads (Pierce 20357) and incubation at 4 ºC for 1 hour. Cleared supernatant was used for labeling with compounds 1 and 2 followed by cycloaddition with probe 2 as previously described. After the cycloaddition reaction, 25 μl of high capacity streptavidin resin was added and incubated for 2 hours at 4 ºC followed by centrifugation at 1,000 rpm for 1 minute. The supernatant was removed and the beads were sequentially washed twice with 1 ml 50 mM HEPES pH 7.4, 150 mM NaCl, 0.2 % SDS, then twice with 1 ml 6 M urea, and finally twice with 1 ml 50 mM HEPES pH 7.4, 150 mM NaCl. For in-gel studies, the beads were resuspended in 50 μl of SDS-PAGE loading buffer and boiled at 95 °C for 5 minutes. For trypsinization directly off the beads for mass spectrometry, the beads were washed with 1 ml of water and submitted for mass spectrometry analysis.

CHAPTER 4

CHARACTERIZATION OF COLLAPSIN RESPONSE MEDIATOR PROTEIN 2 AND OTHER CANDIDATE PROTEINS WITH LACOSAMIDE

4.1 Introduction

Chapter 3 described methods and experiments for selective labeling and capture of putative protein targets that interact with the anticonvulsant (*R*)-lacosamide via chemical biology and mass spectrometry methods. This approach circumvented extensive structural modification and the need for direct immobilization of the drug in order to minimize potential loss of binding affinity to its cognate targets *in vitro*. The proteomic screen generated a list of potential candidate drug targets, many of which provide plausible mechanisms for biological control of seizure disorder.

DPYSL2 (CRMP2), STXBP1 (MUNC18-1), NSF, and ATP1A (Na^+/K^+ ATPase) proteins were chosen for further study. Several general approaches are used to interrogate (*R*)-lacosamide's interaction with these proteins. This included tailoring experiments to individual protein biochemistry. The effect of (*R*)-lacosamide on the DPYSL2 interacting protein calmodulin (CAM) is also investigated.

4.2 Results and Discussion

4.2.1 Identified proteins and their associated pathways

Dihydropyrimidinase like Protein 2 (DPYSL2), also known as Collapsin Response Mediator Protein 2 (CRMP2) and Turned On After Division (TOAD-64), is a

member of a family of cytosolic regulatory proteins implicated in nervous system development and maintenance. Sharing approximately 50-60% sequence homology with dihydropyrimidinase, the 5-member family represents a protein class that has evolutionarily transitioned from an enzymatic role in the cell to a regulator of protein-protein interactions. In the nervous system, DPYSL2 is localized in growth cones and terminal regions of growing axons.[185,186] Its expression promotes axon outgrowth by modulating microtubule assembly through stimulation of tubulin GTPase activity.[185,187]

Overexpression of DPYSL2 results in the formation of multiple axons from both immature and fully mature dendrites. The C-terminal tail of DPYSL2 is a substrate for phosphorylation by CaMKII, Rho kinase, Cdk5 and GSK-3β. Phosphorylation of DPYSL2 by Rho-kinase, Cdk5 and GSK-3β has been shown to prevent binding to tubulin dimers, thereby disrupting the protein's association with microtubules.[171,188,189] Calcium dependent phosphorylation of DPYSL2 by CaMKII occurs after glutamate stimulation of the NMDA receptor, triggering activation of the MAP kinase signaling cascade.[190] Glutamate stimulation of the NMDA receptor also activates the calpain protease that cleaves the DYPSL2 protein at the N-terminus, resulting in a decrease of surface NR2B containing NMDA receptors.[191] The system provides a feedback loop for down regulation of the signaling cascade following glutamate insult and provides a potential mechanism for synaptic plasticity. Increased phosphorylation of DPYSL2 has also been correlated with early stages of Alzheimer's disease.[192]

The crystal structure for a C-terminal truncated DPYSL2 has been resolved at 2.4 Å and 1.9 Å in the presence and absence of the divalent cations Mg^{2+} and Ca^{2+}.[193,194] Both solution and crystal structures suggested metal dependent formation of

homotetramers and heterotetramers exclusively in the presence of Ca^{2+} or Mg^{2+}. A knockout for DPYSL2 has not been reported. DPYSL2 is also a reported calmodulin binding protein with affinities calculated in the low to mid micromolar range.[195] Mapping of the binding regions suggest the functional consequence of calmodulin-binding to DPYSL2 prevents tetramer formation as well as calpain mediated proteolysis.

In addition to its role in microtubule dynamics and axon development, DPYSL2 has been shown to colocalize with N-type calcium channels ($Ca_v2.2$) in immature synapses, growth cones, and dorsal root ganglion (DRG) neurons.[196] Overexpression of DPYSL2 enhanced calcium currents, activation kinetics and neuropeptide release, while siRNA-targeted knockdown of DPYSL2 reduced calcium currents.

STXBP1 and NSF are both proteins involved in synaptic vesicle exocytosis. This highly regulated process involves loading, docking, priming, and fusion of neurotransmitter-loaded vesicles in a calcium dependent fashion.[163] The major machinery for any membrane fusion event includes the core SNARE (Soluble NSF Attachment Receptor) complex comprised of syntaxin-1, SNAP-25, and synaptobrevin proteins. STXBP1 can bind syntaxin-1 in both the "closed" (SNARE inaccessible) conformation and the "open" (SNARE accessible) conformation acting as a key regulator of docking, priming, and fusion. After vesicle fusion, NSF, present at the synapse terminal disassembles the SNARE complex in an ATP dependent fashion. Genetic knockout of STXBP1 in mice leads to a complete loss of neurotransmitter secretion and animals die immediately after birth.[197]

Several clinically observed mutations in STXBP1 have been reported with functional consequences related to seizures. *De novo* mutations in several exons of

STXBP1 were identified in a patient suffering from early infantile epileptic encephalopathy.[182] One mutation (C180Y) in exon 7 resulted in destabilization of the secondary structure of STXBP1 correlating to a decreased binding affinity to the open form of syntaxin-1A (STX1A).

In a separate study, two mutations in STXBP1 were identified from a cohort of 95 patients with mental retardation and non-syndromic epilepsy.[198] One mutation resulted in alteration of the intron splicing site between exon 3 and 4 leading to a longer improperly processed allele transcript containing 7 new amino acids followed by a premature stop codon. The second mutation identified resulted in a premature stop in the coding region of exon 14. The mutations are located in domains that form the cavity for syntaxin-1 binding. Both patients suffered from seizures at early ages and were currently under treatment with anticonvulsants such as phenobarbital, carbamazepine, and clobazam. One patient continues to have 3 seizures per day despite a regimen of multiple anticonvulsants. The clinical association between mutations in STXBP1 and epilepsy highlights its critical role in proper regulation of synaptic transmission and potential as a candidate protein for seizure control.

N-Ethylmaleimide sensitive fusion protein (NSF) is a hexameric protein originally thought to be exclusively associated with membrane fusion but has recently been implicated in a variety of cellular processes. NSF functions as a chaperone for the SNARE complex, regulating its recycling through ATP dependent disassociation of syntaxin, SNAP-25, and synatobrevin post-fusion. The ATPase activity and oligomeric state of NSF is regulated via phosphorylation. Phosphorylation by PKC at Ser237 slows ATP hydrolysis.[199] CDK16 (Pctaire1) phosphorylates NSF at Ser569 within the interface

between monomers preventing oligomerization, thereby potentially providing a mechanism to regulate exocytosis.[200] Overexpression of an ATPase dead mutant of NSF in neurons results in sprouting and overgrowth at neuromuscular junctions.[201] This surprising phenotype is also observed with overexpression of DPYSL2.

In addition to binding SNARE proteins, NSF interacts with cell surface signaling receptors, intracellular proteins, and cytoskeletal elements. Using a yeast two-hybrid system, NSF was found to bind the C-terminal tail of the AMPA receptor, a ligand gated ionotropic excitatory glutamate receptor present in the CNS.[202] The calcium dependent interaction helps tune synaptic strength by maintaining AMPA receptors at the membrane.[203] Disruption of the interaction results in a decrease of miniature excitatory postsynaptic currents (mEPSCs) in cultured hippocampal neurons.

NSF also binds to the intracellular domain of the $GABA_A$ and $GABA_B$ receptors forming a heterotrimeric complex at the postsynaptic membrane.[204,205] Association among the three proteins allows for agonist induced desensitization after stimulation with GABA through recruitment of protein kinase C (PKC) to the membrane which phosphorylates the receptor complex. This property, independent from its role in membrane fusion events, illustrates NSF's role as a modulator of receptor function. Significant interactions have also been illustrated between NSF and D1 and D5 dopamine receptors, β2-adrenergic receptor, M1, M3, M4, and M5 muscarinic recptors.[206-209] These interactions largely relate to receptor recycling and sorting through NSF binding to their intracellular domains.

NSF also binds several members of the small GTPase proteins of the ras-related in brain (Rab) family. This class of proteins are expressed and targeted to different

organelles in the cell regulating the tethering of vesicles for a variety of membrane fusion events.[210] NSF has been shown to intereact with Rab 3, 4, 5, 6 and 11 with NSF. It has been found that Rab 3, 4 and 6 all bind and stimulate the ATPase activity of NSF *in vivo*. The physiological consequences of these interactions are not well understood, but the finding implicates NSF as a regulator of not only vesicle fusion but also intracellular vesicle trafficking.

The final protein chosen for further study was the Na^+/K^+ Transporting ATPase (ATP1A). These integral membrane protein pumps maintain electrochemical gradients through export of three sodium ions and import of two potassium ions at the plasma membrane during one exchange cycle. The complete pump consists of a 110 kDa α-subunit and a 41 kDa β-subunit. Four genes encode the alpha subunit (ATP1A1, ATP1A2, ATP1A3, ATP1A4) that has 10 transmembrane regions.[211] Cardiac glycosides, such as ouabain are natural inhibitors of pump activity that alter neuronal functions *in vitro* and *in vivo*.

Extensive mutations have been identified in genes encoding ATP1A1, ATP1A2, and ATP1A3 that correlate with a variety of neurological disorders. Mutations in ATP1A1, ATP1A2, and ATP1A3 are associated with bipolar disorder.[212] Thirty-nine mutations have been clinically observed in ATP1A2 for patients suffering from familial hemiplegic migraine (FHM2), an autosomal dominant subtype of migraine characterized by migraines with aura including hemiparesis, ataxia, coma, or epileptic seizures.[213,214] The mutations are scattered throughout the proteins extracellular, transmembrane, ATP-binding, and intracellular regions affecting a wide range of pump functionalities, including Na^+ and K^+ ion affinity, ATP-binding, and catalytic turnover.

Five mutations have been reported in ATP1A2 for sporadic hemiplegic migraine (SHM), a migraine disorder in which no first degree relative has similar symptoms.[213] Seven mutations in ATP1A3 are reportedly associated with rapid-onset dystonia Parkinsonism, a syndrome characterized by the abrupt onset of slow movement, altered speech and poor balance. Collectively, the disregulation of pump activity observed by genetic mutation illustrates their effects on neuronal excitability and the importance of maintaining proper electrochemical gradients.

4.2.2 Probing for DPYSL2 in mouse brain lysate

Initial studies investigated the ability of compounds 1 and 2 to label DPYSL2.[103] Soluble mouse brain lysate was labeled with compound 1 (50 μM) for 1 hour followed by click chemistry with probe 1. TAMRA labeled proteins were resolved on an SDS-PAGE gel followed by transfer to a nitrocellulose membrane. After immunoblotting with an antibody recognizing DPYSL2, TAMRA labeled proteins and DPYSL2 were simultaneously detected. The composite image reveals that one of the major bands in the lysate corresponds to DPYSL2 that was detected by both the anti-DPYSL2 antibody and the TAMRA probe (Figure 4.1). The molecular weight of the band corresponds to a truncated version of DPYSL2, (52-55 kDa), suggesting that proteolysis of the full-length DPYSL2 may take place during lysate preparation or during the labeling reaction.

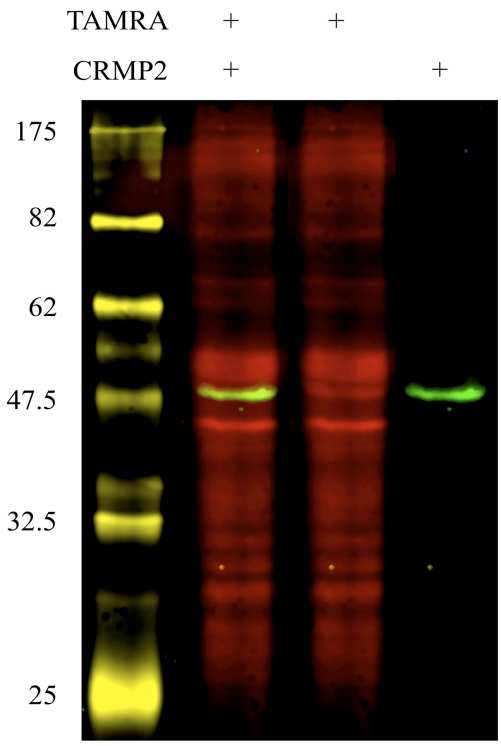

Figure 4.1 Fluorescent western blot detecting DPYSL2 (green) and TAMRA labeled proteins (red). Soluble mouse brain lysate was incubated with compound 1 for 1 hour at room temperature followed by click chemistry with probe 1. Proteins were resolved on a 10% gel followed by transferred to a nitrocellulose membrane. An antibody for DPYSL2 was used to detect the presence of DPYSL2 protein. A Cy5-labeled goat anti-mouse secondary antibody was used to visualize DPYSL2. The nitrocellulose membrane was scanned for DPYSL2 (ex.: 633 nm / em.: 670 nm) and lacosamide adducted proteins (ex.: 532 nm / em.: 580 nm).

The ability of compound 3 to purify endogenous DPYSL2 from mouse brain lysate was investigated next. It was shown previously through in-gel fluorescence that compound 1 labeled a variety of bands in mouse brain lysate as detected by the TAMRA probe (probe 1), including DPYSL2. Fluorescent western blotting for DPYSL2 (Figure 4.1) illustrated an overlap of signal between one strongly labeled protein in the mouse brain lysate and the DPYSL2 antibody signal suggesting that compound 1 labels

endogenous DPYSL2. Without purification of the adducted proteins, however, a single band in the lysate mixture could contain numerous individual proteins.

To evaluate more critically the labeling of endogenous DPYSL2 by the (*R*)-lacosamide derived probes, adducted proteins were purified using biotin streptavidin chemistry followed by probing for the presence of DPYSL2. Using 40 μM of compound 3, proteins were labeled in the presence or absence of an excess of (*S*)-lacosamide followed by purification with streptavidin beads and immunoblotting for DPYSL2 (Figure 4.2). Results indicate that the isothiocyanate affinity bait captures DPYSL2 and that the presence of (*S*)-lacosamide blocks the protein recovery in a dose dependent fashion. Furthermore, the destruction of the isothiocyanate by the addition of methylhydrazine completely blocks the capture of DPYSL2. The affinity bait is therefore essential for maintaining the interaction between DPYSL2 and compound 3.

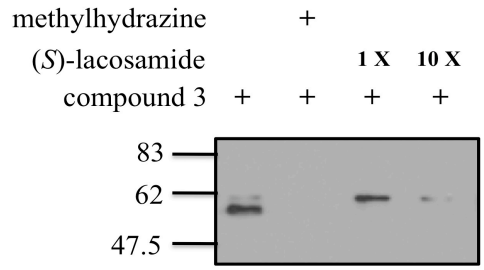

Figure 4.2 Western blot analysis of DPYSL2 from mouse brain lysate captured by compound 3. Compound 3 (40 μM) was reacted with soluble mouse brain lysate (2 mg/ml) for 1 hour at room temperature in the presence of absence of (*S*)-lacosamide. Methylhydrazine was incubated with compound 3 prior to its addition to the lysate for lane 2. Adducted proteins were captured by the addition of 50 μl of streptavidin beads for 1 hour at 4 °C. The beads were washed 10 times and proteins were resolved on a 10% SDS-PAGE gel then transferred to a nitrocellulose membrane followed by immunoblotting for DPYSL2.

4.2.3 Expression and purification of DPYSL2 in *E. coli*

Characterizeing more thoroughly the interaction between (*R*)-lacosamide and the candidate proteins requires a source for pure protein with high quality. Overexpression of proteins in *E. coli* provides a rapid facile means to generate and purify recombinant protein suitable for a variety of biochemical studies. Successful overexpression of DPYSL2 using both GST affinity tags and 6X histidine tags has been reported previously for biochemical investigation and crystal structure determination.[193,188] For the biochemical studies described here, an N-terminal GST-tag and C-terminal HIS tag constructs were created. DPSYSL2 was amplified from a mouse brain cDNA library and insert into pET41 (N terminal GST-tag) or pET28b (C terminal HIS-tag). Sequence verified clones were transformed into Rosetta™ (BL21-DE3) cells for overexpression.

Both constructs allowed for efficient expression and purification of recombinant DPYSL2 fusion protein. The C-terminal HIS tag can purify more full-length DPYSL2 protein by preventing purification of C-terminal truncated isoforms. Column chromatography purification of the GST-DPYSL2 suggested the protein, in solution at high concentrations, migrates at an octamer based on comparison with the migration of known protein standards (Figure 4.3). Stenmark and coworkers determined the crystal structure of DPYSL2 revealing that it forms homotetramers. The apparent migration of the recombinant DPYSL2, therefore, may be an artifact of the tetramer migration on the column or the result of association of two tetramers in solution.

A

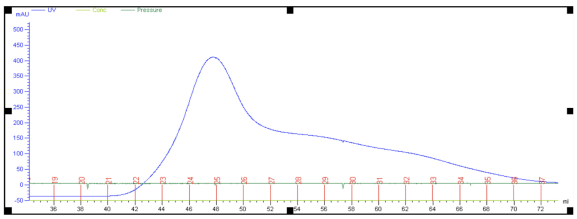

B

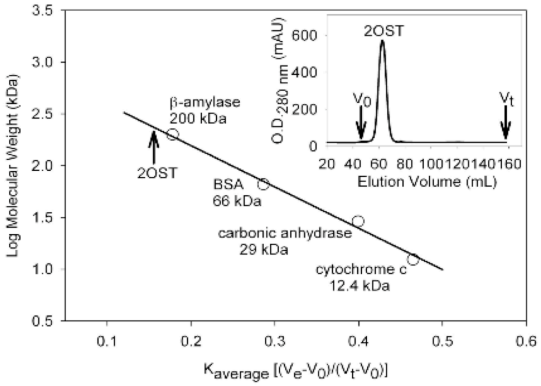

V_{void}= 45 mls
V_{total}= 157.5 mls
$V_{elution}$= 48 mls

$$K_{average} = \frac{(V_e - V_o)}{(V_t - V_o)}$$

Y=(-3.87)(0.0267)+2.93

Y = 2.83 = log MW

MW = 676 kDa

Actual Monomer = 85 kDa for truncated DPYSL2

Figure 4.3 Purification of GST-DPYSL2. (A) Elution profile of GST-DPYSL2 suggests that it migrates as an octamer in solution. (B) $K_{average}$ of proteins with known sizes used to generate a standard curve for calculation of MW (from reference [215]). Calculation of MW using the elution volume of 48 mls suggests that in solution GST-DPYSL2 appears to migrate as an octomer with an apparent molecular weight of 676 kDa.

4.2.4 Functionality of overexpressed DPYSL2

The involvement of DPYSL2 in axonal growth and branching has been linked to its interaction with tubulin heterodimers. The promotion of microtubule formation *in vitro* is considered one hallmark of DPYSL2 activity.[185] To assess the functionality of the recombinant DPYSL2-HIS protein, tubulin polymerization as measured by a change in absorbance at 340 nm was used. The change in OD of purified tubulin in the presence or absence of DPSYSL-HIS protein was evaluated over 1 hour. The results showed an increase in polymerization when 10 μM of DPYSL2-HIS protein was added to the reaction (Figure 4.4).

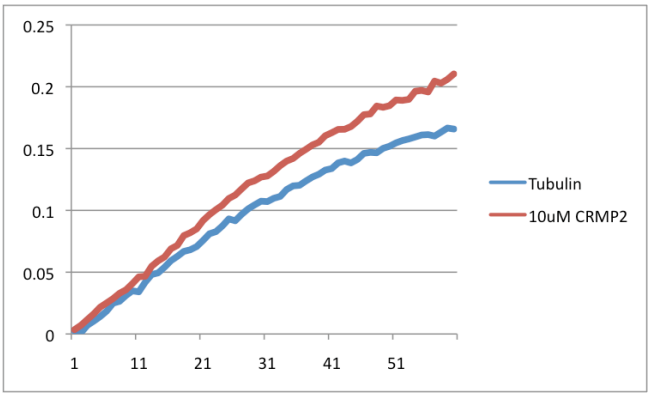

Figure 4.4 DPYSL2-HIS promotes tubulin polymerization *in vitro*. 45 µl of purified tubulin (1 mg/ml) in 80 mM PIPES pH 6.9, 1 mM $MgCl_2$, 1 mM EGTA, and 1 mM GTP was added to a 384 well plate prewarmed to 37 °C containing 10 µM DPYSL2-HIS protein. After brief mixing, the change in OD_{340} was monitored every 30 seconds for 1 hour.

These results are consistent with previous reports that DPYSL2 shows modest polymerization of microtubules suggesting that the recombinant protein is properly folded and functional.[187] Validation of functionality allows for characterization of the interaction between (*R*)-lacosamide and the recombinant protein.

4.2.5 Fluorescent labeling of GST-DPYSL2 by lacosamide probes

The purified recombinant protein permits utilization of the TAMRA probe (probe 1) for *in vitro* labeling to evaluate quantitatively the amount of adduction via in-gel fluorescence. The ability of compound 1 and 2 to label GST-DPYSL2 was evaluated in the induced soluble *E. coli* lysate, GST-column elution fractions, and glutathione free (buffer exchanged) fractions. For induced soluble *E. coli* lysate, cells were collected by centrifugation at 1,000 rpm followed by resuspension of the pellet in a buffer containing 50 mM HEPES pH 7.4 and 150 mM NaCl. Cells were sonicated 3 times and insoluble material removed by centrifugation at 14,000 rpm. Supernatant was used directly for

labeling reactions or purification of GST-fusion proteins with glutathione beads. Elution fractions containing 10 mM glutathione from affinity purification were utilized for labeling reactions or buffer exchanged into 50 mM HEPES pH 7.4 and 150 mM NaCl with a size exclusion column.

Labeling the lysate, elution fraction, and buffer exchanged fractions showed both the nucleophilic and photoaffinity baits resulted in labeling of GST-DPYSL in the soluble lysate using 50 μM of compounds 1 and 2 (Figure 4.5). The nucleophilic isothiocyanate labels the fusion protein to a greater extent than the photoaffinity probe under the same conditions.

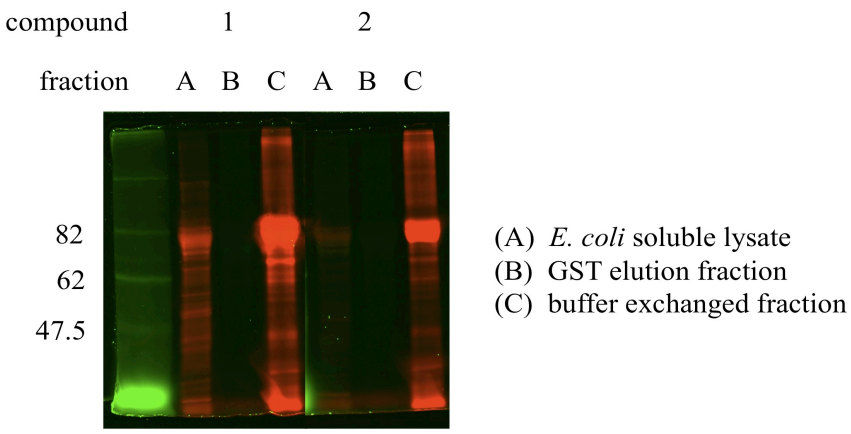

Figure 4.5 In-gel fluorescent labeling of GST-DPYSL2 by compounds 1 and 2. 10μl of protein fractions from GST-DPYSL2 expression were incubated with compounds 1 or 2 (50 μM) for 1 hour at room temperature. Compound 2 was activated for 10 minutes at 312 nm at 4 °C. Adducted proteins were tagged using click chemistry for 1 hour with probe 1. Proteins were resolved on a 10% SDS-PAGE gel followed by in-gel fluorescence (ex.: 532 nm / em.: 580 nm).

Compound 1 also shows substantial reactivity to numerous proteins in the soluble *E. coli* lysate illustrating the high possibility that some of the proteins identified via mass spectrometry are false positives. The reactivity of compound 1, however, does not

directly correlate with abundant proteins in the lysate based on stains for total protein, demonstrating that protein concentration alone does not confer reactivity to the probe. It suggests instead that successful adduction requires a specific interaction between the chemical probe and protein in order for efficient labeling to occur. Compound 2 shows less overall labeling of the lysate fraction with only modest labeling of GST-DPYSL2. Non-specific reactivity of compound 2 is difficult to judge based upon the overall low reactivity.

Labeling of the GST-elution fraction with compounds 1 and 2 demonstrates that the presence of 10 mM glutathione completely blocks the labeling reaction. The phenomenon likely results from destruction of the affinity bait present on each molecule by glutathione. Reaction of glutathione with the isothiocyanate and aromatic azide generates a dithiocarbamate and aromatic amine, respectively, rendering them non-reactive to proteins. Reaction of the activated nitrene with glutathione would also render the affinity bait inactive and reduces the effective labeling of compound 2. Pre-removal of glutathione via buffer exchange restores reactivity of both compounds toward GST-DPYSL2. The extent of labeling between compounds 1 and 2 was equivalent in contrast to the *E. coli* lysate fraction in which a large difference in labeling toward the same protein was observed. Collectively, the in-gel fluorescence results indicate that upon removal of glutathione, both affinity baits strongly label GST-DPYSL2 and that the protein can be successfully used to study the interaction with (*R*)-lacosamide.

The sensitivity of probe 1 in detecting the drug-protein adducts and the amount of protein needed were investigated using purified proteins. Dose dependent labeling from 24 μM to 0.375 μM for compound 1 and 2 showed linear fluorescent labeling across the

dose range with adduction detectable using nanomolar concentrations of drug and 10 μM protein (Figure 4.6). No background fluorescence was seen in the absence of either compound. Using 3 μM of compound 1 the detection limit of protein was approximately 1 μM.

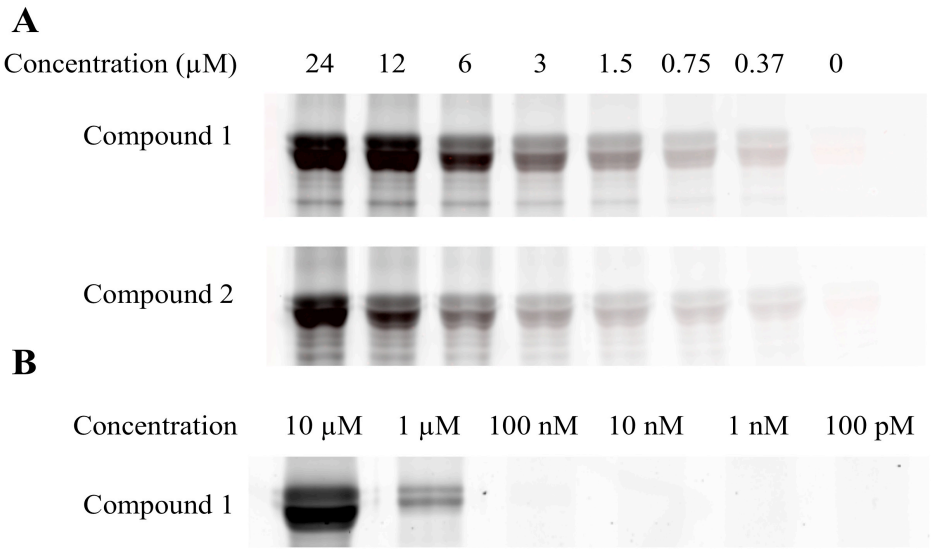

Figure 4.6 In-gel fluorescence illustrating dose dependent labeling of GST-DPYSL2. (A) 10 μl of purified GST-DPYSL2 protein (10 μM in 50 mM HEPES, 150 mM NaCl pH 7.4) was incubated with compound 1 or 2 for 1 hour at room temperature. Samples incubated with compound 2 were activated with UV light (312 nm) for 10 minutes at 4 °C. Click chemistry was performed with probe 1 for 1 hour at room temperature. (B) GST-DPYSL2 protein was diluted from 10 μM to 100 pM in 50 mM HEPES, 150 mM NaCl pH 7.4 then reacted with 3 μM of compound 1 for 1 hour at room temperature. Click chemistry was performed with probe 1 for 1 hour at room temperature. For all samples 5 μl of SDS-PAGE loading buffer was added to reaction after click chemistry and samples boiled for 5 minutes at 95 °C. Proteins were resolved on a 10% SDS-PAGE gel and scanned for in-gel fluorescence (ex.: 532 nm / em.: 580 nm).

4.2.6 Competition with (*R*)-lacosamide and (*S*)-lacosamide

The development of conditions for labeling and detection for GST-DPYSL2 permitted the interrogation of competition with unmodified versions of (*R*)-lacosamide and (*S*)-lacosamide. This approach is used frequently in radioligand binding assays

wherein a specific amount of radiolabeled drug is competed by varying amounts of unlabeled compound. This method, termed homologous competition, has several criteria for accurate K_d measurement.

First, the receptor must have equal affinity for both the labeled and unlabeled ligands. In the case of the AB and CR modified compounds, affinity for the protein targets is unknown. Biological activity provides the only insight for compound efficacy. Although the modified compounds 1 and 2 show diminished activity in animals (ED_{50} 45 and 20 mg/kg respectively, versus 4.5 mg/kg for (*R*)-lacosamide), it is not known whether these activity values represent decreased affinity for the cognate protein target(s) or contributing effects from altered metabolism, transport, pharmacokinetics, or efflux. The homologous competition design provides, therefore, a simple though imperfect assessment of affinity.

In addition to the assumption of equal affinity between radiolabeled and unlabeled ligands, the assay assumes that there is no cooperative binding, no ligand depletion from binding to the receptor, and that non-specific binding will increase proportionally with the amount of labeled ligand added. Under the assay conditions described in the previous section, it is predicted that these assumptions will be true based on the fact that the drug is in molar excess to the protein and that dose dependent labeling is observed when the drug concentration is increased. In the instance of these in-gel fluorescent experiments, the IC_{50} is the concentration of competing ligand at which fluorescent intensity is reduced by 50%. The labeled ligand concentration equals the concentration of AB and CR probe used in the reaction.

Successful competition between an AB and CR probe and (*R*)-lacosamide or its enantiomer requires careful titration of probe reactivity toward the target protein. Competition between binding of (*R*)-lacosamide and the adduction of the AB and CR probe represent two distinct reactions, a reversible and an irreversible binding event. The choice of the affinity bait used for competition reactions should afford tight temporal control of reactivity to allow for total equilibration between the reactive lacosamide analog and the unmodified drug with the target protein. To this end, compound 2 containing the photo-activated aromatic azide was chosen for use in these competition experiments. The photoaffinity probe is unreactive to proteins until specific activation by UV light that can be controlled in both time and intensity. In theory, this allows for a period of equilibration between the labeled and unlabeled compounds to find binding sites present on the protein followed by a short activation of the AB unit to create the adduct.

The use of compound 2 to label GST-DPYSL2 in the presence of increasing concentrations of (*R*) or (*S*)-lacosamide ranging from 1.5 μM to 30 mM revealed a sigmoidal decrease in labeling in the presence of (*R*)-lacosamide but not (*S*)-lacosamide (Figure 4.7). Each sample was repeated in duplicate were resolved on the same gel. The graphed values represent the average normalized pixel intensities calculated for each concentration. The IC_{50} for (*R*)-lacosamide under the assay conditions was calculated to be 451 μM. The high IC_{50} might suggest that the assumptions required for the homologous competition experiment, such as equal affinity between labeled and unlabeled compounds, may not be met. Furthermore, the irreversible adduction reaction

between compound 2 and the protein may mask true binding affinity of the unmodified compound.

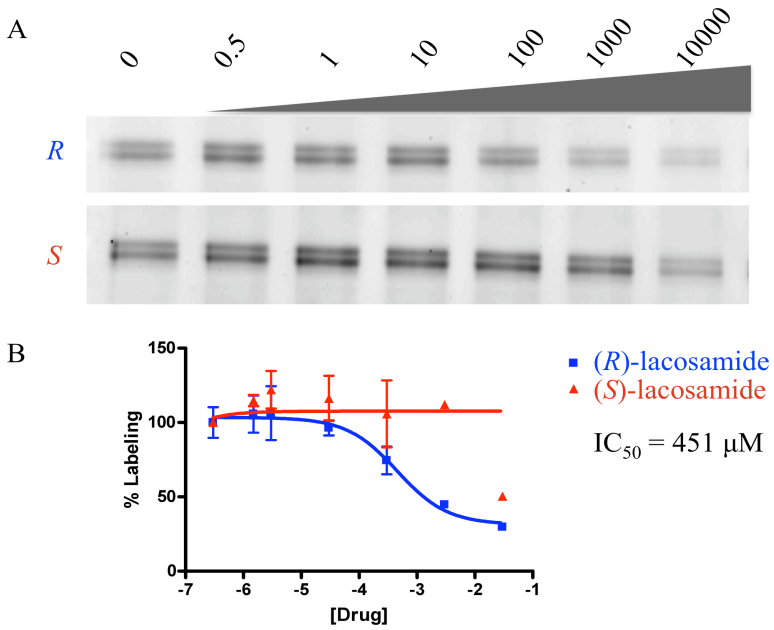

Figure 4.7 Homologous competition assay with GST-DPYSL2. (A) Compound 2 (3 µM) was added to a mastermix of GST-DPYSL2 protein diluted to 1 µM in 50 mM HEPES, 150 mM NaCl pH 7.4. 10 µl of master mix was aliquoted per reaction followed by addition of (*R*) or (*S*)-lacosamide (3 µM to 30 mM). The reactions were incubated for 3 hours at 4 °C followed by photoactivation at 312 nm for 10 minutes on ice. Cycloaddition was initiated by addition of 24 µM probe 1 (0.1 µl of 2.4 mM stock in DMSO), 500 µM of TCEP (5 µl of 1 mM stock in water), 250 µM TBTA (0.625 µl of a 4 mM stock in DMSO) and 1mM $CuSO_4$ (1 µl of a 10 mM stock in water). The reaction was allowed to proceed for 1 hour at room temperature followed by addition of 5 µl of 4X SDS-PAGE loading buffer. Samples were boiled at 95 °C for 5 minutes and the entire sample was loaded to a 10% SDS-PAGE gel. Gels were washed to twice with water for 5 minutes then visualized by fluorescent scanning (ex.: 532 nm / em.: 580 nm). (B) Pixel intensities were quantified using ImageJ (NIH) and curves generated using GraphPad (Prism). Each concentration was repeated in duplicate and graphed values represent the average pixel intensity calculated at each concentration.

In contrast to GST-DPYSL2, two control proteins were also analyzed for labeling by compound 2 in the presence of competing ligands. Enolase, a protein identified during the proteomic screening, represents a potential false positive that was identified by

showing inherent reactivity toward the affinity bait and not a specific interaction with the lacosamide scaffold. Under the same reaction conditions, commercial enolase protein showed modest labeling by compound 2 as detected by in-gel fluorescence. In the presence of excess concentrations of (*R*) and (*S*) lacosamide, however, labeling was diminished in a linear fashion consistent with adduction resulting from a non-specific interaction (Figure 4.8). This trend appears different from the apparent sigmoidal competition curves observed with GST-DPYSL2.

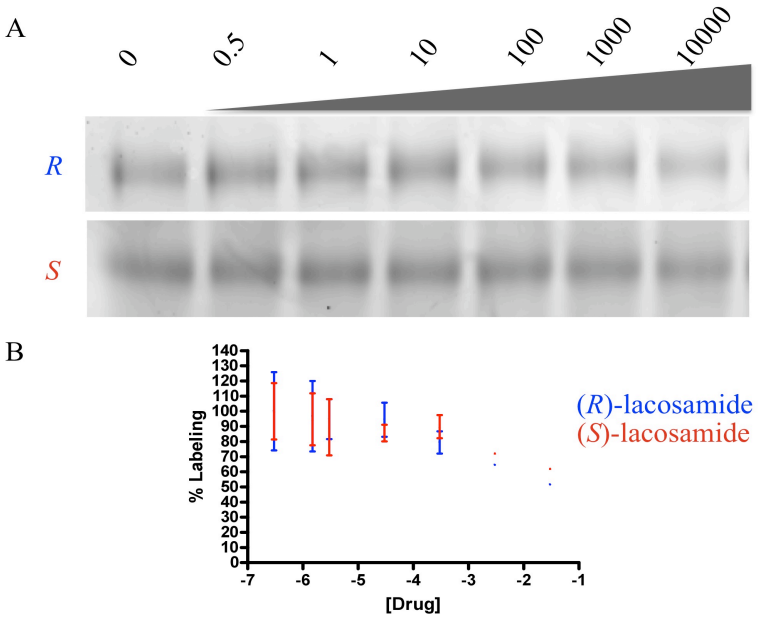

Figure 4.8 Homologous competition assay using enolase protein. (A) Compound 2 (3 μM) was added to a mastermix of enolase protein diluted to 1 μM in 50 mM HEPES, 150 mM NaCl pH 7.4. 10 μl of master mix was aliquoted per reaction followed by addition of (*R*) or (*S*)-lacosamide (3 μM to 30 mM). The reactions were incubated for 3 hours at 4 °C followed by photoactivation at 312 nm for 10 minutes on ice. Cycloaddition was initiated by addition of 24 μM probe 1 (0.1 μl of 2.4 mM stock in DMSO), 500 μM of TCEP (5 μl of 1 mM stock in water), 250 μM TBTA (0.625 μl of a 4 mM stock in DMSO) and 1mM $CuSO_4$ (1 μl of a 10 mM stock in water). The reaction was allowed to proceed for 1 hour at room temperature followed by addition of 5 μl of 4X SDS-PAGE loading buffer. Samples were boiled at 95 °C for 5 minutes and the entire sample was loaded to a 10% SDS-PAGE gel. Gels were washed to twice with water for 5 minutes then visualized by fluorescent scanning (ex.: 532 nm / em.: 580 nm). (B) Pixel intensities were quantified using ImageJ (NIH) and curves generated using GraphPad (Prism). Each

concentration was repeated in duplicate and graphed values represent the average pixel intensity calculated at each concentration.

The second control protein evaluated, bovine serum album (BSA), represents a protein that was not identified during the proteomic screen and can be used to assess the unbiased reactivity of a general protein to the photoaffinity probe. Results show only weak labeling by compound 2 and no obvious trend in competition (Figure 4.9). This suggests that compound 2 does not indiscriminately label all proteins in the proteome equally. Of the proteins that are labeled, some show sigmoidal dose dependent competition with (*R*)-lacosamide while others simply possess favorable interactions for adduction by the photoaffinity probe.

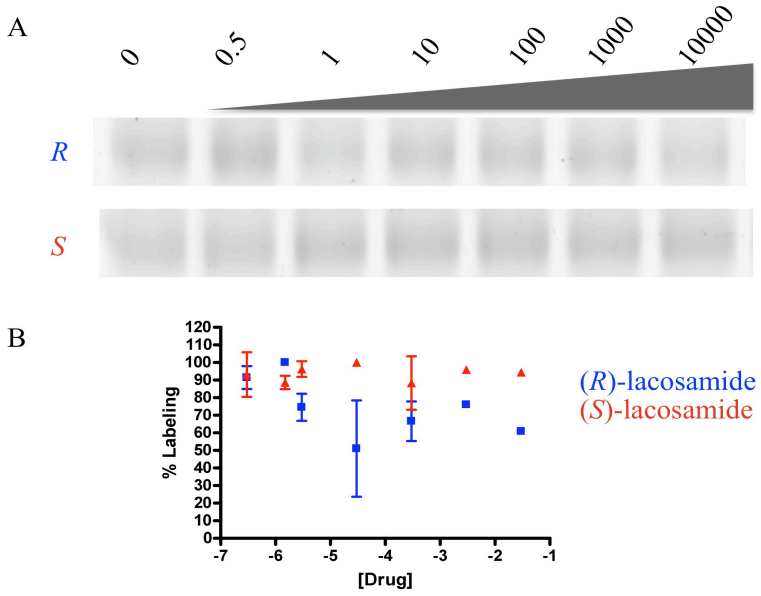

Figure 4.9 Homologous competition assay using BSA protein. (A) Compound 2 (3 μM) was added to a mastermix of enolase protein diluted to 1 μM in 50 mM HEPES, 150 mM NaCl pH 7.4. 10 μl of master mix was aliquoted per reaction followed by addition of (*R*) or (*S*)-lacosamide (3 μM to 30 mM). The reactions were incubated for 3 hours at 4 °C followed by photoactivation at 312 nm for 10 minutes on ice. Cycloaddition was initiated by addition of 24 μM probe 1 (0.1 μl of 2.4 mM stock in DMSO), 500 μM of TCEP (5 μl of 1 mM stock in water), 250 μM TBTA (0.625 μl of a 4 mM stock in DMSO) and 1mM $CuSO_4$ (1 μl of a 10 mM stock in water). The reaction was allowed to

proceed for 1 hour at room temperature followed by addition of 5 μl of 4X SDS-PAGE loading buffer. Samples were boiled at 95 °C for 5 minutes and the entire sample was loaded to a 10% SDS-PAGE gel. Gels were washed to twice with water for 5 minutes then visualized by fluorescent scanning (ex.: 532 nm / em.: 580 nm). (B) Pixel intensities were quantified using ImageJ (NIH) and curves generated using GraphPad (Prism). Each concentration was repeated in duplicate and graphed values represent the average pixel intensity calculated at each concentration.

The homologous competition assays collectively illustrated the reactivity of different classes of proteins to compound 2. Three distinctive displacement profiles were observed in the presence of (*R*) or (*S*)-lacosamide. BSA protein showed minimal labeling with compound 2 and no dose dependent competition, even with a large excess of ligand. Enolase protein showed modest labeling by compound 2, but linear abolishment of labeling with increasing concentrations of competing ligand. This profile implies an inherent reactivity to the photoaffinity bait present in compound 2, but no specific interaction with the lacosamide scaffold. DPYSL2 shows strong labeling by compound 2 and dose dependent abolishment of labeling consistent with a drug-receptor interaction. Although the calculated affinity appears to be weak (451 μM), the results suggest a specific interaction.

4.2.7 Adduction site of DPYSL2-HIS by lacosamide probes

(*R*)-lacosamide and compounds 1 and 2 interact with DPYSL2 protein based on the in-gel fluorescent studies. To understand this interaction better, the site of modification at which the affinity bait labels the protein was investigated. Understanding the amino acid residue(s) provides insight into the interaction of DPYSL2 with (*R*)-lacosamide. In order to observe the modification site via mass spectrometry, a detectable amount of adducted DPYSL2 must be generated. A panel of conditions was evaluated

that could generate maximal labeling of DPYSL2-HIS by compound 1 (Figure 4.10). Condition 5 provided the maximal labeling of DPYSL2-HIS protein and was used to create adducted samples for mass spectrometry analysis.

1	2	3	4	5
pH 7.4	pH 74	pH 7.8	pH 7.8	pH 7.8
100 µM	100 µM	100 µM	100 µM	250 µM
R.T.	37°C	R.T.	37°C	37°C
1 h	4 h	4 h	4 h	4 h

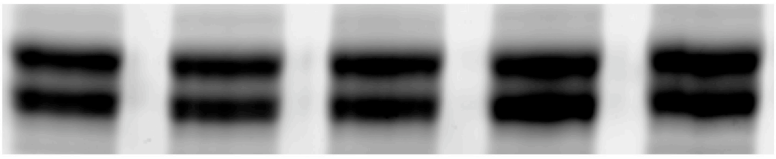

Figure 4.10 Conditions for DPYSL2-HIS adduction by compound 1. 10 µl of DPYSL2-HIS was reacted with the compound 1 under various conditions followed by click chemistry with probe 1 for 1 hour at room temperature. Adducted proteins were resolved on a 10% SDS-PAGE gel followed by scanning for in-gel fluorescence (ex.: 532 nm / em.: 580 nm).

Purified DPYSL2-HIS protein was reacted with 250 µM of (*R*)-lacosamide containing the isothiocyanate affinity bait as in compound 1 for 4 h at 37 °C (Figure 4.11). Unreacted drug was removed and the samples were subject to trypsinization followed by LC-MS/MS nano-electronspray quadrupole time of flight (QToF) mass spectrometry. Comparison of chromatograms of mass to charge ratios (m/z) of trypsinized peptides derived from protein labeled with (*R*)-lacosamide and unlabeled protein identified a triply protonated species (m/z 535.2) corresponding to the modified peptide KPFPDFVYKR specifically present in the labeled sample (Figure 4.12A). Collision-induced disassociation (CID) further fragmented the peptide with the m/z ratio of 535.2 to identify lysine 472 (K472) as the site of modification by the drug analog

within the modified peptide (Figure 4.12B). In this method, the ionized fragments are accelerated in the gas phase to collide with argon gas resulting in the conversion of kinetic energy to internal energy within the peptide. Fragmentation results from migration of a proton from the amino acid side chain to the peptide backbone generating cyclic and linear ionized fragments.

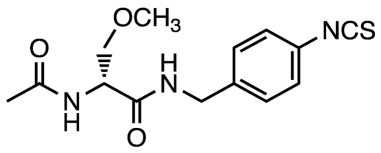

Mice i.p. ED_{50} = 24 mg/kg

Figure 4.11 (*R*)-Lacosamide analog used to generate modified DPYSL2 protein

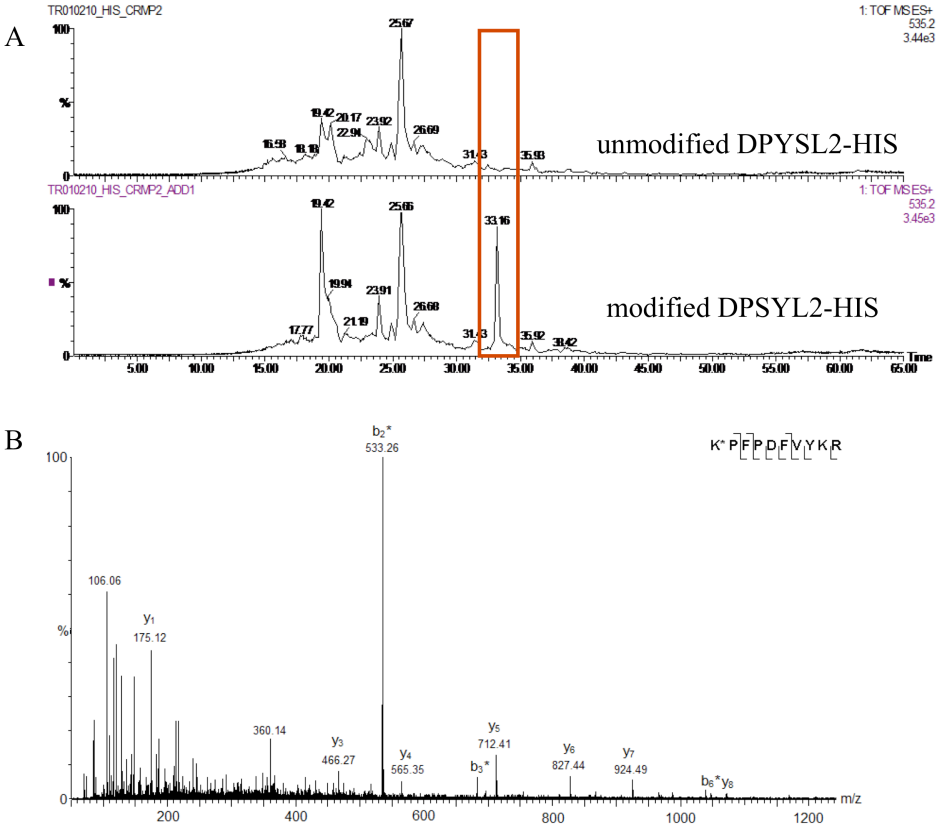

Figure 4.12 Mass spectrometry identification of the modification site of DPYSL2 by (*R*)-lacosamide. DPYSL2-HIS protein was reacted with 250 μM (*R*)-lacosamide containing a reactive isothiocyanate for 4 hours at 37°C. (A) Chromatograms of mass to charge ratios of the ions revealed a new adducted peptide species present in the adducted sample (red box) (B) Collision-induced disassociation identified lysine 472 as the site of modification by (*R*)-lacosamide.

Interestingly, this lysine residue (K472) is located on the surface of the protein adjacent to several regions of DPYSL2 known to be involved in various protein-protein interactions. (Figure 4.13) Amino acids 479-500 are one of three regions in DPYSL2 that has been shown to bind N-type calcium channels ($Ca_v2.2$) using pulldown assays with GST-fusion mutants of DPYSL2.[216] A peptide corresponding to amino acids 475-493 has been shown to bind to calmodulin using isothermal titration calorimetry.[195] The C-

terminus of DPYSL2 has also been shown to be a strong activator of GTP hydrolysis for tubulin.[187]

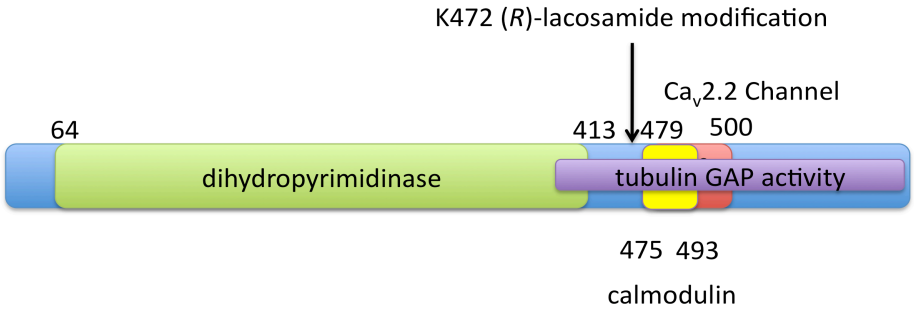

Figure 4.13 Regions adjacent to the K472 modification site involved in protein-protein interactions. Residues 479-500 (red) of DPYSL2 have been shown to bind to the $Ca_v2.2$ calcium channel. Residues 475-493 (yellow) have been shown to bind to calmodulin. The C-terminus of DPYSL2 from 410 (purple) has been shown to have strong GAP activity towards tubulin polymerization of microtubules.

The mapped modification site is close to the interface between monomers of the DPYSL2 protein that are thought to form tetramers *in vivo*. Tetramer formation is dependent upon the presence of divalent cations such as Mg^{2+} and Ca^{2+}.[194] There are a total of 32 lysines in the full-length DPYSL2, of which 13 are located on the outer surface of the protein and not present at the interface between monomers. There are several other lysines that are equally available in regards to solvent accessibility and exposure compared to K472, especially K292 and K422, but no adduction was observed at these residues. The fact that a single lysine modification was found implies the reaction between DPYSL2 and (*R*)-lacosamide was not the result of non-specific reaction with lysines present on the protein surface.

4.2.8 Computational modeling of (*R*)-lacosamide analogs to DPYSL2

Autodock Vina was used to predict the possible interactions that (*R*)-lacosamide might have with the DPYSL2 protein structure.[217] Lysine 472 was identified as the site of modification by the (*R*)-lacosamide analog containing the isothiocyanate affinity bait, therefore initial docking studies used this region on a monomeric version of DPYSL2 for computational studies. Four confirmations of the drug were predicted that positioned the affinity bait containing (*R*)-lacosamide toward lysine 472. Three of the predicted binding sites are shallow pockets and there are few structural clues on the protein that could explain the enantioselective biological activity observed *in vivo* (Figure 4.14). Additionally, structure activity relationships suggest that extensive modifications are not tolerated at the C2 and acetamide positions. Despite this, no obvious steric hindrance is present at these two sites that would inhibit or abolish binding.

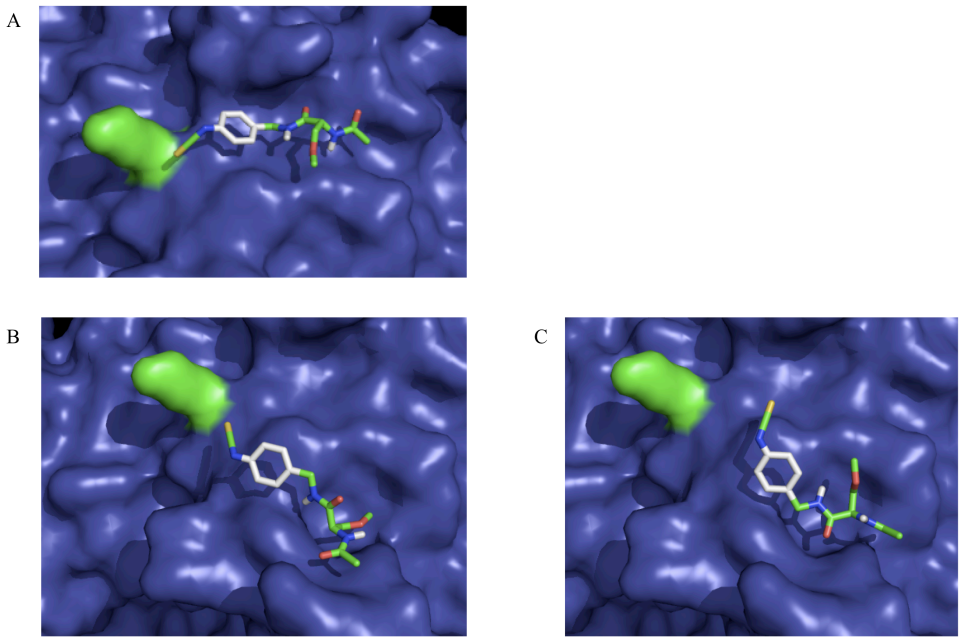

Figure 4.14 Unlikely interactions of the isothiocyanate (*R*)-lacosamide analog predicted by Autodock. The (R)-lacosamide analog containing the isothiocyanate affinity bait was docked to the DPYSL2 monomer using AutoDock Vina. Three predicted interactions between the (*R*)-lacosamide analog used for mass spectrometry using AutoDock Vina were generated near K472 (green).

Autodock predicted a fourth confirmation that positions the molecule in a narrow binding pocket located near the interface of two monomers (Figure 4.15). Several polar contacts are predicted to occur (shown in yellow) with tyrosine 395 (Y395), aspartic acid (D476), and asparagine 393 (N393). The ring is also pointed toward the K472, putting the isothiocyanate closer to the amino acid side chain than other predicted conformations, possibly facilitating adduction of the protein.

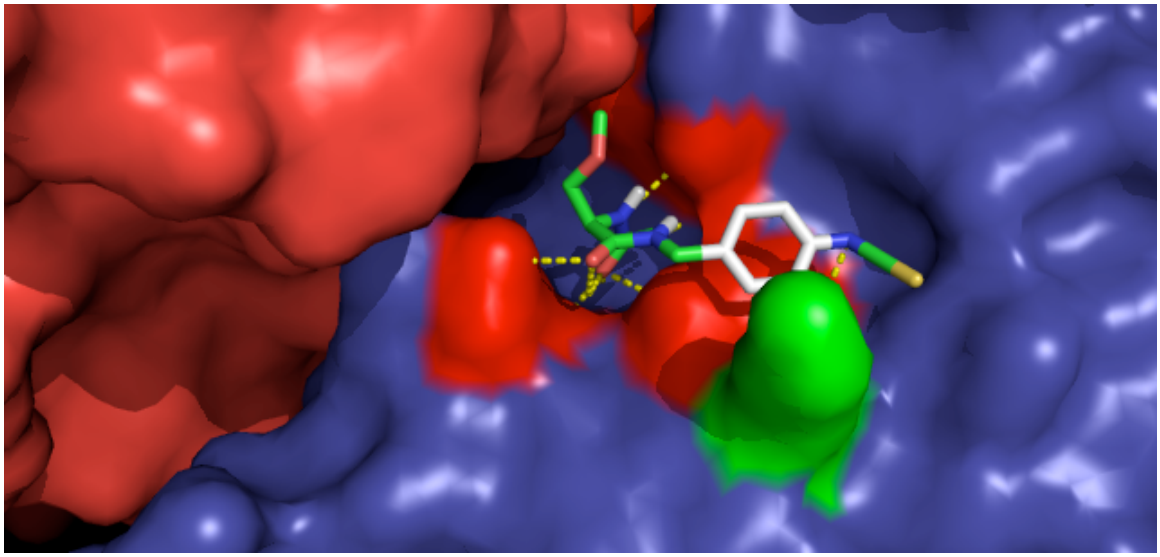

Figure 4.15 Favorable predicted conformation of (*R*)-lacosamide with DPYSL2. The molecule is positioned within a pocket located adjacent to the interface between two monomers. The isothiocyanate is pointed toward K472 (green) and shares several hydrogen bonds (yellow) (Y395, D476, N393) with the protein (red).

Structure activity relationships for (*R*)-lacosamide suggest that extensive modifications are not tolerated at the C2 or acetamide positions. Consistent with these trends, the pocket predicted by AutoDock leaves little room for inversion of C2 side chain of the molecule without steric clash with aspartic acid 476 on DPYSL2. Furthermore, the depth of the pocket prohibits extension of the acetamide end of (*R*)-lacosamide. Based on the three predicted polar contacts, position of the N-benzyl group toward K472, and structural constraints consistent with known SAR, this fourth conformation represents the most likely interaction between the (*R*)-lacosamide analog and DPYSL2 calculated by AutoDock.

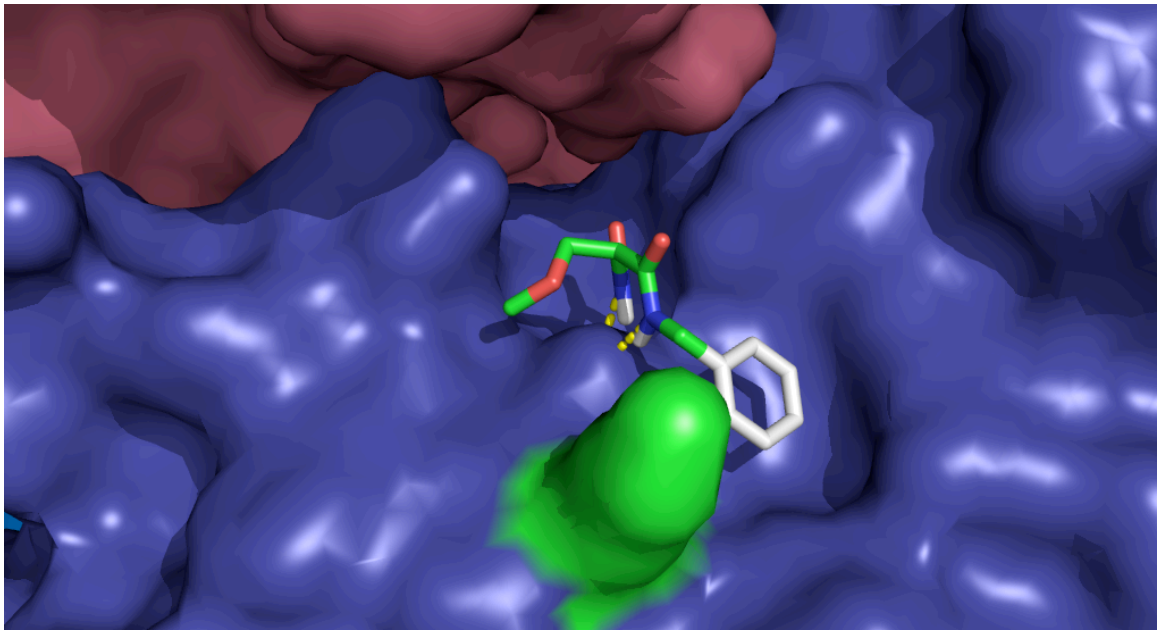

Figure 4.16 Predicted docked conformation of (*S*)-lacosamide with DPYSL2 protein. Conformations were generated with AutoDock Vina near lysine 472 (green). Potential hydrogen bonding with N393 is shown in yellow.

(*S*)-Lacosamide was also docked to DPYSL2 to predicted possible conformations (Figure 4.16). The ring is positioned in a similar fashion to the conformations predicted for the previous compound, but the acetamide group is positioned to hydrogen bond with Asp393 (N393). The side chain, which was previously predicted to extend into the pocket, is now extened around aspartic acid 476 (D476). This model suggests that although (S)-lacosamide may bind to DPYSL2, its conformation is distinct from (R)-lacosamide.

4.2.9 Evaluation of K472A DPYSL2-HIS mutant protein

The identification of the site of modification of DPSYL2 by (*R*)-lacosamide provides great insight into the binding site for the molecule on the protein. Therefore, we mutated lysine 472 to alanine and evaluated whether compound 1 could continue to label

the protein using in-gel fluorescence. The point mutation was generated using mutagenic primers. PCR was used to generate linear double-stranded plasmid DNA containing the point mutation followed by digestion of the methylated wild-type DNA by Dpn1. A sequence confirmed construct was expressed and purified in a similar fashion to the wild-type DPYSL2-HIS protein.

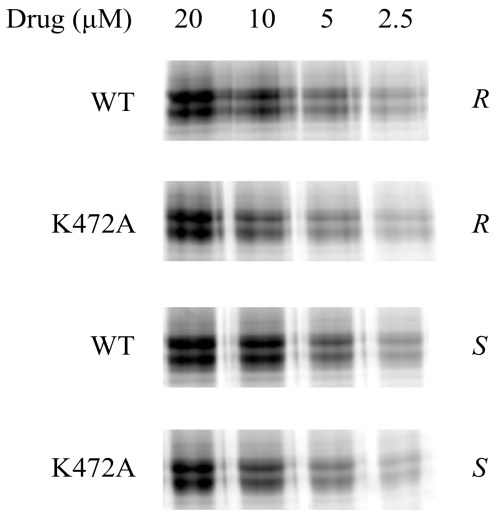

Figure 4.17 In-gel fluorescent labeling of WT and K472A DPYSL2-HIS by compound 1. Compound 1 was added to WT or K472A DPYSL2 protein diluted to 1 μM in 50 mM HEPES, 150 mM NaCl pH 7.4. The reactions were incubated for 1 hour at room temperature. Cycloaddition was initiated by addition of 24 μM probe 1 (0.1 μl of 2.4 mM stock in DMSO), 500 μM of TCEP (5 μl of 1 mM stock in water), 250 μM TBTA (0.625 μl of a 4 mM stock in DMSO) and 1mM $CuSO_4$ (1 μl of a 10 mM stock in water). The reaction was allowed to proceed for 1 hour at room temperature followed by addition of 5 μl of 4X SDS-PAGE loading buffer. Samples were boiled at 95 °C for 5 minutes and the entire sample was loaded to a 10% SDS-PAGE gel. Gels were washed to twice with water for 5 minutes then visualized by fluorescent scanning (ex.: 532 nm / em.: 580 nm).

Dose dependent labeling (20 - 2.5 μM) was observed with both the wild-type and K472A mutant proteins after reaction with compound 1 for 30 minutes at room temperature in 50 mM HEPES and 150 mM NaCl pH 7.4. Despite the removal of the

lysine residue identified as the adduction site for compound 1, the recombinant protein continued to be fluorescently labeled (Figure 4.17). This demonstrates that the isothiocyanate affinity bait can react at multiple sites on the protein in addition to lysine 472. No preference was observed for labeling of the K472A-DPYSL2-HIS protein by the *R* enantiomer under the conditions used.

There are two possible explanations for the continued labeling of K472A DPYSL2-HIS observed by in-gel fluorescence. The sensitivity of the in-gel fluorescence is very high allowing for the detection of tiny amounts of labeled protein. The observed labeling may therefore, be a very small amount of adduction occurring at other surface residues rather than the preferred site at lysine 472. In the absence of K472, other random non-specific modifications would still be visible. Secondly, the conditions used to generate the modified protein for mass spectrometry may have enhanced reactivity of K472 to become preferentially labeled relative to the other lysines that are labeled for in-gel fluorescence. The high concentration of drug (500 μM), increased pH (8.0 versus 7.4), increased temperature (37 °C versus 25 °C) and reaction time (4 hours versus 30 minutes) likely create unforeseen changes on affinity bait specificity and reactivity towards DPYSL2. The harsh conditions used could have encouraged reaction of the high concentration of drug to adduct with lysine 472 instead of a site that is more reactive under lower drug, pH, and temperature conditions.

4.2.10 Affinity evaluated via surface plasmon resonance

An attempt was made to measure the affinity between (*R*)-lacosamide derivatives and DPYSL2 protein using surface plasmon resonance (SPR). This technology relies on

detecting the change in refractive index of a reflected light source from a metal film (plasmon) as a result of mass increase occurring during a binding event. In order to determine the affinity between two molecules, one is immobilized on the metal film while the other is passed over the flow cell containing the immobilized component. The refractive index is monitored in real-time allowing for observation of both association and disassociation between the components.

Three biotinylated (*R*)-lacosamide derivatives were synthesized in the Kohn laboratory, each with the biotin group tethered to a different site on the lacosamide scaffold (Figure 4.18). The commercial availability of a streptavidin coated sensor chip permitted facile immobilization of the three drug analogs using biotin-streptavidin chemistry.

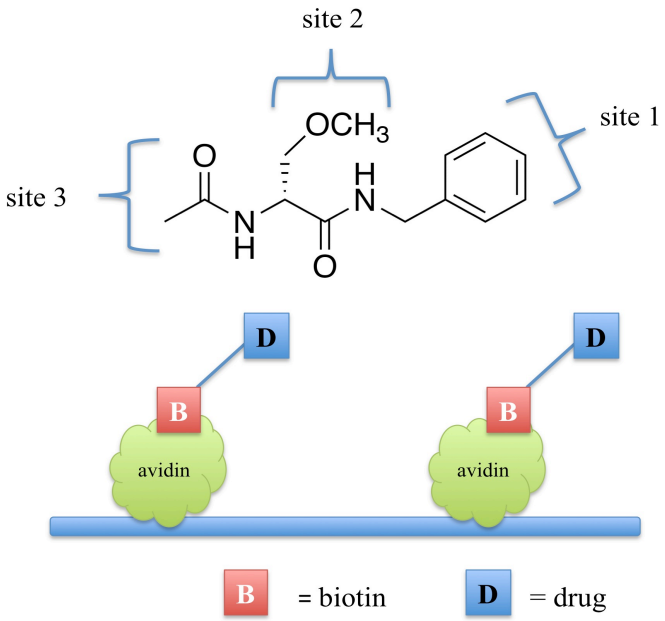

Figure 4.18 The 3 sites for incorporation of biotin for immobilization of (*R*)-lacosamide derivatives on the surface plasmon resonance chip.

Because the lacosamide scaffold cannot tolerate extensive modification without substantial loss of activity, the three sites chosen for immobilization provide a more comprehensive view of the potential interactions that may be critical for binding. Based on previous SAR, it is expected that site 1 can tolerate the most modification and should provide the best "display" of the compound on the sensor chip. This is postulated because larger modifications are tolerated at site 1 without substantial loss of anticonvulsant activity *in vivo*.

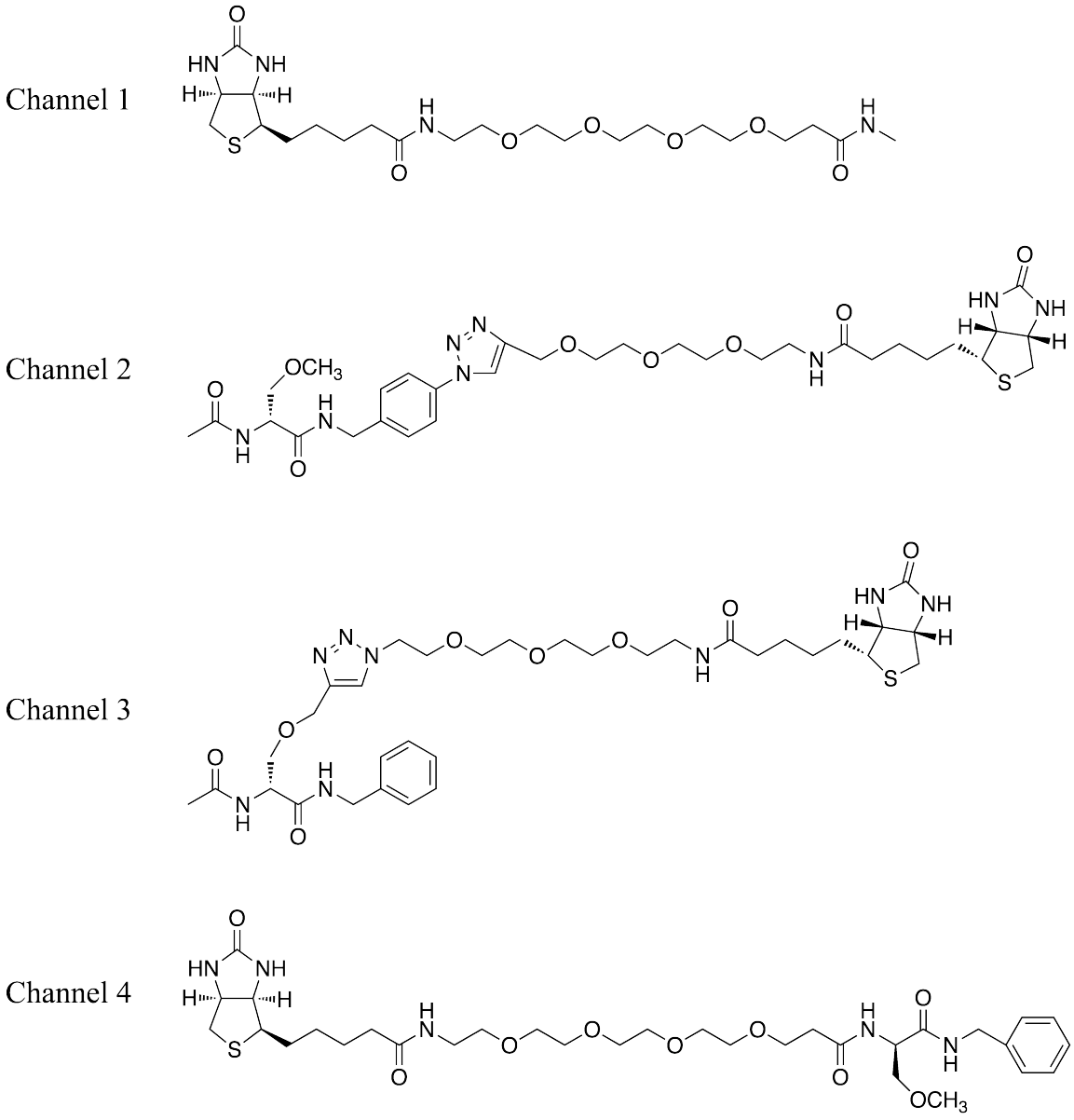

Figure 4.19 The four biotinylated (*R*)-lacosamide derivatives synthesized for immobilization on the streptavidin sensor chip for SPR.

Figure 4.19 illustrates the biotinylated compounds synthesized for immobilization on the streptavidin sensor chip for SPR. Compounds synthesized for sites 1 and 2 utilize azide containing (*R*)-lacosamide derivatives that were reacted with the biotin probe (probe 2) using the Cu(I) mediated Huisgen 1,3 cycloaddition, forming a triazole linkage

between the (*R*)-lacosamide scaffold and the biotin-PEG linker. The compound synthesized for site 3 coupled the biotin-PEG NHS activated ester with (*S*)-N-Benzyl-2-amino-3-methoxypropionamide. For immobilization, each biotinylated compound was sequentially injected into their respective channels on the streptavidin functionalized chip.

The ability of GST-DPYSL2 to bind to the immobilized compounds was evaluated at 0.25 μM, 0.5 μM, and 1 μM (Figure 4.20). Results showed no significant binding to any of the three immobilized compounds. Although there was a change in refractory units (RU), this increase was also seen with the negative control channel (channel 1). These results highlight the challenges of proper immobilization and display of small molecules on the sensor chip. The density of components on the surface and immobilization strategy may have drastic impacts on correct drug-receptor recognition. Furthermore, specific binding conditions or unknown co-factors may be required for observation of the interaction.

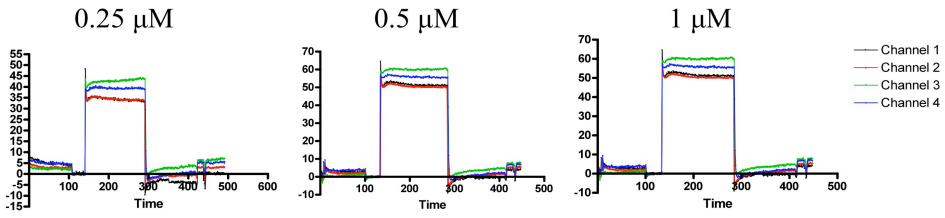

Figure 4.20 SPR binding results for GST-DPYSL2 to the biotinylated (*R*)-lacosamide derivatives. Proteins were extensively dialyzed against the flow buffer (50 mM HEPES, 150 mM NaCl pH 7.4) prior to experiments. 70 μl of protein (0.25 μM, 0.5 μM, and 1 μM) were injected into all four channels at a flow rate of 50 μl/min and their binding kinetics were observed over 3 minutes.

4.2.11 Effect of (*R*)-lacosamide on DPYSL2 and calmodulin

It was recently reported that DPSYL2 is a calmodulin binding protein with an affinity estimated in the low micromolar range.[195] Using both recombinant DPYSL2 protein and mouse brain lysate, we evaluated whether (*R*) or (*S*)-lacosamide affected the interaction between calmodulin and DPYSL2.

Calmodulin immobilized on agarose beads was incubated with recombinant DPYSL2-HIS protein or soluble mouse brain lysate in the presence or absence of 1 mM (*R*) or (*S*)-lacosamide. After washing to remove non-specifically bound proteins, captured DPSYL2 was eluted with 10 mM EGTA. Samples were resolved on an SDS-PAGE gel followed by western blotting for the DPYSL2 (Figure 4.21). The results indicate that the presence of (*R*) or (*S*)-lacosamide did not disrupt the interaction between calmodulin and DPYSL2 under the conditions tested. Eluted fractions from each sample showed that a similar amount of protein was present in all three conditions. The concentration of the compounds evaluated exceeds clinically achievable concentrations and, therefore, it is unlikely that (*R*)-lacosamide affects this interaction *in vivo*.

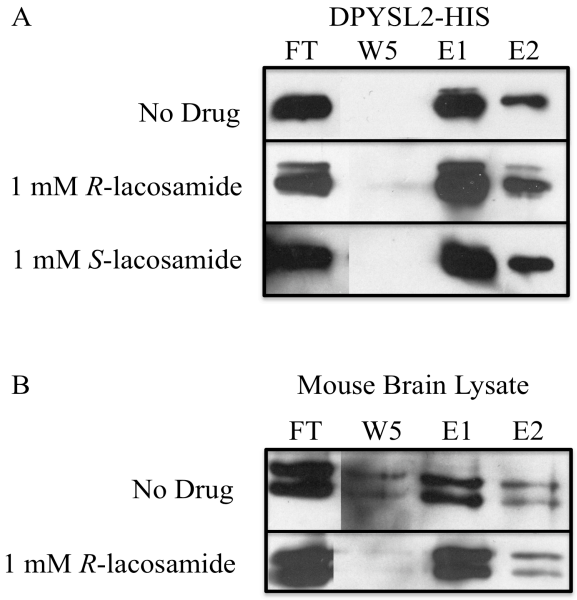

Figure 4.21 Purification of DPYSL2 with calmodulin agarose. (A) Recombinant DPYSL2-HIS was incubated with calmodulin agarose in the presence and absence of (*R*) or (*S*)-lacosamide. After washing, bound samples were eluted with 10 mM EGTA and resolved on a 10% SDS-PAGE gel followed by western blotting for DPYSL2. (B) Calmodulin agarose was added to soluble mouse brain lysate to capture endogenous DPYSL2. Eluted proteins were resolved on a 10% SDS-PAGE gel followed by western blotting for DPYSL2.

4.3 Studies with other candidate proteins

Several other proteins identified during the proteomic screen were examined in addition to evaluating the interaction between (*R*)-lacosamide and DPYSL2. The two proteins involved in the vesicle exocytosis, STXBP1 and NSF were chosen based upon their close association with modulation of neurotransmitter release and receptor trafficking.

4.3.1 STXBP1 (Munc18-1) and NSF

STXBP1 and NSF were overexpressed as N-terminal GST-fusion proteins in a manner identical to DPYSL2. Both compound 1 and compound 2 efficiently labeled the

purified proteins (Figure 4.22). Similar to DPYSL2, the detection limit of both proteins was around 1 μM.

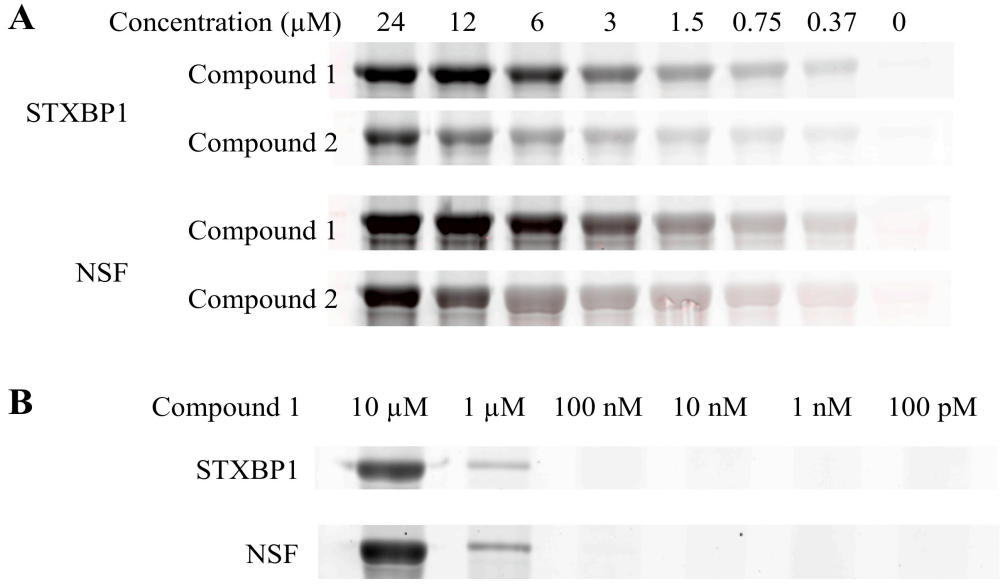

Figure 4.22 Dose dependent labeling of GST-STXBP1 and GST-NSF. (A)10 μl of purified GST-STXBP1 or GST-NSF protein (10 μM in 50 mM HEPES, 150 mM NaCl pH 7.4) was incubated with compound 1 or 2 for 1 hour at room temperature. Samples incubated with compound 2 were activated with UV light (312 nm) for 10 minutes at 4 °C. Click chemistry was performed with probe 1 for 1 hour at room temperature. (B) GST-DPYSL2 protein was diluted from 10 μM to 100 pM in 50 mM HEPES, 150 mM NaCl pH 7.4 then reacted with 3 μM of compound 1 for 1 hour at room temperature. Click chemistry was performed with probe 1 for 1 hour at room temperature. For all samples 5 μl of SDS-PAGE loading buffer was added to reaction after click chemistry and samples boiled for 5 minutes at 95 °C. Proteins were resolved on a 10% SDS-PAGE gel and scanned for in-gel fluorescence (ex.: 532 nm / em.: 580 nm).

Homologous competition assays using excess (*R*) or (*S*)-lacosamide estimated the (*R*)-lacosamide IC_{50} for STXB1 at 694 μM (Figure 4.23) and NSF at 340 μM using compound 2 (Figure 4.24). For these two proteins it appears that there are two sites that can interact with (*R*) or (*S*)-lacosamide in a stereospecific manner. When the (R) stereoisomer was used in the competition experiments the blocking of labeling was much

more pronounced. However when the (S) stereoisomer was used, the labeled is only partially block and plateaus when the competing ligand is at a concentration of 3 mM.

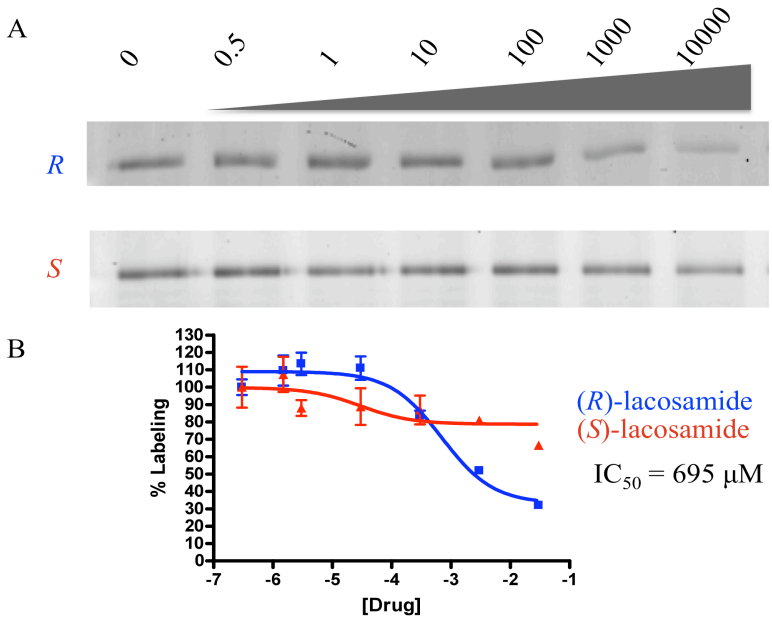

Figure 4.23 Homologous competition assay using GST-STXBP1 protein. (A) Compound 2 (3 µM) was added to a mastermix of GST-STXBP1 protein diluted to 1 µM in 50 mM HEPES, 150 mM NaCl pH 7.4. 10 µl of master mix was aliquoted per reaction followed by addition of (*R*) or (*S*)-lacosamide (3 µM to 30 mM). The reactions were incubated for 3 hours at 4 °C followed by photoactivation at 312 nm for 10 minutes on ice. Cycloaddition was initiated by addition of 24 µM probe 1 (0.1 µl of 2.4 mM stock in DMSO), 500 µM of TCEP (5 µl of 1 mM stock in water), 250 µM TBTA (0.625 µl of a 4 mM stock in DMSO) and 1mM $CuSO_4$ (1 µl of a 10 mM stock in water). The reaction was allowed to proceed for 1 hour at room temperature followed by addition of 5 µl of 4X SDS-PAGE loading buffer. Samples were boiled at 95 °C for 5 minutes and the entire sample was loaded to a 10% SDS-PAGE gel. Gels were washed to twice with water for 5 minutes then visualized by fluorescent scanning (ex.: 532 nm / em.: 580 nm). (B) Pixel intensities were quantified using ImageJ (NIH) and curves generated using GraphPad (Prism). Each concentration was repeated in duplicate and graphed values represent the average pixel intensity calculated at each concentration.

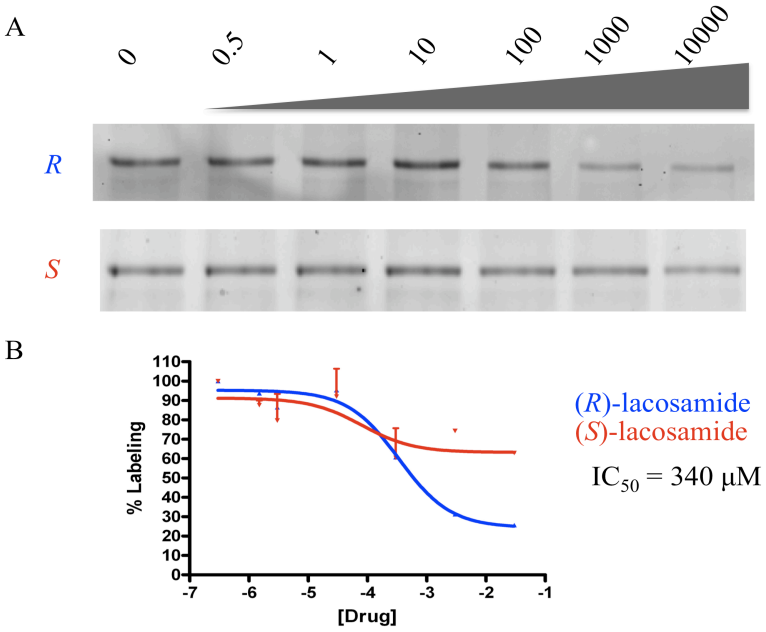

Figure 4.24 Homologous competition assay using GST-NSF protein. (A) Compound 2 (3 µM) was added to a mastermix of GST-NSF protein diluted to 1 µM in 50 mM HEPES, 150 mM NaCl pH 7.4. 10 µl of master mix was aliquoted per reaction followed by addition of (*R*) or (*S*)-lacosamide (3 µM to 30 mM). The reactions were incubated for 3 hours at 4 °C followed by photoactivation at 312 nm for 10 minutes on ice. Cycloaddition was initiated by addition of 24 µM probe 1 (0.1 µl of 2.4 mM stock in DMSO), 500 µM of TCEP (5 µl of 1 mM stock in water), 250 µM TBTA (0.625 µl of a 4 mM stock in DMSO) and 1mM $CuSO_4$ (1 µl of a 10 mM stock in water). The reaction was allowed to proceed for 1 hour at room temperature followed by addition of 5 µl of 4X SDS-PAGE loading buffer. Samples were boiled at 95 °C for 5 minutes and the entire sample was loaded to a 10% SDS-PAGE gel. Gels were washed to twice with water for 5 minutes then visualized by fluorescent scanning (ex.: 532 nm / em.: 580 nm). (B) Pixel intensities were quantified using ImageJ (NIH) and curves generated using GraphPad (Prism). Each concentration was repeated in duplicate and graphed values represent the average pixel intensity calculated at each concentration.

4.3.2 Na^+/K^+ Transporting ATPase

The effect of (*R*)-lacosamide, (*S*)-lacosamide, and an isopropyl derivative (Figure 4.25) were evaluated in a commercial enzyme assay measuring the ATPase activity of the Na^+/K^+ Transporting ATPase. The generation of inorganic phosphate (Pi) was measured using a malachite green photometric assay with tissue derived from porcine cerebral

cortex tissue. Three compounds were tested in triplicate at 10 μM, 30 μM, and 100 μM for modulation of the enzyme activity. The compound ouabain was used as a positive control for inhibition of ATPase activity. Recent research has linked mutations in the Na^+/K^+ ATPase alpha 3 gene with hyperexcitability and epilepsy due to inactivation of the pump.[218]

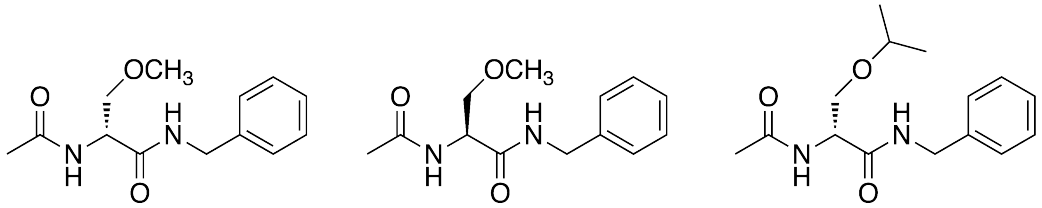

Figure 4.25 Compounds evaluated in the ATPase assay.

Potential rescue of pump activity may contribute to anticonvulsant activity. Therefore, *in vitro*, (*R*)-lacosamide might act as an activator of ATPase activity for the Na^+/K^+ transporting ATPase. Results indicate, however, no significant change in ATPase activity at any concentration tested for all three compounds. (Table 4.1) These findings suggest that *in vitro* (*R*)-lacosamide is not a modulator of the Na^+/K^+ transporting ATPase.

Table 4.1 Evaluation of (*R*)-lacosamide derivatives for inhibition of ATPase activity of the Na^+/K^+ Transporting ATPase. All samples were performed in triplicate.

Compound	Test Concentration	% of Control Values	
		1st	Mean
(*R*)-lacosamide	10 μM	104.1	**104.1**
(*R*)-lacosamide	30 μM	104.8	**104.8**
(*R*)-lacosamide	100 μM	103.3	**103.3**
(*S*)-lacosamide	10 μM	100.0	**100.0**
(*S*)-lacosamide	30 μM	102.0	**102.0**
(*S*)-lacosamide	100 μM	103.5	**103.5**
Compound 4	10 μM	102.1	**102.1**
Compound 4	30 μM	103.7	**103.7**
Compound 4	100 μM	101.8	**101.8**

4.3.3 Carbonic anhydrase II (CAR2) and 14-3-3

The commercial availability of CAR2 and 14-3-3 allowed for rapid testing of binding to (*R*)-lacosamide using the same sensor chip generated for DPYSL2. Injections of 1 μM, 0.5 μM, and 0.25 μM showed different association and disassociation profiles compared with GST-DPYSL2. There was no difference, however, between the channels with immobilized lacosamide derivatives (channels 2-4) and the negative control biotin probe (channel 1) (Figure 4.27). Additionally, the change in RUs was not dose dependent relative to the protein concentration for carbonic anhydrase II (Figure 4.26). The lack of appreciable binding (channels 2-4) relative to the control (channel 1) is surprising due to the fact that (*R*)-lacosamide has been shown to be a nanomolar inhibitor (IC_{50} = 331 nM) for human carbonic anhydrase II. This suggests that the biotinylated lacosamide derivatives may not be properly displayed on the streptavidin chip allowing for recognition by carbonic anhydrase.

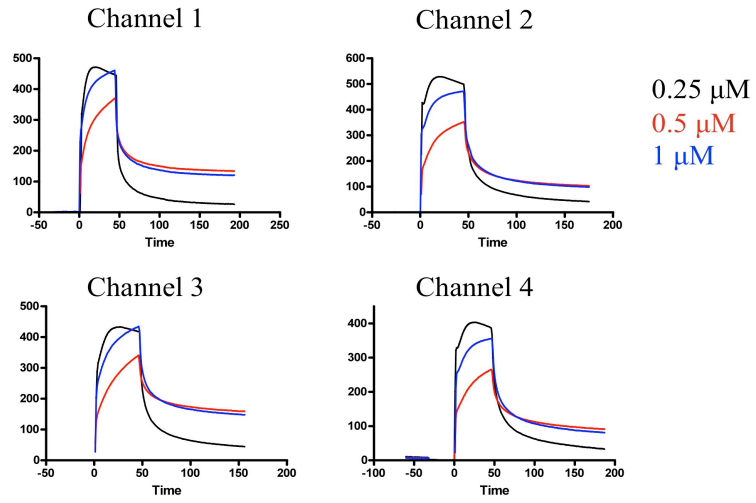

Figure 4.26 SPR binding results for human carbonic anhydrase II to the biotinylated (*R*)-lacosamide derivatives. Proteins were extensively dialyzed against the flow buffer (50 mM HEPES, 150 mM NaCl pH 7.4) prior to experiments. 70 μl of protein (0.25 μM, 0.5 μM, and 1 μM) were injected into all four channels at a flow rate of 50 μl/min and their binding kinetics were observed over 3 minutes.

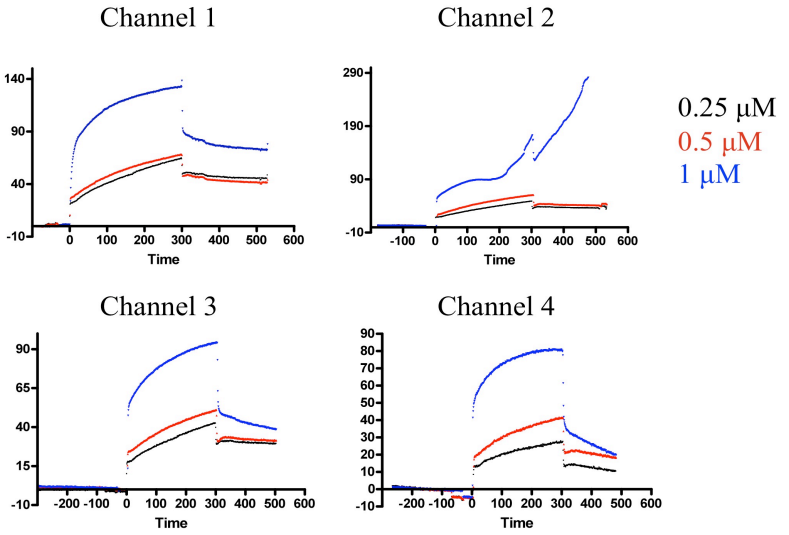

Figure 4.27 SPR binding results for 14-3-3-HIS to the biotinylated (*R*)-lacosamide derivatives. Proteins were extensively dialyzed against the flow buffer (50 mM HEPES, 150 mM NaCl pH 7.4) prior to experiments. 70 μl of protein (0.25 μM, 0.5 μM, and 1 μM) were injected into all four channels at a flow rate of 50 μl/min and their binding kinetics were observed over 3 minutes.

4.4 Concluding remarks

From the list of proteins identified in the proteomic screen, DPYSL2, STXBP1, NSF and Na^+/K^+ ATPase were chosen for in-depth analysis, with a major focus on DPYSL2. In-gel fluorescence with several recombinant proteins illustrated a specific dose dependent interaction with (*R*)-lacosamide. Homologous competition assays calculated IC_{50} values in the mid to high micromolar range (DPYSL2 = 451 μM, STXBP1 = 694 μM, NSF = 340 μM). Attempts at accurate estimation of affinity using SPR with DPYSL2, STXBP1, NSF, CAR2, and 14-3-3 were performed through immobilization of several biotinylated derivatives of (*R*)-lacosamide that revealed a high degree of non-specific binding, for which the cause remains unknown. It is possible that proper display or stability of immobilized compounds or the lack of required co-factors hinders observation of the binding events. Screening of (*R*)-lacosamide's activity on the Na^+/K^+ ATPase transporter in cellular assay demonstrated no inhibition or activation at the concentrations tested.

Using an isothiocyanate containing analog of (*R*)-lacosamide, a site of modification on DPYSL2 was successfully identified using mass spectrometry. Lysine 472 was the only amino acid detected that was modified by (*R*)-lacosamide. The residue is located adjacent to domains involved in binding to N-type calcium channels ($Ca_v2.2$), calmodulin, and tubulin.

Computational studies predicted four potential binding conformations for the (*R*)-lacosamide analog using AutoDock Vina that could allow for adduction by the affinity bait to occur. One model provides a plausible confirmation of (R)-lacosamide docked

into a pocket on DPYSL2 at the interface between two monomers of the crystal structure. The orientation of the molecule is favorable for adduction by the affinity with the modified residue identified via mass spectrometry. Additionally, the SAR observed in mice, namely a dramatic loss of activity from extension of the acetamide end and the *R* versus *S* selectivity, could be explained by steric clash with residues surrounding the predicted binding pocket.

A mutant of DPYSL2 containing an alanine at position 472 instead of lysine was generated. In-gel fluorescent studies using recombinant DPYSL2-K472A-HIS protein showed that despite the mutation, the protein continued to be labeled to a similar extent as the wild type using compound 1. Labeling in buffer alone or a complex mixture of lysate did not affect the extent of labeling. These results demonstrate that the isothiocyanate affinity bait used may label multiple sites on the DPYSL2 protein under the conditions tested.

Collectively, the work presented here successfully applied electrophilic and photo affinity labeling strategies to enrich and identify (*R*)-lacosamide interacting proteins from mouse brain lysate. Mass spectrometry methods were developed to identify the identity of individual proteins from both gel slices and proteins immobilized on a solid surface. From this list of 73 potential targets, 3 proteins were chosen for further study using recombinantly expressed proteins. Lysine 472 was identified as the likely adduction site of compound 1 on DPYSL2. Furthermore, the mutation of the (*R*)-lacosamide adduction site on DPYSL2 did not abolish its labeling by compound 1 when measured by in-gel fluorescence.

The results illustrate the limitations of the affinity labeling strategy to definitively identify physiologically relevant protein targets for (*R*)-lacosamide. Activity of (*R*)-lacosamide to enhance slow inactivation of sodium channels continues to be the likely primary action responsible for its anticonvulsant activity, perhaps in association with one or more proteins identified during our screen. During our proteome search, however, no sodium channels peptides were identified. For that reason, the data obtained should be integrated with multiple data streams for (*R*)-lacosamide such as electrophysiology, animal activity, and gene expression profiling to generate a more comprehensive picture of the compound's complex pharmacology.

4.5 Materials and Methods

4.5.1 Western blot for DPYSL2

Mouse brain lysate was prepared as described in chapter 3 using deoxycholate. For each reaction, 500 μl of lysate was reacted with 40 μM of compound 3 for 1 h at room temperature. For competition samples, (*S*)-lacosamide was added in excess and allowed to equilibrate for 30 minutes prior to addition of compound 3. Methylhydrazine (1 mM) was incubated with compound 3 for 30 minutes prior to addition to lysate for sample 2 to destroy the isothiocyanate affinity bait.

After labeling the lysate for 1 hour, 50 μl of streptavidin beads (Pierce) was added and the mixture rotated for 1 h at 4 °C followed by centrifugation at 1,000 rpm for 1 minute. The supernatant was removed and the beads were sequentially washed twice with 1 ml 50 mM HEPES pH 7.4, 150 mM NaCl, 0.2 % SDS, then twice with 1 ml 6 M urea, and twice with 1 ml 50 mM HEPES pH 7.4 and 150 mM NaCl. 50μl of 4X SDS-

PAGE loading buffer was added to the resin followed by boiling at 95 °C for 5 minutes. After a brief mixing, the beads were centrifuged and 20 μl of supernatant was loaded to a 10 % gel and transferred to a nitrocellulose membrane followed by immunoblotting for DPYSL2.

The membrane was probed with anti-DPYSL2 (Santa Cruz 30228) using a 1:1000 dilution for 1 hour at room temperature followed by addition of secondary anti-rabbit-HRP conjugate antibody (GE Healthcare) 1:1000 for 1 hour at room temperature. HRP substrate was added and image developed immediately.

4.5.2 Fluorescent western blot for DPYSL2

For detection of DPYSL2, lysate was labeled as described previously (3.5.4) with compound 1. After SDS-PAGE, the gel was transferred to a nitrocellulose membrane and blocked for 1 hour with TBST and 5 % milk. The membrane was probed with anti-DPYSL2 (Santa Cruz) using a 1:1000 dilution for 1 hour at room temperature followed by the addition of secondary anti-rabbit-HRP conjugate antibody (GE Healthcare) 1:1000 for 1 hour at room temperature. HRP substrate was added to the membrane and immediately scanned for Cy5 (ladder), TAMRA, and ECL. The composite image was created in ImageJ (NIH).

4.5.3 Construction, expression and purification fusion proteins

PCR products were amplified from mouse brain cDNA library (Ambion) using KOD polymerase (Novagen). GST-fusion proteins were created through insertion into pET41-LIC/Ek through ligation independent cloning according to the manufacturer's

instruction (Novagen). For HIS-tagged fusion proteins, complementary digested PCR products were ligated into pET28b plasmid (NEB) digested with Nco1 and Xho1. Sequence verified clones were transformed into Rosetta *E. coli* (Novagen).

For expression, cultures were grown in LB to an OD_{600} of 0.7 then cooled to 20 °C followed by addition of 1 mM IPTG. Induction was carried out overnight (16 hours) at 20 °C. For GST-fusion proteins, clarified lysate was passed over a 3 mls of GST-Bind resin (Novagen) and washed with 20 column volumes of 50 mM HEPES, 150 mM NaCl pH 7.4. Bound proteins were eluted with 3 column volumes of 1 mM glutathione in wash buffer. Free glutathione was removed using a NAP-10 column (GE Healthcare).

For HIS-tagged fusion proteins, clarified lysate was passed over 3 mls of Talon cobalt resin (Clonetech) and washed with 20 column volumes of 50 mM HEPES, 150 mM NaCl, and 10 mM imidazole pH 7.4. Bound proteins were eluted with 3 column volumes of 100 mM imidazole, 50 mM HEPES and 150 mM NaCl pH 7.4. Eluted fractions were dialyzed against 2 liters of 50 mM HEPES, 150 mM NaCl to remove imidazole. Samples were aliquoted and stored at -80 °C until use.

The K472A DPYSL2-HIS mutant was generated via mutagenic PCR. Primers containing the mutation were used for amplification of pET28b vector containing the wild-type version of the DPYSL2 sequence.

CRMP2K472A.F

CTGGACGCTACATTCCCCGGGCGCCCTTCCCTGATTTTGTTTAC

CRMP2K472A.R

GTAAACAAAATCAGGGAAGGGCGCCCGGGGAATGTAGCGTCCAG

50 ng of pET28b vector containing DPYSL2 was amplified with 1.25 μg of each primer using clone Pfu Polymerase (Stratagene) for 16 cycles followed by digestion of 1 μl of Dpn1 at 37 C for 1 h. 95 °C for 2 minutes, (95 °C for 30 seconds, 55 °C for 30 seconds, 72 °C for 10 minutes) 15 times, 72 °C for 7 minutes, 4 °C. 7 μl of plasmid was transformed into TOP10 cells and sequence verified clones were transformed into Rosetta *E. coli* (Novagen) for expression.

4.5.4 Autodock Vina Docking Studies

Autodock Tools 1.5.4 was used to generate PDBQT files with proper Gasteiger charges for DPYSL2 (2GSE.pdb) and (*R*)-lacosamide. A monomeric crystal structure of DPYSL2 was used for docking studies. Grid size and spacial orientation were estimated around K472 using Autodock Tools. Autodock Vina (1.0) was run on Mac OS X Leopard using extensiveness set to 100 and a total of 30 conformations calculated. The predicted conformations were visualized in MacPyMol with the 2GSE.pdb crystal structure of DPYSL2.

4.5.5 Tubulin polymerization assay

Tubulin (Cytoskeleton) was resuspended in 80 mM PIPES, 0.5 mM EGTA, 2 mM $MgCl_2$, 0.05% glycerol pH 6.9 to a concentration of 1 mg/ml (10 μM). GTP was added to 1 mM and the mixture was equilibrated on ice for 15 minutes. Recombinant DPYSL2, taxol, (*R*)-lacosamide, or buffer were added to their respective wells of the 384 well plate followed by incubation in the microplate reader at 37 °C for 5 minutes. Polymerization

was initiated by addition of 44 μl of tubulin to each well. OD_{340} measurements were captured every 30 seconds for 1 hour at 37 °C.

4.5.6 DPYSL2 pulldown using calmodulin agarose

Calmodulin-agarose beads (25 μl resin) (Stratagene) were equilibrated in 50 mM HEPES pH 7.4, 150 mM NaCl, and 10 mM $CaCl_2$. Recombinant DPYSL2-HIS protein (100 ng in 500 μl of buffer) or deoxycholate treated mouse brain lysate (2 mg/ml) were added to the resin and rotated at 4 °C for 2 hours. For those samples evaluating the effect of small molecules drugs, (*R*) or (*S*)-lacosamide was added to 1 mM. Beads were pelleted at 1000 rpm for 1 minute and supernatant removed. The beads were washed 5X with 167 μl of 50 mM HEPES pH 7.4, 150 mM NaCl, and 1 mM $CaCl_2$. Bound proteins were eluted with 50 μl of 50 mM HEPES pH 7.4, 150 mM NaCl, and 10 mM EGTA and resolved on a 10 % SDS-PAGE gel followed by western blotting for DPYSL2.

4.5.7 In-gel fluorescent labeling of purified proteins

For in-gel fluorescent studies, 10 μl of protein was diluted to various concentrations in 50 mM HEPES, 150 mM NaCl pH 7.4 and labeled with compound 1 or 2. For compound 1, reactions were incubated for 1 hour at room temperature. For compound 2, reactions were incubated for 50 minutes at 4 °C followed by photoactivation at 312 nm (Spectroline EB-280C, 115V, 60 Hz, 0.4 Amps) at distance of 2 millimeters for 10 minutes on ice. Cycloaddition was initiated by addition of 24 μM probe 1 (0.1 μl of 2.4 mM stock in DMSO), 500 μM of TCEP (5 μl of 1 mM stock in water), 250 μM TBTA (0.625 μl of a 4 mM stock in DMSO) and 1mM $CuSO_4$ (1 μl of a

10 mM stock in water). The reaction was allowed to proceed for 1 hour at room temperature followed by addition of 5 μl of 4X SDS-PAGE loading buffer. Samples were boiled at 95 °C for 5 minutes and 10 μl were loaded to a 10% SDS-PAGE gel. Gels were washed twice with water for 5 minutes then visualized by fluorescent scanning using a Typhoon 9400 (GE Healthcare) with excitation at 532 nm and detection at 580 nm.

4.5.8 Homologous competition assay

For homologous competition assays, 3 μM of compound 2 was added to a mastermix of GST-fusion protein diluted to 1 μM. 10 μl of master mix was aliquoted per reaction followed by addition of (*R*) or (*S*)-lacosamide (3 μM to 30 mM). The reactions were incubated for 3 hours at 4 °C followed by photoactivation at 312 nm for 10 minutes on ice. Cycloaddition was initiated by addition of 24 μM probe 1 (0.1 μl of 2.4 mM stock in DMSO), 500 μM of TCEP (5 μl of 1 mM stock in water), 250 μM TBTA (0.625 μl of a 4 mM stock in DMSO) and 1mM $CuSO_4$ (1 μl of a 10 mM stock in water). The reaction was allowed to proceed for 1 hour at room temperature followed by addition of 5 μl of 4X SDS-PAGE loading buffer. Samples were boiled at 95 °C for 5 minutes and the entire sample was loaded to a 10% SDS-PAGE gel. Gels were washed to twice with water for 5 minutes then visualized by fluorescent scanning using a Typhoon 9400 (GE Healthcare) with excitation at 532 nm and detection at 580 nm. Images were quantified using ImageJ (NIH) and curves generated using GraphPad (Prism).

4.5.9 Surface plasmon resonance

Biotinylated lacosamide compounds dissolved in DMSO were immobilized on a streptavidin chip (SA chip/GE Healthcare) using a BIAcore2000 according to the manufacturer's instructions. Proteins were extensively dialyzed against the flow buffer (50 mM HEPES, 150 mM NaCl pH 7.4) prior to experiments. Proteins were injected at a flow rate of 50 μl/min and their binding kinetics were observed over 3 minutes. Data were analyzed with BIAevaluation 3.0 software (BIAcore).

CHAPTER 5

FUTURE WORK AND FORWARD LOOKING STUDIES

5.1 Introduction

The previous chapters outlined efforts to identify the protein targets of the novel anticonvulsant (*R*)-lacosamide (Vimpat®). A proteomic screen of the mouse brain proteome identified 73 proteins via mass spectrometry that were captured with nucleophillic and photoaffinity reactive groups installed on (*R*) and (*S*)-lacosamide derived probes. DPYSL2 was chosen for further study using recombinant protein expressed in *E. coli*. Lysine 472 on DPYSL2 was identified as the residue that was modified by reaction with an isothiocyanate containing (*R*)-lacosamide analog. The residue is adjacent to several sites important for phosporylation by Rho-kinase, Cdk5 and GSK-3β. Additionally, mapped adduction site is close to the C-terminus of the protein that has been implicated in a variety of interactions with other proteins such as calmodulin, tubulin, and $Ca_v2.2$. Several approaches could expand upon the work presented to characterize better the physiologically relevant interactions with DPYSL2 and other proteins identified during the proteomic screen with (*R*)-lacosamide.

5.2 Effects of DPYSL2 phosphorylation on (*R*)-lacosamide binding

It is predicted that phosphorylation of DPYSL2 protein *in vivo* modulates its functionality.[171,188-190,192,219] DPYSL2 can be phosphorylated at Thr-555 by Rho kinase,

Ser-522 by Cdk5, and Ser-518 and Thr-514 by GSK-3β. The phosphorylation status of recombinant DPSYL2 protein was never evaluated in our studies; therefore, binding to (*R*)-lacosamide may be conditional based on kinase phosphorylation. To test this hypothesis, *in vitro* kinase assays can be used to phosphorylate recombinant DPYSL2 protein prior to binding experiments. Cdk5 (Upstate) and GSK-3β (New England Biolabs) are commercially available in sufficient quantities to be used for phosphorylation of purified recombinant DPYSL2 protein. If normal ATP is added to the kinase reaction, the phosphorylated recombinant protein can be used for Isothermal Titration Calorimetry (ITC) or Surface Plasmon Resosance (SPR) using (*R*)-lacosamide or the chip designed in chapter 4, respectively, to measure binding affinity.

[γ-^{32}P]ATP can be substituted for ATP in the kinase assay to generate phosphorylated DPYSL2 protein that is radiolabeled. This labeled protein can be used in several ways. First, using the AB and CR strategy with compounds 1 and 2 followed by enrichment with streptavidin beads, the amount of radiolabeled DPYSL2 can be measured in the presence or absence of competing amounts of (*R*) or (*S*)-lacosamide. Enriched proteins can be resolved on a SDS-PAGE gel and the amount of DPYSL2 can be detected by autoradiography.

Another hypothesis is that (*R*)-lacosamide can inhibit DPYSL2 phosphorylation. Using a similar approach, [γ-^{32}P]ATP can be used to investigate whether (*R*)-lacosamide can modulate the phosphorylation of DPYSL2 by kinases such as Cdk5 or GSK-3β. The *in vitro* kinase assay used in the previous experiments can be repeated in the presence of increasing amount of (*R*) or (*S*)-lacosamide. After the kinase reaction, the amount of phosphorylated protein can be measured directly using autoradiography.

5.3 Screening of (*R*)-lacosamide against metabotropic glutamate receptors

Extensive screening of (*R*)-lacosamide against a variety of GPCRs and ion channels has been reported previously but only partial binding was seen at voltage gated sodium channels.[150] Binding to additional receptors is worth investigating, however. It has been reported that (*R*)-lacosamide effectively reduces harmaline induced essential tremor in rats.[220] Traditionally, it has been thought that harmaline tremor is mediated by activity at the NMDA receptor.[221] It has been demonstrated recently that harmaline induced tremors are enhanced by the selective metabotropic glutamate receptor 1 (mGluR1) antagoinist JNJ 16259685, suggesting a possible inhibitory influence between mGlu receptors and harmaline induced tremor.[222]

One series of mGluR2/3 agonists show potent anticonvulsant activity in a kindled rat model.[223] Ligands for mGlu receptors tend to have molecular weights less than 300 daltons and have structures that are derivatives of amino acids. These characteristics are also shared by (*R*)-lacosamide and other functionalized amino acids, therefore activity at one or more metabotropic glutamate receptor may be possible. To this end, receptor binding assays against metabotropic glutamate receptors at the Psychoactive Drug Screening Program (PDSP) using (*R*)-lacosamide is recommended. Currently there are 7 human metabotropic receptor assays available for testing (human mGluR1-7).

Alternatively, animal evaluation of (*R*)-lacosamide in the presence of the glutamate receptor antagonist (2*S*,1′*S*,2′*S*)-2-methyl-2-(carboxycyclopropyl)glycine (MCCG) would provide a similar assessment of activity at the mGluR (group II) receptors. This receptor antagonist has been used to evaluate the anticonvulsant activity of DCG-IV on the mGluR (group II) family.

5.4 Screening of (*R*)-lacosamide to latrophilin toxin receptors

During the proteomic search, the calcium-independent α-latrotoxin receptor was identified using compounds 1 and 2. This protein belongs to a family of 3 large G-protein coupled receptors (~1000 AA) that bind α-latrotoxin, a toxin peptide from black widow spiders that stimulates strong release of glutamate.[224] Currently their roles *in vivo* and natural ligands are unknown. Stimulation of vesicle exocytosis appears to occur in a calcium independent fashion, but the receptor requires the core vesicle fusion proteins synaptobrevin, SNAP-25, Stxbp1, and syntaxin.

Knowing whether (*R*)-lacosamide could affect the potent activity of α-latrotoxin in stimulating glutamate release would be of great interest. To assess this, individual latrophilin receptors could be transfected into PC12 cells and calcium release measured in the presence or absence of (*R*)-lacosamide as previously described.[225] Alternatively, the release of radiolabeled glutamate or GABA could be measured from purified synaptosomes after treatment with α-latrotoxin.[226]

Single and double mutant knock-out mice for latrophilin-1 and 2 are available and show normal development and survival rates. Using these strains, the efficacy of (*R*)-lacosamide in the MES seizure test could be reevaluated to investigate what changes may occur in the absence of the receptor. If (*R*)-lacosamide shows activity at latrophilin-1 or 2, protection from seizure development may be diminished.

5.5 ATPase activity of NSF protein

Neuronal sprouting has recently been reported to be a phenotype of neurons treated with (*R*)-lacosamide. Although a number of unique pathways involving multiple

proteins may mediate this process, some proteins identified in our proteomic search have been associated with this phenomenon. NSF, the hexameric ATPase involved in disassembly of the SNARE complex, was identified specifically with the (*R*) entantiomer during the proteomic screen and the IC_{50} calculated to be 340 μM using the homologous competition assay. This was the lowest IC_d of all three proteins tested. Expression of a dominant negative (ATPase inactive) mutant in drosophila results in outgrowth at the neuromuscular synapse during development.[227] If the ATPase activity of NSF contributes to synpase sprouting, then potentially (*R*)-lacosamide may affect NSF activity. A standard ATPase assay using recombinant protein in the presence or absence of (*R*) and (*S*)-lacosamide would evaluate whether this hypothesis warrants further investigation.

5.6 Metabolic profiling of (*R*)-lacosamide treated mice

The majority of our efforts have relied solely on the results of a proteomic screen to identify potential protein targets that interact with (*R*)-lacosamide coupled with *in vitro* methods to measure labeling and binding affinity. Alternative methods that provide greater insight into the biochemical changes elicited by (*R*)-lacosamide would help distinguish between physiologically relevant proteins identified during our screen with those that should be considered background. As mentioned in chapter 2, advances in mass spectrometry now allow for simultaneous detection of hundreds of cellular metabolites from tissues to discern biochemical changes between samples. This methodology has been successfully applied for the identification of the protein targets of several drug candidates.[141]

A similar approach could be taken with (*R*)-lacosamide by profiling the four sets of mouse brain tissue used to generate the mRNA-display libraries [normal (sham stimulated), (*R*)-lacosamide treated (20 mg/kg), 6 Hz stimulated (32 mA 3 sec), and 6 Hz stimulated (*R*)-lacosamide treated]. The results would generate unique metabolic profiles for each tissue treatment that could readily be mapped to biochemical pathways in the cell. Changes in metabolites upon administration of (*R*)-lacosamide could then be integrated with the results of our proteomic screen, providing a better understanding of which biochemical pathways to pursue.

Bibliography

(1) World Health Organization *Atlas Epilepsy Care in the World 2005*; World Health Organization, 2005.

(2) Proposal for revised clinical and electroencephalographic classification of epileptic seizures. From the Commission on Classification and Terminology of the International League Against Epilepsy. *Epilepsia* **1981**, *22*, 489-501.

(3) Squire, L. R. *Fundamental neuroscience*; Academic Press, 2008.

(4) Allen, N. J.; Barres, B. A. Neuroscience: Glia - more than just brain glue. *Nature* **2009**, *457*, 675-677.

(5) Collingridge, G. L.; Olsen, R. W.; Peters, J.; Spedding, M. A nomenclature for ligand-gated ion channels. *Neuropharmacology* **2009**, *56*, 2-5.

(6) Miller, P. S.; Smart, T. G. Binding, activation and modulation of Cys-loop receptors. *Trends Pharmacol Sci* **2010**.

(7) Shorvon, S. D. (. D.). *Handbook of epilepsy treatment : forms, causes and therapy in children and adults*; 2nd ed.; Blackwell Pub.,: Malden, Mass., 2005.

(8) Fisher, J. L. A mutation in the GABAA receptor alpha 1 subunit linked to human epilepsy affects channel gating properties. *Neuropharmacology* **2004**, *46*, 629-637.

(9) Baulac, S.; Huberfeld, G.; Gourfinkel-An, I.; Mitropoulou, G.; Beranger, A.; Prud'homme, J. F.; Baulac, M.; Brice, A.; Bruzzone, R.; LeGuern, E. First genetic evidence of GABA(A) receptor dysfunction in epilepsy: a mutation in the gamma2-subunit gene. *Nat. Genet* **2001**, *28*, 46-48.

(10) Wallace, R. H.; Marini, C.; Petrou, S.; Harkin, L. A.; Bowser, D. N.; Panchal, R. G.; Williams, D. A.; Sutherland, G. R.; Mulley, J. C.; Scheffer, I. E.; Berkovic, S. F. Mutant GABA(A) receptor gamma2-subunit in childhood absence epilepsy and febrile seizures. *Nat. Genet* **2001**, *28*, 49-52.

(11) Harkin, L. A.; Bowser, D. N.; Dibbens, L. M.; Singh, R.; Phillips, F.; Wallace, R. H.; Richards, M. C.; Williams, D. A.; Mulley, J. C.; Berkovic, S. F.; Scheffer, I. E.; Petrou, S. Truncation of the GABA(A)-receptor gamma2 subunit in a family with generalized epilepsy with febrile seizures plus. *Am. J. Hum. Genet* **2002**, *70*, 530-536.

(12) Bianchi, M. T.; Song, L.; Zhang, H.; Macdonald, R. L. Two different mechanisms of disinhibition produced by GABAA receptor mutations linked to epilepsy in humans. *J. Neurosci* **2002**, *22*, 5321-5327.

(13) Steinlein, O. K.; Mulley, J. C.; Propping, P.; Wallace, R. H.; Phillips, H. A.; Sutherland,

G. R.; Scheffer, I. E.; Berkovic, S. F. A missense mutation in the neuronal nicotinic acetylcholine receptor alpha 4 subunit is associated with autosomal dominant nocturnal frontal lobe epilepsy. *Nat. Genet* **1995**, *11*, 201-203.

(14) Leniger, T.; Kananura, C.; Hufnagel, A.; Bertrand, S.; Bertrand, D.; Steinlein, O. K. A new Chrna4 mutation with low penetrance in nocturnal frontal lobe epilepsy. *Epilepsia* **2003**, *44*, 981-985.

(15) Hirose, S.; Iwata, H.; Akiyoshi, H.; Kobayashi, K.; Ito, M.; Wada, K.; Kaneko, S.; Mitsudome, A. A novel mutation of CHRNA4 responsible for autosomal dominant nocturnal frontal lobe epilepsy. *Neurology* **1999**, *53*, 1749-1753.

(16) Chen, Y.; Wu, L.; Fang, Y.; He, Z.; Peng, B.; Shen, Y.; Xu, Q. A novel mutation of the nicotinic acetylcholine receptor gene CHRNA4 in sporadic nocturnal frontal lobe epilepsy. *Epilepsy Res* **2009**, *83*, 152-156.

(17) Weiland, S.; Witzemann, V.; Villarroel, A.; Propping, P.; Steinlein, O. An amino acid exchange in the second transmembrane segment of a neuronal nicotinic receptor causes partial epilepsy by altering its desensitization kinetics. *FEBS Lett* **1996**, *398*, 91-96.

(18) Steinlein, O. K.; Magnusson, A.; Stoodt, J.; Bertrand, S.; Weiland, S.; Berkovic, S. F.; Nakken, K. O.; Propping, P.; Bertrand, D. An insertion mutation of the CHRNA4 gene in a family with autosomal dominant nocturnal frontal lobe epilepsy. *Hum. Mol. Genet* **1997**, *6*, 943-947.

(19) McLellan, A.; Phillips, H. A.; Rittey, C.; Kirkpatrick, M.; Mulley, J. C.; Goudie, D.; Stephenson, J. B. P.; Tolmie, J.; Scheffer, I. E.; Berkovic, S. F.; Zuberi, S. M. Phenotypic comparison of two Scottish families with mutations in different genes causing autosomal dominant nocturnal frontal lobe epilepsy. *Epilepsia* **2003**, *44*, 613-617.

(20) De Fusco, M.; Becchetti, A.; Patrignani, A.; Annesi, G.; Gambardella, A.; Quattrone, A.; Ballabio, A.; Wanke, E.; Casari, G. The nicotinic receptor beta 2 subunit is mutant in nocturnal frontal lobe epilepsy. *Nat. Genet* **2000**, *26*, 275-276.

(21) Figl, A.; Viseshakul, N.; Shafaee, N.; Forsayeth, J.; Cohen, B. N. Two mutations linked to nocturnal frontal lobe epilepsy cause use-dependent potentiation of the nicotinic ACh response. *J. Physiol. (Lond.)* **1998**, *513 (Pt 3)*, 655-670.

(22) Phillips, H. A.; Marini, C.; Scheffer, I. E.; Sutherland, G. R.; Mulley, J. C.; Berkovic, S. F. A de novo mutation in sporadic nocturnal frontal lobe epilepsy. *Ann. Neurol* **2000**, *48*, 264-267.

(23) Steinlein, O. K.; Bertrand, D. Nicotinic receptor channelopathies and epilepsy. *Pflugers Arch* **2009**.

(24) Rogawski, M. A. KCNQ2/KCNQ3 K+ channels and the molecular pathogenesis of epilepsy: implications for therapy. *Trends Neurosci* **2000**, *23*, 393-398.

(25) Singh, N. A.; Charlier, C.; Stauffer, D.; DuPont, B. R.; Leach, R. J.; Melis, R.; Ronen, G. M.; Bjerre, I.; Quattlebaum, T.; Murphy, J. V.; McHarg, M. L.; Gagnon, D.; Rosales, T. O.; Peiffer, A.; Anderson, V. E.; Leppert, M. A novel potassium channel gene, KCNQ2, is mutated in an inherited epilepsy of newborns. *Nat. Genet* **1998**, *18*, 25-29.

(26) Biervert, C.; Schroeder, B. C.; Kubisch, C.; Berkovic, S. F.; Propping, P.; Jentsch, T. J.; Steinlein, O. K. A potassium channel mutation in neonatal human epilepsy. *Science* **1998**, *279*, 403-406.

(27) Watanabe, H.; Nagata, E.; Kosakai, A.; Nakamura, M.; Yokoyama, M.; Tanaka, K.; Sasai, H. Disruption of the epilepsy KCNQ2 gene results in neural hyperexcitability. *J. Neurochem* **2000**, *75*, 28-33.

(28) Heilstedt, H. A.; Burgess, D. L.; Anderson, A. E.; Chedrawi, A.; Tharp, B.; Lee, O.; Kashork, C. D.; Starkey, D. E.; Wu, Y. Q.; Noebels, J. L.; Shaffer, L. G.; Shapira, S. K. Loss of the potassium channel beta-subunit gene, KCNAB2, is associated with epilepsy in patients with 1p36 deletion syndrome. *Epilepsia* **2001**, *42*, 1103-1111.

(29) Zuberi, S. M.; Eunson, L. H.; Spauschus, A.; De Silva, R.; Tolmie, J.; Wood, N. W.; McWilliam, R. C.; Stephenson, J. B.; Stephenson, J. P.; Kullmann, D. M.; Hanna, M. G. A novel mutation in the human voltage-gated potassium channel gene (Kv1.1) associates with episodic ataxia type 1 and sometimes with partial epilepsy. *Brain* **1999**, *122 (Pt 5)*, 817-825.

(30) Eunson, L. H.; Rea, R.; Zuberi, S. M.; Youroukos, S.; Panayiotopoulos, C. P.; Liguori, R.; Avoni, P.; McWilliam, R. C.; Stephenson, J. B.; Hanna, M. G.; Kullmann, D. M.; Spauschus, A. Clinical, genetic, and expression studies of mutations in the potassium channel gene KCNA1 reveal new phenotypic variability. *Ann. Neurol* **2000**, *48*, 647-656.

(31) Mulley, J. C.; Scheffer, I. E.; Petrou, S.; Dibbens, L. M.; Berkovic, S. F.; Harkin, L. A. SCN1A mutations and epilepsy. *Hum. Mutat* **2005**, *25*, 535-542.

(32) Lulic, D.; Ahmadian, A.; Baaj, A. A.; Benbadis, S. R.; Vale, F. L. Vagus nerve stimulation. *Neurosurg Focus* **2009**, *27*, E5.

(33) Uthman, B. M.; Reichl, A. M.; Dean, J. C.; Eisenschenk, S.; Gilmore, R.; Reid, S.; Roper, S. N.; Wilder, B. J. Effectiveness of vagus nerve stimulation in epilepsy patients: a 12-year observation. *Neurology* **2004**, *63*, 1124-1126.

(34) Groves, D. A.; Brown, V. J. Vagal nerve stimulation: a review of its applications and potential mechanisms that mediate its clinical effects. *Neurosci Biobehav Rev* **2005**, *29*, 493-500.

(35) Epilepsy Foundation-Surgery. *Treatment Options: Surgery*.

(36) Nylen, K.; Likhodii, S.; Burnham, W. M. The ketogenic diet: proposed mechanisms of action. *Neurotherapeutics* **2009**, *6*, 402-405.

(37) Beniczky, S.; Jose Miranda, M.; Alving, J.; Heber Povlsen, J.; Wolf, P. Effectiveness of the ketogenic diet in a broad range of seizure types and EEG features for severe childhood epilepsies. *Acta Neurol. Scand* **2010**, *121*, 58-62.

(38) Bough, K. Energy metabolism as part of the anticonvulsant mechanism of the ketogenic diet. *Epilepsia* **2008**, *49 Suppl 8*, 91-93.

(39) Bough, K. J.; Rho, J. M. Anticonvulsant mechanisms of the ketogenic diet. *Epilepsia* **2007**, *48*, 43-58.

(40) Weinshenker, D.; Szot, P. The role of catecholamines in seizure susceptibility: new results using genetically engineered mice. *Pharmacol. Ther* **2002**, *94*, 213-233.

(41) Yan, Q. S.; Jobe, P. C.; Dailey, J. W. Noradrenergic mechanisms for the anticonvulsant effects of desipramine and yohimbine in genetically epilepsy-prone rats: studies with microdialysis. *Brain Res* **1993**, *610*, 24-31.

(42) *Epilepsy: A Comprehensive Textbook*; 2nd ed.; Wolters Kluwer Health/Lippincott Williams & Wilkins: Philadelphia, 2008.

(43) Ben-Menachem, E. Eslicarbazepine acetate: a well-kept secret? *Epilepsy Curr* **2010**, *10*, 7-8.

(44) Pearce, R. E.; Lu, W.; Wang, Y.; Uetrecht, J. P.; Correia, M. A.; Leeder, J. S. Pathways of carbamazepine bioactivation in vitro. III. The role of human cytochrome P450 enzymes in the formation of 2,3-dihydroxycarbamazepine. *Drug Metab. Dispos* **2008**, *36*, 1637-1649.

(45) Bialer, M.; Johannessen, S. I.; Levy, R. H.; Perucca, E.; Tomson, T.; White, H. S. Progress report on new antiepileptic drugs: a summary of the Ninth Eilat Conference (EILAT IX). *Epilepsy Res* **2009**, *83*, 1-43.

(46) Kuo, C. C. A common anticonvulsant binding site for phenytoin, carbamazepine, and lamotrigine in neuronal Na+ channels. *Mol. Pharmacol* **1998**, *54*, 712-721.

(47) Mintzer, S.; Mattson, R. T. Should enzyme-inducing antiepileptic drugs be considered first-line agents? *Epilepsia* **2009**, *50 Suppl 8*, 42-50.

(48) Gidal, B. E.; French, J. A.; Grossman, P.; Le Teuff, G. Assessment of potential drug interactions in patients with epilepsy: impact of age and sex. *Neurology* **2009**, *72*, 419-425.

(49) Taverna, S.; Sancini, G.; Mantegazza, M.; Franceschetti, S.; Avanzini, G. Inhibition of transient and persistent Na+ current fractions by the new anticonvulsant topiramate. *J. Pharmacol. Exp. Ther* **1999**, *288*, 960-968.

(50) Gryder, D. S.; Rogawski, M. A. Selective antagonism of GluR5 kainate-receptor-mediated synaptic currents by topiramate in rat basolateral amygdala neurons. *J.*

Neurosci **2003**, *23*, 7069-7074.

(51) White, H. S.; Brown, S. D.; Woodhead, J. H.; Skeen, G. A.; Wolf, H. H. Topiramate enhances GABA-mediated chloride flux and GABA-evoked chloride currents in murine brain neurons and increases seizure threshold. *Epilepsy Res* **1997**, *28*, 167-179.

(52) Braga, M. F. M.; Aroniadou-Anderjaska, V.; Li, H.; Rogawski, M. A. Topiramate reduces excitability in the basolateral amygdala by selectively inhibiting GluK1 (GluR5) kainate receptors on interneurons and positively modulating GABAA receptors on principal neurons. *J. Pharmacol. Exp. Ther* **2009**, *330*, 558-566.

(53) Kaminski, R. M.; Banerjee, M.; Rogawski, M. A. Topiramate selectively protects against seizures induced by ATPA, a GluR5 kainate receptor agonist. *Neuropharmacology* **2004**, *46*, 1097-1104.

(54) Angehagen, M.; Ben-Menachem, E.; Shank, R.; Rönnbäck, L.; Hansson, E. Topiramate modulation of kainate-induced calcium currents is inversely related to channel phosphorylation level. *J. Neurochem* **2004**, *88*, 320-325.

(55) Kwan, P.; Brodie, M. J. Phenobarbital for the treatment of epilepsy in the 21st century: a critical review. *Epilepsia* **2004**, *45*, 1141-1149.

(56) MacDonald, R. L.; Rogers, C. J.; Twyman, R. E. Barbiturate regulation of kinetic properties of the GABAA receptor channel of mouse spinal neurones in culture. *J. Physiol. (Lond.)* **1989**, *417*, 483-500.

(57) Twyman, R. E.; Rogers, C. J.; Macdonald, R. L. Differential regulation of gamma-aminobutyric acid receptor channels by diazepam and phenobarbital. *Ann. Neurol* **1989**, *25*, 213-220.

(58) Rho, J. M.; Donevan, S. D.; Rogawski, M. A. Direct activation of GABAA receptors by barbiturates in cultured rat hippocampal neurons. *J. Physiol. (Lond.)* **1996**, *497 (Pt 2)*, 509-522.

(59) van der Laan, J. W.; de Boer, T.; Bruinvels, J. Di-n-propylacetate and GABA degradation. Preferential inhibition of succinic semialdehyde dehydrogenase and indirect inhibition of GABA-transaminase. *J. Neurochem* **1979**, *32*, 1769-1780.

(60) Johannessen, C. U. Mechanisms of action of valproate: a commentatory. *Neurochem. Int* **2000**, *37*, 103-110.

(61) Toth, M. The epsilon theory: a novel synthesis of the underlying molecular and electrophysiological mechanisms of primary generalized epilepsy and the possible mechanism of action of valproate. *Med. Hypotheses* **2005**, *64*, 267-272.

(62) Bazinet, R. P.; Weis, M. T.; Rapoport, S. I.; Rosenberger, T. A. Valproic acid selectively inhibits conversion of arachidonic acid to arachidonoyl-CoA by brain microsomal long-chain fatty acyl-CoA synthetases: relevance to bipolar disorder. *Psychopharmacology*

(Berl.) **2006**, *184*, 122-129.

(63) Rosenberg, G. The mechanisms of action of valproate in neuropsychiatric disorders: can we see the forest for the trees? *Cell. Mol. Life Sci* **2007**, *64*, 2090-2103.

(64) Hendrich, J.; Van Minh, A. T.; Heblich, F.; Nieto-Rostro, M.; Watschinger, K.; Striessnig, J.; Wratten, J.; Davies, A.; Dolphin, A. C. Pharmacological disruption of calcium channel trafficking by the alpha2delta ligand gabapentin. *Proc. Natl. Acad. Sci. U.S.A* **2008**, *105*, 3628-3633.

(65) Abdul-Ghani, A. S.; Coutinho-Netto, J.; Bradford, H. F. The action of gamma-vinyl-GABA and gamma-acetylenic-GABA on the resting and stimulated release of GABA in vivo. *Brain Res* **1980**, *191*, 471-481.

(66) Petroff, O. A.; Behar, K. L.; Mattson, R. H.; Rothman, D. L. Human brain gamma-aminobutyric acid levels and seizure control following initiation of vigabatrin therapy. *J. Neurochem* **1996**, *67*, 2399-2404.

(67) Nakamura, F.; Suzuki, S.; Nishimura, S.; Yagi, K.; Seino, M. Effects of clobazam and its active metabolite on GABA-activated currents in rat cerebral neurons in culture. *Epilepsia* **1996**, *37*, 728-735.

(68) Coulter, D. A.; Huguenard, J. R.; Prince, D. A. Characterization of ethosuximide reduction of low-threshold calcium current in thalamic neurons. *Ann. Neurol* **1989**, *25*, 582-593.

(69) Kito, M.; Maehara, M.; Watanabe, K. Mechanisms of T-type calcium channel blockade by zonisamide. *Seizure* **1996**, *5*, 115-119.

(70) Suzuki, S.; Kawakami, K.; Nishimura, S.; Watanabe, Y.; Yagi, K.; Seino, M.; Miyamoto, K. Zonisamide blocks T-type calcium channel in cultured neurons of rat cerebral cortex. *Epilepsy Res* **1992**, *12*, 21-27.

(71) Schauf, C. L. Zonisamide enhances slow sodium inactivation in Myxicola. *Brain Res* **1987**, *413*, 185-188.

(72) Mimaki, T.; Suzuki, Y.; Tagawa, T.; Karasawa, T.; Yabuuchi, H. Interaction of zonisamide with benzodiazepine and GABA receptors in rat brain. *Med J Osaka Univ* **1990**, *39*, 13-17.

(73) Macdonald, R. L.; Greenfield, L. J. Mechanisms of action of new antiepileptic drugs. *Curr. Opin. Neurol* **1997**, *10*, 121-128.

(74) Sander, J. W.; Patsalos, P. N. An assessment of serum and red blood cell folate concentrations in patients with epilepsy on lamotrigine therapy. *Epilepsy Res* **1992**, *13*, 89-92.

(75) Cheung, H.; Kamp, D.; Harris, E. An in vitro investigation of the action of lamotrigine on

neuronal voltage-activated sodium channels. *Epilepsy Res* **1992**, *13*, 107-112.

(76) Rekling, J. C.; Jahnsen, H.; Mosfeldt Laursen, A. The effect of two lipophilic gamma-aminobutyric acid uptake blockers in CA1 of the rat hippocampal slice. *Br. J. Pharmacol* **1990**, *99*, 103-106.

(77) Nielsen, E. B.; Suzdak, P. D.; Andersen, K. E.; Knutsen, L. J.; Sonnewald, U.; Braestrup, C. Characterization of tiagabine (NO-328), a new potent and selective GABA uptake inhibitor. *Eur. J. Pharmacol* **1991**, *196*, 257-266.

(78) Pellock, J. M. Felbamate in epilepsy therapy: evaluating the risks. *Drug Saf* **1999**, *21*, 225-239.

(79) Harty, T. P.; Rogawski, M. A. Felbamate block of recombinant N-methyl-D-aspartate receptors: selectivity for the NR2B subunit. *Epilepsy Res* **2000**, *39*, 47-55.

(80) Taglialatela, M.; Ongini, E.; Brown, A. M.; Di Renzo, G.; Annunziato, L. Felbamate inhibits cloned voltage-dependent Na+ channels from human and rat brain. *Eur. J. Pharmacol* **1996**, *316*, 373-377.

(81) Kume, A.; Greenfield, L. J.; Macdonald, R. L.; Albin, R. L. Felbamate inhibits [3H]t-butylbicycloorthobenzoate (TBOB) binding and enhances Cl- current at the gamma-aminobutyric AcidA (GABAA) receptor. *J. Pharmacol. Exp. Ther* **1996**, *277*, 1784-1792.

(82) Rho, J. M.; Donevan, S. D.; Rogawski, M. A. Mechanism of action of the anticonvulsant felbamate: opposing effects on N-methyl-D-aspartate and gamma-aminobutyric acidA receptors. *Ann. Neurol* **1994**, *35*, 229-234.

(83) Kuo, C.; Lin, B.; Chang, H.; Hsieh, C. Use-dependent inhibition of the N-methyl-D-aspartate currents by felbamate: a gating modifier with selective binding to the desensitized channels. *Mol. Pharmacol* **2004**, *65*, 370-380.

(84) Lynch, B. A.; Lambeng, N.; Nocka, K.; Kensel-Hammes, P.; Bajjalieh, S. M.; Matagne, A.; Fuks, B. The synaptic vesicle protein SV2A is the binding site for the antiepileptic drug levetiracetam. *Proc. Natl. Acad. Sci. U.S.A* **2004**, *101*, 9861-9866.

(85) Janz, R.; Goda, Y.; Geppert, M.; Missler, M.; Südhof, T. C. SV2A and SV2B function as redundant Ca2+ regulators in neurotransmitter release. *Neuron* **1999**, *24*, 1003-1016.

(86) Matagne, A.; Margineanu, D.; Kenda, B.; Michel, P.; Klitgaard, H. Anti-convulsive and anti-epileptic properties of brivaracetam (ucb 34714), a high-affinity ligand for the synaptic vesicle protein, SV2A. *Br. J. Pharmacol* **2008**, *154*, 1662-1671.

(87) Zona, C.; Pieri, M.; Carunchio, I.; Curcio, L.; Klitgaard, H.; Margineanu, D. G. Brivaracetam (ucb 34714) inhibits Na(+) current in rat cortical neurons in culture. *Epilepsy Res* **2010**, *88*, 46-54.

(88) White, H. S.; Franklin, M. R.; Kupferberg, H. J.; Schmutz, M.; Stables, J. P.; Wolf, H. H.

The anticonvulsant profile of rufinamide (CGP 33101) in rodent seizure models. *Epilepsia* **2008**, *49*, 1213-1220.

(89) McLean, M. J.; Schmutz, M. The Influence of Rufinamide on Sodium Currents and Action Potential Firing in Rodent Neurons. *Epilepsia* **2005**, *46*, 296.

(90) UCB :: UCB's Vimpat® approved by U.S. FDA as adjunctive therapy for partial onset seizures in adults.

(91) Clinical Trials.gov Search of: Lacosamide neuropathic pain - List Results - ClinicalTrials.gov.

(92) Conley, J. D.; Kohn, H. Functionalized DL-amino acid derivatives. Potent new agents for the treatment of epilepsy. *J. Med. Chem* **1987**, *30*, 567-574.

(93) Shorvon, S. D.; Fish, D.; Dodson, W. E. *The treatment of epilepsy*; Wiley-Blackwell, 2004.

(94) Choi, D.; Stables, J. P.; Kohn, H. The anticonvulsant activities of functionalized N-benzyl 2-acetamidoacetamides. The importance of the 2-acetamido substituent. *Bioorg. Med. Chem* **1996**, *4*, 2105-2114.

(95) Kohn, H.; Sawhney, K. N.; LeGall, P.; Conley, J. D.; Robertson, D. W.; Leander, J. D. Preparation and anticonvulsant activity of a series of functionalized alpha-aromatic and alpha-heteroaromatic amino acids. *J. Med. Chem* **1990**, *33*, 919-926.

(96) Kohn, H.; Sawhney, K. N.; Bardel, P.; Robertson, D. W.; Leander, J. D. Synthesis and anticonvulsant activities of alpha-heterocyclic alpha-acetamido-N-benzylacetamide derivatives. *J. Med. Chem* **1993**, *36*, 3350-3360.

(97) Bardel, P.; Bolanos, A.; Kohn, H. Synthesis and anticonvulsant activities of alpha-acetamido-N-benzylacetamide derivatives containing an electron-deficient alpha-heteroaromatic substituent. *J. Med. Chem* **1994**, *37*, 4567-4571.

(98) Choi, D.; Stables, J. P.; Kohn, H. Synthesis and anticonvulsant activities of N-Benzyl-2-acetamidopropionamide derivatives. *J. Med. Chem* **1996**, *39*, 1907-1916.

(99) LeTiran, A.; Stables, J. P.; Kohn, H. Design and evaluation of affinity labels of functionalized amino acid anticonvulsants. *J. Med. Chem* **2002**, *45*, 4762-4773.

(100) Stöhr, T.; Kupferberg, H. J.; Stables, J. P.; Choi, D.; Harris, R. H.; Kohn, H.; Walton, N.; White, H. S. Lacosamide, a novel anti-convulsant drug, shows efficacy with a wide safety margin in rodent models for epilepsy. *Epilepsy Res* **2007**, *74*, 147-154.

(101) Bialer, M.; White, H. S. Key factors in the discovery and development of new antiepileptic drugs. *Nat Rev Drug Discov* **2010**, *9*, 68-82.

(102) EMEA Assesment Report for Vimpat: EMEA 460925/2008 **2008**.

(103) Schwarz Pharma Lacosamide Has a Novel Dual Mode of Action **2006**.

(104) Sheets, P. L.; Heers, C.; Stoehr, T.; Cummins, T. R. Differential block of sensory neuronal voltage-gated sodium channels by lacosamide [(2R)-2-(acetylamino)-N-benzyl-3-methoxypropanamide], lidocaine, and carbamazepine. *J. Pharmacol. Exp. Ther* **2008**, *326*, 89-99.

(105) Errington, A. C.; Stöhr, T.; Heers, C.; Lees, G. The investigational anticonvulsant lacosamide selectively enhances slow inactivation of voltage-gated sodium channels. *Mol. Pharmacol* **2008**, *73*, 157-169.

(106) Temperini, C.; Innocenti, A.; Scozzafava, A.; Parkkila, S.; Supuran, C. T. The coumarin-binding site in carbonic anhydrase accommodates structurally diverse inhibitors: the antiepileptic lacosamide as an example and lead molecule for novel classes of carbonic anhydrase inhibitors. *J. Med. Chem* **2010**, *53*, 850-854.

(107) Park, K. D.; Morieux, P.; Salomé, C.; Cotten, S. W.; Reamtong, O.; Eyers, C.; Gaskell, S. J.; Stables, J. P.; Liu, R.; Kohn, H. Lacosamide Isothiocyanate-Based Agents: Novel Agents To Target and Identify Lacosamide Receptors. *J. Med. Chem* **2009**.

(108) Koul, A.; Dendouga, N.; Vergauwen, K.; Molenberghs, B.; Vranckx, L.; Willebrords, R.; Ristic, Z.; Lill, H.; Dorange, I.; Guillemont, J.; Bald, D.; Andries, K. Diarylquinolines target subunit c of mycobacterial ATP synthase. *Nat. Chem. Biol* **2007**, *3*, 323-324.

(109) Brehmer, D.; Greff, Z.; Godl, K.; Blencke, S.; Kurtenbach, A.; Weber, M.; Müller, S.; Klebl, B.; Cotten, M.; Kéri, G.; Wissing, J.; Daub, H. Cellular targets of gefitinib. *Cancer Res* **2005**, *65*, 379-382.

(110) Harding, M. W.; Galat, A.; Uehling, D. E.; Schreiber, S. L. A receptor for the immunosuppressant FK506 is a cis-trans peptidyl-prolyl isomerase. *Nature* **1989**, *341*, 758-760.

(111) Taunton, J.; Hassig, C. A.; Schreiber, S. L. A mammalian histone deacetylase related to the yeast transcriptional regulator Rpd3p. *Science* **1996**, *272*, 408-411.

(112) Vodovozova, E. L. Photoaffinity labeling and its application in structural biology. *Biochemistry Mosc* **2007**, *72*, 1-20.

(113) Hatanaka, Y.; Sadakane, Y. Photoaffinity labeling in drug discovery and developments: chemical gateway for entering proteomic frontier. *Curr Top Med Chem* **2002**, *2*, 271-288.

(114) Hashimoto, M.; Hatanaka, Y. Recent Progress in Diazirine-Based Photoaffinity Labeling. *European Journal of Organic Chemistry* **2008**, *2008*, 2513-2523.

(115) Dormán, G.; Prestwich, G. D. Using photolabile ligands in drug discovery and development. *Trends Biotechnol* **2000**, *18*, 64-77.

(116) Fuks, B.; Gillard, M.; Michel, P.; Lynch, B.; Vertongen, P.; Leprince, P.; Klitgaard, H.;

Chatelain, P. Localization and photoaffinity labelling of the levetiracetam binding site in rat brain and certain cell lines. *Eur. J. Pharmacol* **2003**, *478*, 11-19.

(117) Lynch, B. A.; Lambeng, N.; Nocka, K.; Kensel-Hammes, P.; Bajjalieh, S. M.; Matagne, A.; Fuks, B. The synaptic vesicle protein SV2A is the binding site for the antiepileptic drug levetiracetam. *Proc. Natl. Acad. Sci. U.S.A* **2004**, *101*, 9861-9866.

(118) MacKinnon, A. L.; Garrison, J. L.; Hegde, R. S.; Taunton, J. Photo-leucine incorporation reveals the target of a cyclodepsipeptide inhibitor of cotranslational translocation. *J. Am. Chem. Soc* **2007**, *129*, 14560-14561.

(119) Gunther, E. C.; Stone, D. J.; Gerwien, R. W.; Bento, P.; Heyes, M. P. Prediction of clinical drug efficacy by classification of drug-induced genomic expression profiles in vitro. *Proc. Natl. Acad. Sci. U.S.A* **2003**, *100*, 9608-9613.

(120) Sinha, B.; Cao, Z.; Murray, T. F.; Aldrich, J. V. Discovery of dermorphin-based affinity labels with subnanomolar affinity for mu opioid receptors. *J. Med. Chem* **2009**, *52*, 7372-7375.

(121) Burke, T. R.; Bajwa, B. S.; Jacobson, A. E.; Rice, K. C.; Streaty, R. A.; Klee, W. A. Probes for narcotic receptor mediated phenomena. 7. Synthesis and pharmacological properties of irreversible ligands specific for mu or delta opiate receptors. *J. Med. Chem* **1984**, *27*, 1570-1574.

(122) de Costa, B. R.; Rothman, R. B.; Bykov, V.; Jacobson, A. E.; Rice, K. C. Selective and enantiospecific acylation of kappa opioid receptors by (1S,2S)-trans-2-isothiocyanato-N-methyl-N-[2-(1-pyrrolidinyl) cyclohexy l] benzeneacetamide. Demonstration of kappa receptor heterogeneity. *J. Med. Chem* **1989**, *32*, 281-283.

(123) Maeda, D. Y.; Ishmael, J. E.; Murray, T. F.; Aldrich, J. V. Synthesis and evaluation of N,N-dialkyl enkephalin-based affinity labels for delta opioid receptors. *J. Med. Chem* **2000**, *43*, 3941-3948.

(124) Choi, H.; Murray, T. F.; Aldrich, J. V. Synthesis and evaluation of potential affinity labels derived from endomorphin-2. *J. Pept. Res* **2003**, *61*, 58-62.

(125) Li, X.; Cao, J.; Li, Y.; Rondard, P.; Zhang, Y.; Yi, P.; Liu, J.; Nan, F. Activity-based probe for specific photoaffinity labeling gamma-aminobutyric acid B (GABAB) receptors on living cells: design, synthesis, and biological evaluation. *J. Med. Chem* **2008**, *51*, 3057-3060.

(126) Williams, E. F.; Rice, K. C.; Paul, S. M.; Skolnick, P. Heterogeneity of benzodiazepine receptors in the central nervous system demonstrated with kenazepine, an alkylating benzodiazepine. *J. Neurochem* **1980**, *35*, 591-597.

(127) de Costa, B. R.; Lewin, A. H.; Rice, K. C.; Skolnick, P.; Schoenheimer, J. A. Novel site-directed affinity ligands for GABA-gated chloride channels: synthesis, characterization, and molecular modeling of 1-(isothiocyanatophenyl)-4-tert-butyl-2,6,7-

trioxabicyclo[2.2.2]octanes. *J. Med. Chem* **1991**, *34*, 1531-1538.

(128) Atlas, D.; Plotek, Y.; Miskin, I. An affinity label for alpha 2-adrenergic receptors in rat brain. *Eur. J. Biochem* **1982**, *126*, 537-541.

(129) Soskić, V.; Maelicke, A.; Petrovic, G.; Ristic, B.; Petrović, J. Synthesis of some phenothiazine derivatives as potential affinity ligands for the central dopamine receptors. *J. Pharm. Pharmacol* **1991**, *43*, 27-30.

(130) Campbell, D. A.; Szardenings, A. K. Functional profiling of the proteome with affinity labels. *Curr Opin Chem Biol* **2003**, *7*, 296-303.

(131) Kho, Y.; Kim, S. C.; Jiang, C.; Barma, D.; Kwon, S. W.; Cheng, J.; Jaunbergs, J.; Weinbaum, C.; Tamanoi, F.; Falck, J.; Zhao, Y. A tagging-via-substrate technology for detection and proteomics of farnesylated proteins. *Proc. Natl. Acad. Sci. US A* **2004**, *101*, 12479-84.

(132) Salisbury, C. M.; Cravatt, B. F. Activity-based probes for proteomic profiling of histone deacetylase complexes. *Proc Natl Acad Sci U S A* **2007**, *104*, 1171-6.

(133) Schmidinger; Hermetter; Birner-Gruenberger Activity-based proteomics: enzymatic activity profiling in complex proteomes. *Amino Acids* **2006**, *30*, 333-350.

(134) Weerapana, E.; Simon, G. M.; Cravatt, B. F. Disparate proteome reactivity profiles of carbon electrophiles. *Nat. Chem. Biol* **2008**, *4*, 405-7.

(135) Adam, G. C.; Burbaum, J.; Kozarich, J. W.; Patricelli, M. P.; Cravatt, B. F. Mapping enzyme active sites in complex proteomes. *J. Am. Chem. Soc.* **2004**, *126*, 1363-8.

(136) Adam, G. C.; Sorensen, E. J.; Cravatt, B. F. Proteomic profiling of mechanistically distinct enzyme classes using a common chemotype. *Nat. Biotechnol* **2002**, *20*, 805-809.

(137) Greenbaum, D. C.; Baruch, A.; Grainger, M.; Bozdech, Z.; Medzihradszky, K. F.; Engel, J.; DeRisi, J.; Holder, A. A.; Bogyo, M. A role for the protease falcipain 1 in host cell invasion by the human malaria parasite. *Science* **2002**, *298*, 2002-2006.

(138) von Rechenberg, M.; Blake, B. K.; Ho, Y. J.; Zhen, Y.; Chepanoske, C. L.; Richardson, B. E.; Xu, N.; Kery, V. Ampicillin/penicillin-binding protein interactions as a model drug-target system to optimize affinity pull-down and mass spectrometric strategies for target and pathway identification. *Proteomics* **2005**, *5*, 1764-1773.

(139) Marton, M. J.; DeRisi, J. L.; Bennett, H. A.; Iyer, V. R.; Meyer, M. R.; Roberts, C. J.; Stoughton, R.; Burchard, J.; Slade, D.; Dai, H.; Bassett, D. E.; Hartwell, L. H.; Brown, P. O.; Friend, S. H. Drug target validation and identification of secondary drug target effects using DNA microarrays. *Nat. Med* **1998**, *4*, 1293-1301.

(140) Lindsay, M. A. Target discovery. *Nat Rev Drug Discov* **2003**, *2*, 831-838.

(141) Watson, M.; Roulston, A.; Bélec, L.; Billot, X.; Marcellus, R.; Bédard, D.; Bernier, C.; Branchaud, S.; Chan, H.; Dairi, K.; Gilbert, K.; Goulet, D.; Gratton, M.; Isakau, H.; Jang, A.; Khadir, A.; Koch, E.; Lavoie, M.; Lawless, M.; Nguyen, M.; Paquette, D.; Turcotte, E.; Berger, A.; Mitchell, M.; Shore, G. C.; Beauparlant, P. The small molecule GMX1778 is a potent inhibitor of NAD+ biosynthesis: strategy for enhanced therapy in nicotinic acid phosphoribosyltransferase 1-deficient tumors. *Mol. Cell. Biol* **2009**, *29*, 5872-5888.

(142) Kolb, H. C.; Finn, M. G.; Sharpless, K. B. Click Chemistry: Diverse Chemical Function from a Few Good Reactions. *Angew. Chem. Int. Ed. Engl* **2001**, *40*, 2004-2021.

(143) Prescher, J. A.; Bertozzi, C. R. Chemistry in living systems. *Nat Chem Biol* **2005**, *1*, 13-21.

(144) Kolb, H. C.; Sharpless, K. B. The growing impact of click chemistry on drug discovery. *Drug Discov. Today* **2003**, *8*, 1128-1137.

(145) Agard, N. J.; Baskin, J. M.; Prescher, J. A.; Lo, A.; Bertozzi, C. R. A comparative study of bioorthogonal reactions with azides. *ACS. Chem. Biol.* **2006**, *1*, 644-8.

(146) Ballell, L.; Scherpenzeel, M. V.; Buchalova, K.; Liskamp, R. M. J.; Pieters, R. J. A new chemical probe for the detection of the cancer-linked galectin-3. *Org. Biomol. Chem.* **2006**, *4*, 4387-4394.

(147) Saxon, E.; Bertozzi, C. R. Cell surface engineering by a modified Staudinger reaction. *Science* **2000**, *287*, 2007-10.

(148) Swieten, P. F. V.; Leeuwenburgh, M. A.; Kessler, B. M.; Overkleeft, H. S. Bioorthogonal organic chemistry in living cells: novel strategies for labeling biomolecules. *Org. Biomol. Chem.* **2005**, *3*, 20-27.

(149) Cohen, M. S.; Hadjivassiliou, H.; Taunton, J. A clickable inhibitor reveals context-dependent autoactivation of p90 RSK. *Nat. Chem. Biol.* **2007**, *3*, 156-60.

(150) Errington, A. C.; Coyne, L.; Stöhr, T.; Selve, N.; Lees, G. Seeking a mechanism of action for the novel anticonvulsant lacosamide. *Neuropharmacology* **2006**, *50*, 1016-29.

(151) Choi, D.; Stables, J. P.; Kohn, H. Synthesis and anticonvulsant activities of N-Benzyl-2-acetamidopropionamide derivatives. *J. Med. Chem.* **1996**, *39*, 1907-16.

(152) Conley, J. D.; Kohn, H. Functionalized DL-amino acid derivatives. Potent new agents for the treatment of epilepsy. *J Med Chem* **1987**, *30*, 567-74.

(153) LeTiran, A.; Stables, J. P.; Kohn, H. Design and evaluation of affinity labels of functionalized amino acid anticonvulsants. *J. Med. Chem* **2002**, *45*, 4762-4773.

(154) Shen, M.; LeTiran, A.; Xiao, Y.; Golbraikh, A.; Kohn, H.; Tropsha, A. Quantitative structure-activity relationship analysis of functionalized amino acid anticonvulsant agents

using k nearest neighbor and simulated annealing PLS methods. *J. Med. Chem* **2002**, *45*, 2811-2823.

(155) Speers, A. E.; Cravatt, B. F. Profiling enzyme activities in vivo using click chemistry methods. *Chem. Biol* **2004**, *11*, 535-546.

(156) Huisgen, R. 1,3-Dipolar Cycloadditions. Past and Future. *Angew. Chem. Int. Edn. Engl.* **1963**, *2*, 565-598.

(157) Rostovtsev, V. V.; Green, L. G.; Fokin, V. V.; Sharpless, K. B. A stepwise huisgen cycloaddition process: copper(I)-catalyzed regioselective "ligation" of azides and terminal alkynes. *Angew. Chem. Int. Ed. Engl* **2002**, *41*, 2596-2599.

(158) Rodionov, V. O.; Presolski, S. I.; Díaz, D. D.; Fokin, V. V.; Finn, M. G. Ligand-accelerated Cu-catalyzed azide-alkyne cycloaddition: a mechanistic report. *J. Am. Chem. Soc* **2007**, *129*, 12705-12712.

(159) Siuzdak, G. *The Expanding Role of Mass Spectrometry in Biotechnology*; MCC Press, 2003.

(160) Wenthold, R. J.; Blahos, J.; Huh, K. H.; Petralia, R. S. Detergent solubilization and immunoprecipitation of native NMDA receptors. *Methods Mol. Biol* **1999**, *128*, 113-119.

(161) Andreu, J. M. Interaction of tubulin with non-denaturing amphiphiles. *EMBO J* **1982**, *1*, 1105-1110.

(162) Park, K. D.; Liu, R.; Kohn, H. Useful tools for biomolecule isolation, detection, and identification: acylhydrazone-based cleavable linkers. *Chem. Biol* **2009**, *16*, 763-772.

(163) Rizo, J.; Südhof, T. C. Snares and Munc18 in synaptic vesicle fusion. *Nat. Rev. Neurosci* **2002**, *3*, 641-53.

(164) Coleman, W. L.; Bykhovskaia, M. Rab3a-mediated vesicle recruitment regulates short-term plasticity at the mouse diaphragm synapse. *Mol. Cell. Neurosci* **2009**, *41*, 286-296.

(165) Sollner, T.; Whiteheart, S. W.; Brunner, M.; Erdjument-Bromage, H.; Geromanos, S.; Tempst, P.; Rothman, J. E. SNAP receptors implicated in vesicle targeting and fusion. *Nature* **1993**, *362*, 318-324.

(166) Toonen, R. F. G.; Verhage, M. Munc18-1 in secretion: lonely Munc joins SNARE team and takes control. *Trends Neurosci* **2007**, *30*, 564-72.

(167) Takemura, M.; Mishima, T.; Wang, Y.; Kasahara, J.; Fukunaga, K.; Ohashi, K.; Mizuno, K. Ca2+/calmodulin-dependent protein kinase IV-mediated LIM kinase activation is critical for calcium signal-induced neurite outgrowth. *J. Biol. Chem* **2009**, *284*, 28554-28562.

(168) Ybot-Gonzalez, P.; Savery, D.; Gerrelli, D.; Signore, M.; Mitchell, C. E.; Faux, C. H.;

Greene, N. D. E.; Copp, A. J. Convergent extension, planar-cell-polarity signalling and initiation of mouse neural tube closure. *Development* **2007**, *134*, 789-799.

(169) Reilly, S. C.; Kipar, A.; Hughes, D. J.; Quinn, J. P.; Cossins, A. R.; Sneddon, L. U. Investigation of Van Gogh-like 2 mRNA regulation and localisation in response to nociception in the brain of adult common carp (Cyprinus carpio). *Neurosci. Lett* **2009**, *465*, 290-294.

(170) Charrier, E.; Reibel, S.; Rogemond, V.; Aguera, M.; Thomasset, N.; Honnorat, J. Collapsin response mediator proteins (CRMPs): involvement in nervous system development and adult neurodegenerative disorders. *Mol Neurobiol* **2003**, *28*, 51-64.

(171) Yoshimura, T.; Kawano, Y.; Arimura, N.; Kawabata, S.; Kikuchi, A.; Kaibuchi, K. GSK-3beta regulates phosphorylation of CRMP-2 and neuronal polarity. *Cell* **2005**, *120*, 137-49.

(172) Li, Y.; Wu, Y.; Li, R.; Zhou, Y. The role of 14-3-3 dimerization in its modulation of the CaV2.2 channel. *Channels (Austin)* **2007**, *1*, 1-2.

(173) Südhof, T. C. alpha-Latrotoxin and its receptors: neurexins and CIRL/latrophilins. *Annu. Rev. Neurosci* **2001**, *24*, 933-962.

(174) McCudden, C. R.; Hains, M. D.; Kimple, R. J.; Siderovski, D. P.; Willard, F. S. G-protein signaling: back to the future. *Cell. Mol. Life Sci* **2005**, *62*, 551-577.

(175) Nakata, H.; Kozasa, T. Functional Characterization of Gαo Signaling through G Protein-Regulated Inducer of Neurite Outgrowth 1. *Molecular Pharmacology* **2005**, *67*, 695-702.

(176) Korshunova, I.; Caroni, P.; Kolkova, K.; Berezin, V.; Bock, E.; Walmod, P. S. Characterization of BASP1-mediated neurite outgrowth. *J. Neurosci. Res* **2008**, *86*, 2201-2213.

(177) Schulze, A. Creatine deficiency syndromes. *Mol Cell Biochem* **2003**, *244*, 143-50.

(178) Streijger, F.; Scheenen, W. J. J. M.; van Luijtelaar, G.; Oerlemans, F.; Wieringa, B.; Van der Zee, C. E. E. M. Complete brain-type creatine kinase deficiency in mice blocks seizure activity and affects intracellular calcium kinetics. *Epilepsia* **2009**.

(179) Temperini, C.; Innocenti, A.; Scozzafava, A.; Parkkila, S.; Supuran, C. T. The Coumarin-Binding Site in Carbonic Anhydrase Accommodates Structurally Diverse Inhibitors: The Antiepileptic Lacosamide As an Example and Lead Molecule for Novel Classes of Carbonic Anhydrase Inhibitors. *J Med Chem* **2009**.

(180) Clapcote, S. J.; Duffy, S.; Xie, G.; Kirshenbaum, G.; Bechard, A. R.; Rodacker Schack, V.; Petersen, J.; Sinai, L.; Saab, B. J.; Lerch, J. P.; Minassian, B. A.; Ackerley, C. A.; Sled, J. G.; Cortez, M. A.; Henderson, J. T.; Vilsen, B.; Roder, J. C. Mutation I810N in the alpha3 isoform of Na+,K+-ATPase causes impairments in the sodium pump and hyperexcitability in the CNS. *Proc. Natl. Acad. Sci. U.S.A* **2009**, *106*, 14085-14090.

(181) de Carvalho Aguiar, P.; Sweadner, K. J.; Penniston, J. T.; Zaremba, J.; Liu, L.; Caton, M.; Linazasoro, G.; Borg, M.; Tijssen, M. A. J.; Bressman, S. B.; Dobyns, W. B.; Brashear, A.; Ozelius, L. J. Mutations in the Na+/K+ -ATPase alpha3 gene ATP1A3 are associated with rapid-onset dystonia parkinsonism. *Neuron* **2004**, *43*, 169-175.

(182) Saitsu, H.; Kato, M.; Mizuguchi, T.; Hamada, K.; Osaka, H.; Tohyama, J.; Uruno, K.; Kumada, S.; Nishiyama, K.; Nishimura, A.; Okada, I.; Yoshimura, Y.; Hirai, S.; Kumada, T.; Hayasaka, K.; Fukuda, A.; Ogata, K.; Matsumoto, N. De novo mutations in the gene encoding STXBP1 (MUNC18-1) cause early infantile epileptic encephalopathy. *Nat Genet* **2008**, *40*, 782-8.

(183) Shen, X.; Valencia, C. A.; Szostak, J. W.; Szostak, J.; Dong, B.; Liu, R. Scanning the human proteome for calmodulin-binding proteins. *Proc Natl Acad Sci U S A* **2005**, *102*, 5969-74.

(184) Shen, X.; Valencia, C. A.; Gao, W.; Cotten, S. W.; Dong, B.; Huang, B.; Liu, R. Ca(2+)/Calmodulin-binding proteins from the C. elegans proteome. *Cell Calcium* **2008**, *43*, 444-56.

(185) Fukata, Y.; Itoh, T. J.; Kimura, T.; Ménager, C.; Nishimura, T.; Shiromizu, T.; Watanabe, H.; Inagaki, N.; Iwamatsu, A.; Hotani, H.; Kaibuchi, K. CRMP-2 binds to tubulin heterodimers to promote microtubule assembly. *Nat. Cell Biol* **2002**, *4*, 583-591.

(186) Inagaki, N.; Chihara, K.; Arimura, N.; Ménager, C.; Kawano, Y.; Matsuo, N.; Nishimura, T.; Amano, M.; Kaibuchi, K. CRMP-2 induces axons in cultured hippocampal neurons. *Nat. Neurosci* **2001**, *4*, 781-782.

(187) Chae, Y. C.; Lee, S.; Heo, K.; Ha, S. H.; Jung, Y.; Kim, J. H.; Ihara, Y.; Suh, P.; Ryu, S. H. Collapsin response mediator protein-2 regulates neurite formation by modulating tubulin GTPase activity. *Cell. Signal* **2009**, *21*, 1818-1826.

(188) Arimura, N.; Ménager, C.; Kawano, Y.; Yoshimura, T.; Kawabata, S.; Hattori, A.; Fukata, Y.; Amano, M.; Goshima, Y.; Inagaki, M.; Morone, N.; Usukura, J.; Kaibuchi, K. Phosphorylation by Rho kinase regulates CRMP-2 activity in growth cones. *Mol. Cell. Biol* **2005**, *25*, 9973-84.

(189) Uchida, Y.; Ohshima, T.; Sasaki, Y.; Suzuki, H.; Yanai, S.; Yamashita, N.; Nakamura, F.; Takei, K.; Ihara, Y.; Mikoshiba, K.; Kolattukudy, P.; Honnorat, J.; Goshima, Y. Semaphorin3A signalling is mediated via sequential Cdk5 and GSK3beta phosphorylation of CRMP2: implication of common phosphorylating mechanism underlying axon guidance and Alzheimer's disease. *Genes Cells* **2005**, *10*, 165-179.

(190) Hou, S. T.; Jiang, S. X.; Aylsworth, A.; Ferguson, G.; Slinn, J.; Hu, H.; Leung, T.; Kappler, J.; Kaibuchi, K. CaMKII phosphorylates collapsin response mediator protein 2 and modulates axonal damage during glutamate excitotoxicity. *J. Neurochem* **2009**, *111*, 870-881.

(191) Bretin, S.; Rogemond, V.; Marin, P.; Maus, M.; Torrens, Y.; Honnorat, J.; Glowinski, J.;

Prémont, J.; Gauchy, C. Calpain product of WT-CRMP2 reduces the amount of surface NR2B NMDA receptor subunit. *J Neurochem* **2006**, *98*, 1252-65.

(192) Cole, A. R.; Noble, W.; van Aalten, L.; Plattner, F.; Meimaridou, R.; Hogan, D.; Taylor, M.; LaFrancois, J.; Gunn-Moore, F.; Verkhratsky, A.; Oddo, S.; LaFerla, F.; Giese, K. P.; Dineley, K. T.; Duff, K.; Richardson, J. C.; Yan, S. D.; Hanger, D. P.; Allan, S. M.; Sutherland, C. Collapsin response mediator protein-2 hyperphosphorylation is an early event in Alzheimer's disease progression. *J. Neurochem* **2007**, *103*, 1132-1144.

(193) Stenmark, P.; Ogg, D.; Flodin, S.; Flores, A.; Kotenyova, T.; Nyman, T.; Nordlund, P.; Kursula, P. The structure of human collapsin response mediator protein 2, a regulator of axonal growth. *J. Neurochem* **2007**, *101*, 906-917.

(194) Majava, V.; Löytynoja, N.; Chen, W.; Lubec, G.; Kursula, P. Crystal and solution structure, stability and post-translational modifications of collapsin response mediator protein 2. *FEBS J* **2008**, *275*, 4583-4596.

(195) Zhang, Z.; Majava, V.; Greffier, A.; Hayes, R. L.; Kursula, P.; Wang, K. K. W. Collapsin response mediator protein-2 is a calmodulin-binding protein. *Cell. Mol. Life Sci* **2009**, *66*, 526-536.

(196) Chi, X. X.; Schmutzler, B. S.; Brittain, J. M.; Wang, Y.; Hingtgen, C. M.; Nicol, G. D.; Khanna, R. Regulation of N-type voltage-gated calcium channels (Cav2.2) and transmitter release by collapsin response mediator protein-2 (CRMP-2) in sensory neurons. *J. Cell. Sci* **2009**, *122*, 4351-4362.

(197) Verhage, M.; Maia, A. S.; Plomp, J. J.; Brussaard, A. B.; Heeroma, J. H.; Vermeer, H.; Toonen, R. F.; Hammer, R. E.; van den Berg, T. K.; Missler, M.; Geuze, H. J.; Südhof, T. C. Synaptic assembly of the brain in the absence of neurotransmitter secretion. *Science* **2000**, *287*, 864-9.

(198) Hamdan, F. F.; Piton, A.; Gauthier, J.; Lortie, A.; Dubeau, F.; Dobrzeniecka, S.; Spiegelman, D.; Noreau, A.; Pellerin, S.; Côté, M.; Henrion, E.; Fombonne, E.; Mottron, L.; Marineau, C.; Drapeau, P.; Lafrenière, R. G.; Lacaille, J. C.; Rouleau, G. A.; Michaud, J. L. De novo STXBP1 mutations in mental retardation and nonsyndromic epilepsy. *Ann. Neurol* **2009**, *65*, 748-753.

(199) Matveeva, E. A.; Whiteheart, S. W.; Vanaman, T. C.; Slevin, J. T. Phosphorylation of the N-ethylmaleimide-sensitive factor is associated with depolarization-dependent neurotransmitter release from synaptosomes. *J. Biol. Chem* **2001**, *276*, 12174-12181.

(200) Liu, Y.; Cheng, K.; Gong, K.; Fu, A. K. Y.; Ip, N. Y. Pctaire1 phosphorylates N-ethylmaleimide-sensitive fusion protein: implications in the regulation of its hexamerization and exocytosis. *J. Biol. Chem* **2006**, *281*, 9852-9858.

(201) Peyre, J.; Seabrooke, S.; Randlett, O.; Kisiel, M.; Aigaki, T.; Stewart, B. A. Interaction of cytoskeleton genes with NSF2-induced neuromuscular junction overgrowth. *Genesis* **2006**, *44*, 595-600.

(202) Song, I.; Kamboj, S.; Xia, J.; Dong, H.; Liao, D.; Huganir, R. L. Interaction of the N-ethylmaleimide-sensitive factor with AMPA receptors. *Neuron* **1998**, *21*, 393-400.

(203) Hanley, J. G. NSF binds calcium to regulate its interaction with AMPA receptor subunit GluR2. *J. Neurochem* **2007**, *101*, 1644-1650.

(204) Pontier, S. M.; Lahaie, N.; Ginham, R.; St-Gelais, F.; Bonin, H.; Bell, D. J.; Flynn, H.; Trudeau, L.; McIlhinney, J.; White, J. H.; Bouvier, M. Coordinated action of NSF and PKC regulates GABAB receptor signaling efficacy. *EMBO J* **2006**, *25*, 2698-2709.

(205) Goto, H.; Terunuma, M.; Kanematsu, T.; Misumi, Y.; Moss, S. J.; Hirata, M. Direct interaction of N-ethylmaleimide-sensitive factor with GABA(A) receptor beta subunits. *Mol. Cell. Neurosci* **2005**, *30*, 197-206.

(206) Cong, M.; Perry, S. J.; Hu, L. A.; Hanson, P. I.; Claing, A.; Lefkowitz, R. J. Binding of the beta2 adrenergic receptor to N-ethylmaleimide-sensitive factor regulates receptor recycling. *J. Biol. Chem* **2001**, *276*, 45145-45152.

(207) Zou, S.; Li, L.; Pei, L.; Vukusic, B.; Van Tol, H. H. M.; Lee, F. J. S.; Wan, Q.; Liu, F. Protein-protein coupling/uncoupling enables dopamine D2 receptor regulation of AMPA receptor-mediated excitotoxicity. *J. Neurosci* **2005**, *25*, 4385-4395.

(208) Heydorn, A.; Søndergaard, B. P.; Hadrup, N.; Holst, B.; Haft, C. R.; Schwartz, T. W. Distinct in vitro interaction pattern of dopamine receptor subtypes with adaptor proteins involved in post-endocytotic receptor targeting. *FEBS Lett* **2004**, *556*, 276-280.

(209) Heydorn, A.; Søndergaard, B. P.; Ersbøll, B.; Holst, B.; Nielsen, F. C.; Haft, C. R.; Whistler, J.; Schwartz, T. W. A library of 7TM receptor C-terminal tails. Interactions with the proposed post-endocytic sorting proteins ERM-binding phosphoprotein 50 (EBP50), N-ethylmaleimide-sensitive factor (NSF), sorting nexin 1 (SNX1), and G protein-coupled receptor-associated sorting protein (GASP). *J. Biol. Chem* **2004**, *279*, 54291-54303.

(210) Wickner, W.; Schekman, R. Membrane fusion. *Nat. Struct. Mol. Biol* **2008**, *15*, 658-664.

(211) Jack H. Kaplan BIOCHEMISTRY OF NA,K-ATPASE **2003**.

(212) Goldstein, I.; Lerer, E.; Laiba, E.; Mallet, J.; Mujaheed, M.; Laurent, C.; Rosen, H.; Ebstein, R. P.; Lichtstein, D. Association between sodium- and potassium-activated adenosine triphosphatase alpha isoforms and bipolar disorders. *Biol. Psychiatry* **2009**, *65*, 985-991.

(213) Morth, J. P.; Poulsen, H.; Toustrup-Jensen, M. S.; Schack, V. R.; Egebjerg, J.; Andersen, J. P.; Vilsen, B.; Nissen, P. The structure of the Na+,K+-ATPase and mapping of isoform differences and disease-related mutations. *Philos. Trans. R. Soc. Lond., B, Biol. Sci* **2009**, *364*, 217-227.

(214) De Fusco, M.; Marconi, R.; Silvestri, L.; Atorino, L.; Rampoldi, L.; Morgante, L.;

Ballabio, A.; Aridon, P.; Casari, G. Haploinsufficiency of ATP1A2 encoding the Na+/K+ pump alpha2 subunit associated with familial hemiplegic migraine type 2. *Nat. Genet* **2003**, *33*, 192-6.

(215) Bethea, H. N.; Xu, D.; Liu, J.; Pedersen, L. C. Redirecting the substrate specificity of heparan sulfate 2-O-sulfotransferase by structurally guided mutagenesis. *Proc. Natl. Acad. Sci. U.S.A* **2008**, *105*, 18724-18729.

(216) Brittain, J. M.; Piekarz, A. D.; Wang, Y.; Kondo, T.; Cummins, T. R.; Khanna, R. An atypical role for collapsin response mediator protein 2 (CRMP-2) in neurotransmitter release via interaction with presynaptic voltage-gated calcium channels. *J. Biol. Chem* **2009**, *284*, 31375-31390.

(217) Trott, O.; Olson, A. J. AutoDock Vina: improving the speed and accuracy of docking with a new scoring function, efficient optimization, and multithreading. *J Comput Chem* **2010**, *31*, 455-461.

(218) Clapcote, S. J.; Duffy, S.; Xie, G.; Kirshenbaum, G.; Bechard, A. R.; Rodacker Schack, V.; Petersen, J.; Sinai, L.; Saab, B. J.; Lerch, J. P.; Minassian, B. A.; Ackerley, C. A.; Sled, J. G.; Cortez, M. A.; Henderson, J. T.; Vilsen, B.; Roder, J. C. Mutation I810N in the alpha3 isoform of Na+,K+-ATPase causes impairments in the sodium pump and hyperexcitability in the CNS. *Proc. Natl. Acad. Sci. U.S.A* **2009**, *106*, 14085-14090.

(219) Yamashita, N.; Morita, A.; Uchida, Y.; Nakamura, F.; Usui, H.; Ohshima, T.; Taniguchi, M.; Honnorat, J.; Thomasset, N.; Takei, K.; Takahashi, T.; Kolattukudy, P.; Goshima, Y. Regulation of spine development by semaphorin3A through cyclin-dependent kinase 5 phosphorylation of collapsin response mediator protein 1. *J. Neurosci* **2007**, *27*, 12546-12554.

(220) Stöhr, T.; Lekieffre, D.; Freitag, J. Lacosamide, the new anticonvulsant, effectively reduces harmaline-induced tremors in rats. *Eur. J. Pharmacol* **2008**, *589*, 114-116.

(221) Du, W.; Aloyo, V. J.; Harvey, J. A. Harmaline competitively inhibits [3H]MK-801 binding to the NMDA receptor in rabbit brain. *Brain Res* **1997**, *770*, 26-29.

(222) Kolasiewicz, W.; Kuter, K.; Wardas, J.; Ossowska, K. Role of the metabotropic glutamate receptor subtype 1 in the harmaline-induced tremor in rats. *J Neural Transm* **2009**, *116*, 1059-1063.

(223) Attwell, P. J.; Singh Kent, N.; Jane, D. E.; Croucher, M. J.; Bradford, H. F. Anticonvulsant and glutamate release-inhibiting properties of the highly potent metabotropic glutamate receptor agonist (2S,2'R, 3'R)-2-(2',3'-dicarboxycyclopropyl)glycine (DCG-IV). *Brain Res* **1998**, *805*, 138-143.

(224) Südhof, T. C. alpha-Latrotoxin and its receptors: neurexins and CIRL/latrophilins. *Annu. Rev. Neurosci* **2001**, *24*, 933-962.

(225) Hlubek, M. D.; Stuenkel, E. L.; Krasnoperov, V. G.; Petrenko, A. G.; Holz, R. W.

Calcium-independent receptor for alpha-latrotoxin and neurexin 1alpha [corrected] facilitate toxin-induced channel formation: evidence that channel formation results from tethering of toxin to membrane. *Mol. Pharmacol* **2000**, *57*, 519-528.

(226) Ichtchenko, K.; Khvotchev, M.; Kiyatkin, N.; Simpson, L.; Sugita, S.; Südhof, T. C. alpha-latrotoxin action probed with recombinant toxin: receptors recruit alpha-latrotoxin but do not transduce an exocytotic signal. *EMBO J* **1998**, *17*, 6188-6199.

(227) Laviolette, M. J.; Nunes, P.; Peyre, J.; Aigaki, T.; Stewart, B. A. A genetic screen for suppressors of Drosophila NSF2 neuromuscular junction overgrowth. *Genetics* **2005**, *170*, 779-792.

APPENDIX

Mass Spectrometry Experiment Number 1 (03/04/08)

Sample	Drug	Protein (ul)	[Drug]	Probe	Purification	Elution
1	Compound 1	500 (0.8mg)	12 uM	Biotin	Muetin Streptavidin beads	Biotin (4mM)
2	Compound 1	500 (0.8mg)	12 uM	Biotin	Streptavidin beads	Sample Buffer
3	Compound 2	500 (0.8mg)	12 uM	Biotin	Muetin Streptavidin beads	Biotin (4mM)
4	Compound 3	500 (0.8mg)	12 uM	Biotin	Muetin Streptavidin beads	Biotin (4mM)
5	Compound 3	500 (0.8mg)	12 uM	Biotin	Streptavidin beads	Sample Buffer
5	No Drug	500 (0.8mg)		Biotin	Streptavidin Beads	Biotin (4mM)

Protocol

1. Aliquot 500ul of lysate (1.71mg/ml) per reaction**.**
2. Add appropriate amount of drug
3. Incubate at room temperature for 1h for NCS, for N_3 UV crosslink for 15 min
4. ***QUENCH*** reactions with 4mM methylhydrazine for **1**h at R.T. for NCS compounds, for N_3, pass through a Zeba column
5. Add SDS to [1 %], boil for 5 minutes
6. Add Click chemistry reagents Biotin-N_3, TBTA, TCEP, CuSO4 (1:1:10:25)
7. Incubate for 2h at R.T. rotating
8. Add 100ul (Resin) streptavidin beads
9. Incubate for 2h at 4°C
10. Wash 4X with 1ml of 50mM HEPES pH 7.2 for regular streptavidin beads, wash muetin streptavidin beads with 3CV of wash buffer
11. Elute with 100ul of elution buffer
    a. SDS-PAGE sample buffer
    b. 4mM Biotin
12. Run eluted products on gel

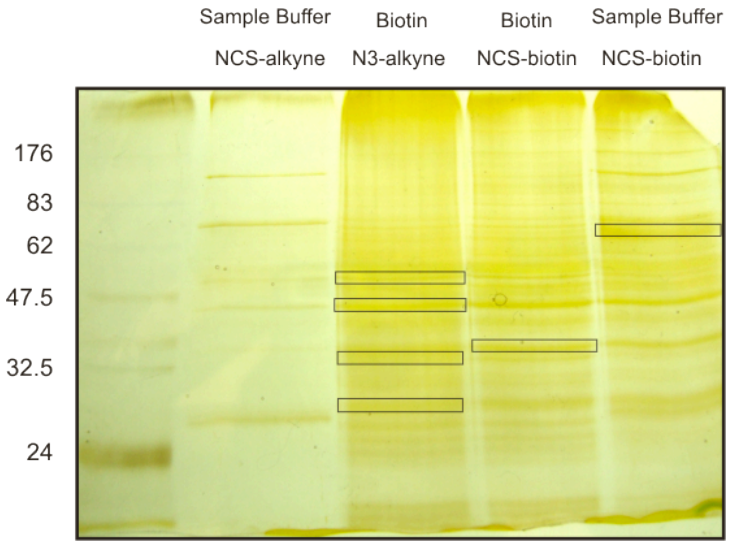

Results of Experiment 1

SCBO1	ATP synthase subunit beta, mitochodrial precursor ATP synthase subunit alpha, mitochondrial precursor Brain acid soluble protein 1 AP-2 complex subunit mu-1
SCBO2	Actin, cytoplasmic 1 Citrate synthase Creatine kinase, ubiquitous mitochondrial precursor Creatine kinase, B-type 2',3'-cyclic-nucleotide 3'-phosphodiesterase Phosphoglycerate kinase1 Phosphoglycerate kinase2
SCBO3	Aspartate aminotransferase, mitochondrial precursor Aspartate aminotransferase, cytoplasmic Fructose-bisphosphate aldolase A actin (can not identify isoform) Fructose-bisphosphate aldolase C Guanine nucleotide-binding protein G (can not identify isoform) Calcium-independent alpha-latrotoxin receptor
SCBO4	3-monooxygenase/tryptophan 5-monooxygenase activation protein zeta/delta 3-monooxygenase/tryptophan 5-monooxygenase activation protein gamma 3-monooxygenase/tryptophan 5-monooxygenase activation protein eta 3-monooxygenase/tryptophan 5-monooxygenase activation protein beta/alpha 3-monooxygenase/tryptophan 5-monooxygenase activation protein sigma 3-monooxygenase/tryptophan 5-monooxygenase activation protein theta ADP/ATP translocase 1 ADP/ATP translocase 2 Carbonic anhydrase 2
SCBO5	Malate dehydrogenase, cytoplasmic Malate dehydrogenase, mitochondrial precursor Guanine nucleotide-binding protein G (can not identify isoform) Syntaxin-1B Clathrin light chain B
SCBO6	Syntaxin-binding protein1 Dihydropyrimidinase-related protein 1 Dihydropyrimidinase-related protein 2 Serum albumin precursor Myelin proteolipid protein

Mass Spectrometry Experiment 2 (04/20/08)

Sample	Drug	Protein (ul)	[Drug]	Probe	Purification	Elution
1	Compound 1	500 (0.8mg)	40 uM	Biotin	Streptavidin beads	Sample Buffer
2	AB-R-LCM	500 (0.8mg)	40 uM	Biotin	Streptavidin beads	Sample Buffer
3	No Drug	500 (0.8mg)	40 uM	Biotin	Streptavidin beads	Sample Buffer

Protocol

1. Aliquot 500ul of lysate (1.71mg/ml) per reaction**.**
2. Add appropriate amount of drug
3. Incubate at room temperature for 1h for NCS
4. ***QUENCH*** reactions with 4mM methylhydrazine for **1**h at R.T. for NCS compounds
5. Add Click Chemistry Reagents in accordance with (Salisbury Cravatte JACS 2008 DOI ja074138u)
    a. 1ul of 20mM Biotin Probe
    b. .25ul of 1M TCEP
    c. 2.5 ul of 20mM TBTA
    d. .5 ul of 1M $CuSO_4$
6. Incubate for 2h at R.T. rotating
7. Add 50ul (Resin) streptavidin beads
8. Wash 2X with 50mM HEPES, 150mM NaCl with .2% SDS
9. Wash 2X with 6M urea
10. Wash 3X with 50mM HEPES, 150mM NaCl
11. Elute with 50ul of elution buffer
    a. SDS-PAGE sample buffer
12. Run eluted products on gel

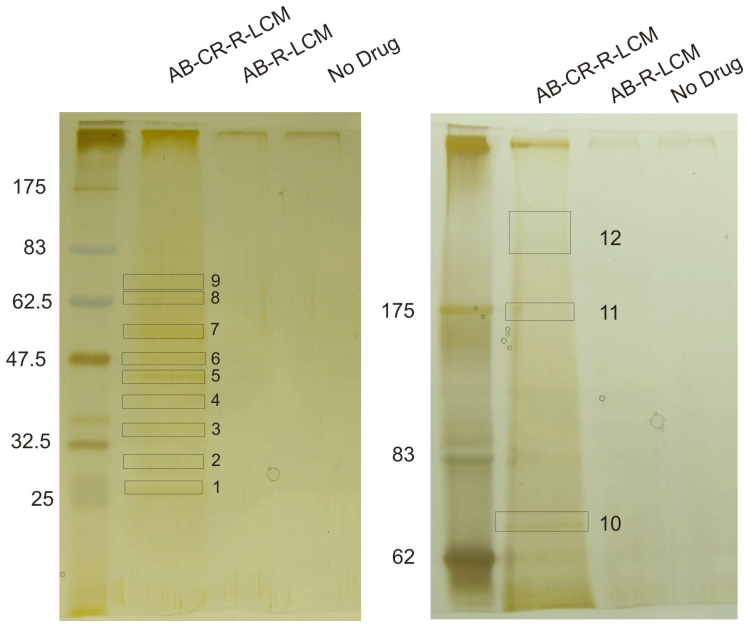

Results of Experiment 2

No.	AB&CR
1	ADP/ATP translocase 1 (MW 32883) 3-monooxygenase/tryptophan 5-monooxygenase activation protein zeta/delta (MW 27754) Keratin, type II cytoskeletal 1 Keratin, type I cytoskeletal 14 Keratin, type I cytoskeletal 15 Keratin, type I cytoskeletal 17 Keratin, type II cytoskeletal 8 Keratin, type II cytoskeletal 5
2	Keratin, type II cytoskeletal 1b Keratin, type I cytoskeletal 10
3	Glyceraldehyde-3-phosphate dehydrogenase (MW 35787) Malate dehydrogenase, mitochondrial precursor (MW 35589) Keratin, type II cytoskeletal 1 Keratin, type I cytoskeletal 10 Keratin, type II cytoskeletal 2 epidermal Keratin, type II cytoskeletal 4 Keratin, type II cytoskeletal 6A
4	Actin, cytoplasmic 1 (MW 41710) Keratin, type I cytoskeletal 10
5	Elongation factor 1-alpha 1 (MW 50082) Alpha-enolase (MW 47111) Keratin, type II cytoskeletal 1b Keratin, type II cytoskeletal 2 epidermal
6	ATP synthase subunit alpha, mitochondrial precursor (MW 59716) Spermatogenesis-associated protein 7 homolog (MW 65613) observed only one peptide Tubulin alpha-1A chain Keratin, type II cytoskeletal 1b Tubulin beta-3 chain Tubulin alpha-4A chain Keratin, type I cytoskeletal 10 Keratin, type I cytoskeletal 18 Tubulin beta-2A chain
7	Dihydropyrimidinase-related protein 1 or 2 (MW 62239) Spermatogenesis-associated protein 7 homolog (MW 65613) observed only one peptide Histone H4 (MW 11360) Keratin, type I cytoskeletal 10

	Keratin, type I cytoskeletal 14 Keratin, type II cytoskeletal 8 Keratin, type II cytoskeletal 5 Keratin, type I cuticular Ha1 Keratin, type II cytoskeletal 1 Keratin type II cuticular Hb5
8	-
9	-
10	-
11	-
12	-

Mass Spectrometry Experiment 3 (05/21/08)

Sample	Drug	Protein (ul)	[Drug]	Click	Probe	Purification	Elution
1	Compound 1 (*R*)	500 (2.25mg)	40 uM	$CuSO_4$	Biotin	Streptavidin beads	Sample Buffer
2	Compound 1 (*S*)	500 (2.25mg)	40 uM	$CuSO_4$	Biotin	Streptavidin beads	Sample Buffer
3	Compound 2 (*R*)	500 (2.25mg)	40 uM	$CuSO_4$	Biotin	Streptavidin beads	Sample Buffer
4	Compound 2 (*S*)	500 (2.25mg)	40 uM	$CuSO_4$	Biotin	Streptavidin beads	Sample Buffer
5	No Drug			$CuSO_4$	Biotin	Streptavidin beads	Sample Buffer

Protocol

1. Preclear lysate with 500ul 50% slurry streptavidin beads
2. Aliquot 500ul of lysate (4.5mg/ml) per reaction
3. Incubate at room temperature for 30 min
4. Add appropriate amount of drug
5. Incubate at room temperature for 1h for NCS, for N3 incubate at R.T. for 30 min then hv crosslink for 20 min
6. ***QUENCH*** reactions with 4mM methylhydrazine for **1**h at R.T. for NCS and TCEP for N_3
7. Add Click Chemistry Reagents in accordance with (Salisbury Cravatte JACS 2008 DOI ja074138u)
    a. 1ul of 20mM Biotin Probe
    b. .25ul of 1M TCEP
    c. 2.5 ul of 20mM TBTA
    d. .5 ul of 1M $CuSO_4$
8. Incubate for 2h at R.T. rotating
9. Add 50ul (Resin) streptavidin beads
10. Wash 2X with 50mM HEPES, 150mM NaCl with .2% SDS
11. Wash 2X with 6M urea
12. Wash 3X with 50mM HEPES, 150mM NaCl
13. Remove 1/3 of the beads to submit for mass spec
14. Elute with 50ul of elution buffer
    a. SDS-PAGE sample buffer
15. Run eluted products on gel

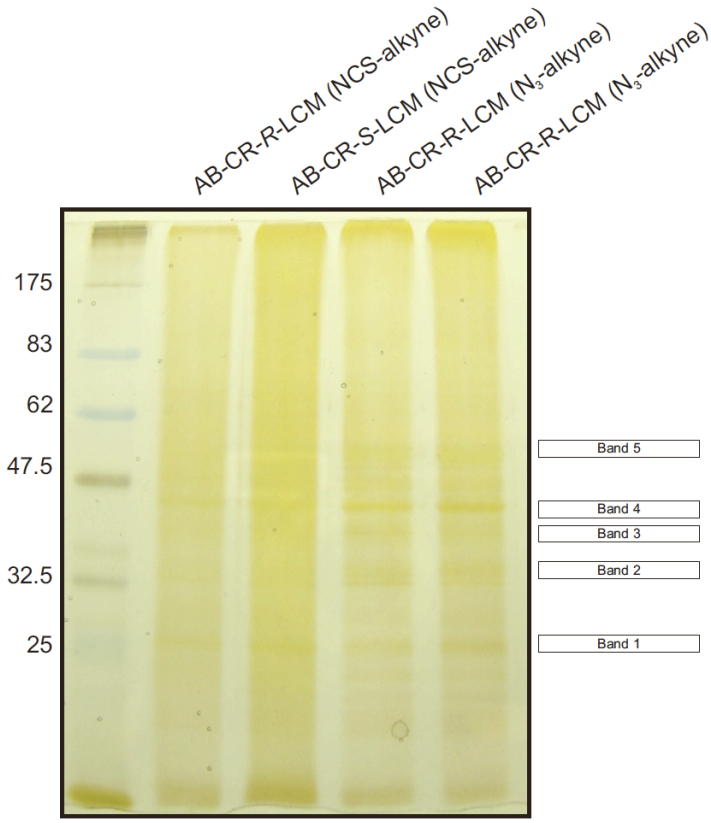

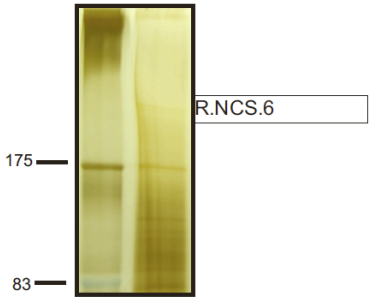

Sample Number	Sample Name	Sample Type	Drug
1	R.NCS.1	Gel Band	Compound 1 (*R*)
2	R.NCS.2	Gel Band	Compound 1 (*R*)
3	R.NCS.3	Gel Band	Compound 1 (*R*)
4	R.NCS.4	Gel Band	Compound 1 (*R*)
5	R.NCS.5	Gel Band	Compound 1 (*R*)
6	R.NCS.6	Gel Band	Compound 1 (*R*)
7	S.NCS.1	Gel Band	Compound 1 (*S*)
8	S.NCS.2	Gel Band	Compound 1 (*S*)
9	S.NCS.3	Gel Band	Compound 1 (*S*)
10	S.NCS.4	Gel Band	Compound 1 (*S*)
11	S.NCS.5	Gel Band	Compound 1 (*S*)
12	R.N3.1	Gel Band	Compound 2 (*R*)
13	R.N3.2	Gel Band	Compound 2 (*R*)
14	R.N3.3	Gel Band	Compound 2 (*R*)

15	R.N3.4	Gel Band	Compound 2 (*R*)
16	R.N3.5	Gel Band	Compound 2 (*R*)
17	S.N3.1	Gel Band	Compound 2 (*S*)
18	S.N3.2	Gel Band	Compound 2 (*S*)
19	S.N3.3	Gel Band	Compound 2 (*S*)
20	S.N3.4	Gel Band	Compound 2 (*S*)
21	S.N3.5	Gel Band	Compound 2 (*S*)
22	1	Streptavidin Beads	Compound 1 (*R*)
24	2	Streptavidin Beads	Compound 1 (*S*)
25	3	Streptavidin Beads	Compound 2 (*R*)
25	4	Streptavidin Beads	Compound 2 (*S*)
26	5	Streptavidin Beads	No Drug

Results of Experiment 3

Protein	**Bead R-NCS**	**Gel R-NCS**	**Bead S-NCS**	**Gel S-NCS**	**Bead R-N3**	**Gel R-N3**	**Bead S-N3**	**Gel S-N3**
Sodium/potassium-transporting ATPase subunit alpha-3	15		13		9		11	2
Sodium/potassium-transporting ATPase subunit alpha-2 precursor	9				7		6	
Sodium/potassium-transporting ATPase subunit alpha-1 precursor	9		6				5	
Sodium/potassium-transporting ATPase subunit beta-1	2		1				1	
ADP/ATP translocase 1	4			6			2	6
ADP/ATP translocase 2	2			4				5
ADP/ATP translocase 4	2							
3-monooxygenase/tryptophan 5-monooxygenase activation protein zeta/delta	3		2	9	3			6
3-monooxygenase/tryptophan 5-monooxygenase			3					

activation protein epsilon								
3-monooxygenase/tryptophan 5-monooxygenase activation protein gamma					3		3	
3-monooxygenase/tryptophan 5-monooxygenase activation protein sigma					2		2	
ATP synthase subunit beta	5		2				3	
ATP synthase subunit alpha, mitochondrial precursor			4	6			2	7
Heat shock cognate 71 kDa protein			2			4		3
Heat shock protein HSP 90-alpha							2	
Heat shock protein HSP 90-beta							2	
Heat shock protein 75 kDa, mitochondrial precursor							1	
Actin, cytoplasmic 1	9	6	11	5	7	16	9	12
Gamma-enolase	2	2				2		3
Alpha-enolase				5			2	
Potassium-transporting ATPase alpha chain 1	2							
Dihydropyrimidinase-related protein 2	8	2	5	3		6		
Triosephosphate isomerase	3		4		1	3		
Fructose-bisphosphate aldolase A	4	2		2				2
Pyruvate kinase isozymes M1/M2	1				3			
Cofilin-1	1							
Hemoglobin subunit beta-1	2		3				1	

Guanine nucleotide-binding protein G(o) subunit alpha 1	2		2	2			2	
2',3'-cyclic-nucleotide 3'-phosphodiesterase	3	2	4				4	
Histone (can not identify isoform)	1		2				2	
Clathrin heavy chain	3		6				4	
Peptidyl-prolyl cis-trans isomerase A	3							
Myelin proteolipid protein	3				2	1	4	1
Creatine kinase B-type	2		3				1	
4-aminobutyrate aminotransferase, mitochondrial precursor			1					
Succinate dehydrogenase [ubiquinone] flavoprotein subunit, mitochondrial precursor			2					
Glyceraldehyde-3-phosphate dehydrogenase			3	2	1		6	
Ras-related protein (can not identify isoform)			1					
Malate dehydrogenase, mitochondrial precursor			1	1				3
Malate dehydrogenase, cytoplasmic								1
Dynamin-1			2					
Excitatory amino acid transporter 2			1					
Symplekin					2			
Vang-like protein 2					1			
Retinoblastoma-binding protein 6					1			
2-oxoglutarate dehydrogenase E1 component, mitochondrial precursor							2	

Elongation factor 1-alpha 1				1	2
G1 to S phase transition protein 1 homolog				1	
Structural maintenance of chromosomes protein 1A				1	
Syntaxin-binding protein 1		2	3		
Vesicle-fusing ATPase			3		
Stress-70 protein, mitochondrial precursor					
Carbonic anhydrase 2					3
Ubiquinol-cytochrome-c reductase complex core protein 2, mitochondrial precursor					3

Mass Spectrometry Experiment 4 (06/29/08)

Sample	Drug	Protein (ul)	[Drug]	Click	Probe	Purification	Competition
1	Compound 1 (*R*)	500 (2.25mg)	40 uM	$CuSO_4$	Biotin	Streptavidin beads	None
2	Compound 1 (*S*)	500 (2.25mg)	40 uM	$CuSO_4$	Biotin	Streptavidin beads	None
3	Compound 2 (*R*)	500 (2.25mg)	40 uM	$CuSO_4$	Biotin	Streptavidin beads	None
4	Compound 2 (*S*)	500 (2.25mg)	40 uM	$CuSO_4$	Biotin	Streptavidin beads	None
5	Compound 1 (*R*)	500 (2.25mg)	40 uM	$CuSO_4$	Biotin	Streptavidin beads	4mM NCS-R
6	Compound 1 (*S*)	500 (2.25mg)	40 uM	$CuSO_4$	Biotin	Streptavidin beads	4mM NCS-R
7	Compound 2 (*R*)	500 (2.25mg)	40 uM	$CuSO_4$	Biotin	Streptavidin beads	4mM NCS-R
8	Compound 2 (*S*)	500 (2.25mg)	40 uM	$CuSO_4$	Biotin	Streptavidin beads	4mM NCS-R

Protocol

1. Preclear lysate with 500ul 50% slurry streptavidin beads
2. Aliquot 500ul of lysate (4.5mg/ml) per reaction
3. Add competing Drug
4. Incubate at room temperature for 30 min
5. Add appropriate amount of drug
6. Incubate at room temperature for 1h for NCS, for N3 incubate at R.T. for 30 min then hv crosslink for 20 min
7. *QUENCH* reactions with 4mM methylhydrazine for 1h at R.T. for NCS and TCEP for N_3
8. Add Click Chemistry Reagents in accordance with (Salisbury Cravatte JACS 2008 DOI ja074138u)
    a. 1ul of 20mM Biotin Probe
    b. .25ul of 1M TCEP
    c. 2.5 ul of 20mM TBTA
    d. .5 ul of 1M $CuSO_4$
9. Incubate for 2h at R.T. rotating
10. Add 50ul (Resin) streptavidin beads
11. Wash 2X with 50mM HEPES, 150mM NaCl with .2% SDS
12. Wash 2X with 6M urea
13. Wash 3X with 50mM HEPES, 150mM NaCl
14. Remove 1/3 of the beads to submit for mass spec

Results of Experiment 4

Protein	no. of peptides							
	R-NCS	S-NCS	R-N3	S-N3	R-NCS	S-NCS	R-N3	S-N3
Sodium/potassium-transporting ATPase subunit alpha-3	10	9	6	10			8	
Sodium/potassium-transporting ATPase subunit alpha-2 precursor	12	9	7	11				
Actin, (can not identify isoform)	6	6	7	5	2		6	9
Sodium/potassium-transporting ATPase subunit alpha-1 precursor	8							
ATP synthase subunit alpha, mitochondrial precursor	4		4				4	3
Syntaxin-binding protein 1	2	3	1	3			3	2
Hemoglobin subunit beta-1	1			2			3	2
Fructose-bisphosphate aldolase A	2							
Glyceraldehyde-3-phosphate dehydrogenase	2	3	4	2			3	2
2',3'-cyclic-nucleotide 3'-phosphodiesterase	2	2	3	4	1		2	3

14-3-3 protein zeta/delta	2	6	1	3				
Ras-related protein Rab-3A	2							
Ras-related protein Rab-30	2							
ATP synthase subunit beta, mitochondrial precursor	4	2					4	2
ADP/ATP translocase 1	3	5	3	1			5	
Elongation factor 1-alpha 1	1							
Guanine nucleotide-binding protein (can not identify isoform)	1	1		2				
Heat shock protein HSP 90-alpha	2	2						
ADP/ATP translocase 4	3	3	4					
Pyruvate kinase isozymes M1/M2	1			3			3	
Plasma membrane calcium-transporting ATPase 2	1							
Heat shock cognate 71 kDa protein (can not identify isoform)	2	4					2	2
14-3-3 protein epsilon		4	1					
14-3-3 protein gamma		4						1
Pyruvate kinase isozymes M1/M2		2						2
Malate dehydrogenase, mitochondrial precursor		3						
Excitatory amino acid transporter 2		1	1	2				
14-3-3 protein theta		3						
Potassium-transporting ATPase alpha chain 1		3						
Abhydrolase domain-containing protein 8		1	1					
Heat shock 70 kDa protein (can not identify isoform)		2					2	
Serine/threonine-protein kinase 6		1		1	1			
Creatine kinase B-type		2		2			3	1
Clathrin heavy chain		3					2	2
Myelin proteolipid protein		3		4		3	2	3
Glutamate dehydrogenase 1, mitochondrial precursor				2			3	
Gamma-enolase				2				
Fructose-bisphosphate aldolase A							1	
Phosphate carrier protein, mitochondrial precursor							1	